

Energy Loss of High Energy Partons In Quark-Gluon Plasma

By

TRAMBAK BHATTACHARYYA

Enrolment No: PHYS04200904015

Variable Energy Cyclotron Centre, Kolkata

*A thesis submitted to
The Board of Studies in Physical Sciences*

In partial fulfillment of requirements

For the Degree of

DOCTOR OF PHILOSOPHY

of

HOMI BHABHA NATIONAL INSTITUTE

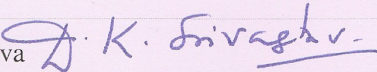
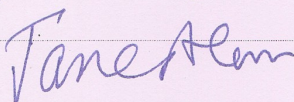
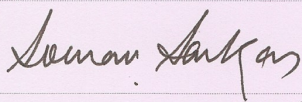
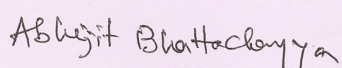


March, 2015

Homi Bhabha National Institute¹

Recommendations of the Viva Voce Committee

As members of the Viva Voce Committee, we certify that we have read the dissertation prepared by Trambak Bhattacharyya entitled "Energy Loss of High Energy Partons in Quark Gluon Plasma" and recommend that it may be accepted as fulfilling the thesis requirement for the award of Degree of Doctor of Philosophy.

Chairman—Dr. D. K. Srivastava		Date: 13/3/2015
Guide / Convener -Dr. Jan-e Alam		Date: 13/3/2015
Co-guide -<Name> (if any)	—	Date: —
Member1—Dr. Sourav Sarkar		Date: 13/3/2015
Member2—Dr. Munshi Golam Mustafa		Date: 13/03/2015
MemberN—Dr. Abhijit Bhattacharyya		Date: 13/3/15

Final approval and acceptance of this thesis is contingent upon the candidate's submission of the final copies of the thesis to HBNI.

I/We hereby certify that I/we have read this thesis prepared under my/our direction and recommend that it may be accepted as fulfilling the thesis requirement.

Date: March 13, 2015

Place: VECE/Kolkata

<Signature>

Co-guide (if applicable)


<Signature> 13/3/2015

Guide

¹ This page is to be included only for final submission after successful completion of viva voce.

Version approved during the meeting of Standing Committee of Deans held during 29-30 Nov 2013.

STATEMENT BY AUTHOR

This dissertation has been submitted in partial fulfilment of requirements for an advanced degree at Homi Bhabha National Institute (HBNI) and is deposited in the Library to be made available to borrowers under rules of the HBNI.

Brief quotation from this dissertation are allowable without special permission, provided that accurate acknowledgement of source is made. Requests for permission for extended quotation from or reproduction of this manuscript in whole or in part may be granted by the Competent Authority of HBNI when in his or her judgement the proposed use of the material is in the interests of scholarship. In all other instances, however, permission must be obtained from the author.


Trambak Bhattacharyya

DECLARATION

I, hereby declare that the investigation presented in the thesis has been carried out by me. The work is original and has not been submitted earlier as a whole or in part for a degree/diploma at this or any other Institution/University.

Trambak Bhattacharyya

Trambak Bhattacharyya

List of Publications arising from this thesis

Journals :

1. Examination of the Gunion-Bertsch formula for soft gluon radiation.
Trambak Bhattacharyya, Surasree Mazumder, Santosh K Das, Jan-e Alam.
Phys. Rev. D **85**, 034033-(1-6)(2012).
2. Dead cone due to parton virtuality
Trambak Bhattacharyya and Jan-e Alam
Int. Jour. of Mod. Phys. A, **28** 1350031-(1-9)(2013).

Conferences:

1. Proceedings of the DAE Symposium on Nuclear Physics, 2011, 56 (2011) 904.
2. Proceedings of the QGP Meet, 2012, held at VECC
3. Proceedings of the 'International Symposium on Matter at Extreme Conditions: Now & Then', 15-17 January, 2014, Bose Institute, Kolkata, India.

Others:

Communicated

1. Color synchrotron off heavy flavor jet deluges the "dead cone"
Trambak Bhattacharyya, Surasree Mazumder and Raktim Abir


Trambak Bhattacharyya

DEDICATION

To my Grand-pa

ACKNOWLEDGEMENTS

I acknowledge my family, my friends and my teachers for their unfathomable support.

SYNOPSIS

Introduction

A time machine helps us move in time as we walk or move in space. Heavy-ion Collision (HIC) experiments are like the time-machines which help us understand Quark-Gluon Plasma (QGP), the form of matter existed when the universe was only micro-second (μS) old. When hadrons are subjected to an ambience of 3-4 times the density of nuclear matter ($\sim .16 \text{ fm}^{-3}$), the individual quarks and gluons of the hadrons would no longer be confined within them but melt into a deconfined state of quarks and gluons. The idea that Quark Matter might form by compressing protons and neutrons was suggested in 1970 by Naoki Itoh [1]. Just after the discovery of asymptotic freedom [2, 3, 4], Collins and Perry [5] also suggested that at very high density the degrees of freedom of the strongly interacting matters are not hadrons but quarks and gluons. The same is true when the quantum chromodynamic (QCD) vacuum is excited to high temperatures, too ([6]). With increasing temperature, new and new hadrons are produced thereby increasing the corresponding number density; and at a certain temperature ($\sim 175 \text{ MeV}$), there is an overlap of hadrons. Such a phase of matter is called Quark Gluon Plasma (QGP) and its study needs QCD, the theory of strong interaction which is extremely successful in vacuum, to be applied in a thermal medium. So, the deconfined state of quarks and gluons gives an opportunity to peruse ‘condensed matter physics’ [7] of elementary particles in the new domain of non-abelian gauge theory.

After big bang took place, the universe has undergone several phase transitions like GUT, Electro-weak, quarks and gluons to hadrons etc. Quarks to hadrons phase transition can be simulated by the present day accelerators like RHIC and LHC (200 GeV/A and $\sim 2.76 \text{ TeV/A}$ respectively). The study of this transition demands special importance in understanding the evolution of the μS old early universe. The issue is very crucial for astrophysics too, as the

core of the compact astrophysical objects like neutron stars may contain quark matter at high baryon density and low temperature. So there is a multitude of reasons behind creating and studying the properties of QGP in laboratories.

Once QGP is created, we must try to understand the transport properties of it. In general, the interaction of probes with a medium brings out useful information about the nature of the bath. The magnitudes of the transport coefficients are sensitive to the coupling strength and so these quantities are used to characterize a medium. In the present discussion, we make use of high energy gluons/light quarks/heavy quarks for probes. The probes interact with the medium mainly via elastic and/or radiative processes. While for transverse momentum (p_T) ~ 2 GeV we expect elastic losses to be dominant, the radiative loss overrides in larger p_T regions.

The present dissertation will mainly concentrate on radiative energy loss of high energy particle probes inside the quark-gluon plasma medium. The integration of radiation spectrum over the phase space yields the energy depletion due to radiation. The energy loss, thus obtained, can be utilized to get the transport coefficients of the medium. However, before embarking upon the discussion about the energy loss of swift partons in quark-gluon plasma, we must briefly explain the physical scenarios and the succession of events while energy loss of a high energy parton takes place in the QGP.

The physical scenarios behind the energy loss phenomenon

Heavy ion collision is about colliding two heavy nuclei with large energies. Quarks and gluons, the constituents of protons, neutrons etc. are also in a Lorentz boosted frame. Now, every charge, electric or colour, in a Lorentz boosted frame acquires photons/gluons/sea quarks. This picture of imagining the field of a rapidly (but uniformly) moving charge as collection of

virtual particles is called the Weizsäcker-Williams picture. This picture relies on the fact that there is a similarity between the fields of a rapidly moving charge and the fields of a pulse [8]. A violent collision of nuclei results in acceleration imparted to the moving charges. While the fast Fourier components of the field, whose transverse momenta $k \geq a_0$, where a_0 is the inverse acceleration time, can manage to follow the charge, the softer part is ‘left behind’ [9]. The Weizsäcker-Williams gluons which are now detached from the charge are regenerated along a new direction. So, there is a radiation – the vacuum radiation of highly virtual (Virtuality $Q \sim p_T$, the transverse momentum of parton) particles.

The fast particle alongwith the associated gluons is called the jet-shower (loosely jet); and we observe the interaction of this jet shower with the medium formed after the softer particles, produced much after the birth of the hard partons, jostle among themselves and thermalize.

There are two main processes, the elastic and the radiative processes, by which the jet interacts with the medium. The radiative energy loss of a representative particle in the jet-shower, called the leading particle, calls for counting the number of gluons emitted. The more the number of gluons given off, the more the radiative loss is. So we want the distribution of gluons for computing the energy depletion due to radiation.

Approximations widely used in energy loss models

Finding out the radiation distribution involves kinematics and dynamics of interaction. The dynamics is obtained by dint of the Feynman diagrams method applied for the perturbative QCD (pQCD). As far as the kinematics is concerned, we will perform all the calculations in the centre of momentum (COM) frame. The kinematic approximations widely used in these calculations are:

- soft radiation (energy of radiation is much smaller compared to the parent parton)

- eikonal approximation (no recoil of the leading parton due to scattering and radiation)
- and
- collinear radiation (radiated gluons almost graze the trajectory of the parent particle).

Works presented in the dissertation

A significant part of the present dissertation is devoted to the discussions about relaxing kinematic approximations used in computing the radiation distribution. While successful attempts have been observed in calling off the collinearity (in [10]) and the eikonal approximation due to scattering (in [11]), withdrawal of the soft approximation, which implies and is implied by the eikonal approximation due to radiation, still awaits.

After a broad classification of the nature of the work presented in the thesis, we will devote few paragraphs for a pithier description of what the thesis is about emphasizing the findings of the thesis. We will try to order them in the next few paragraphs.

Examination of the Gunion-Bertsch formula for soft gluon radiation.

Non-eikonal corrections to the Gunion-Bertsch formula [12] for the radiation distribution has been found out from the unapproximated matrix element of the $gg \rightarrow ggg$ process obtained from [13]. Non-eikonal becomes of particular importance if we consider the recoil of the incident jet due to scattering with the medium particles. The distribution, thus obtained, has been employed to compute the equilibration rate and the energy loss of gluons in gluonic plasma [14]. The radiation distribution off gluon jets with non-eikonal corrections is given by:

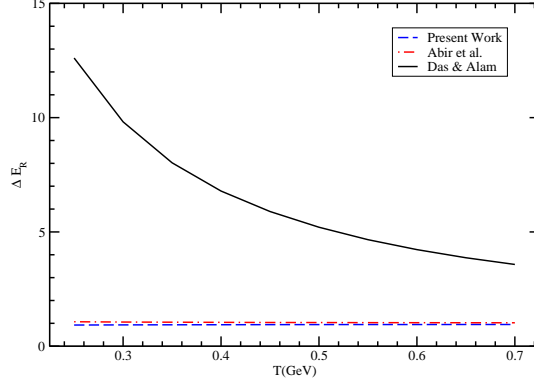


Figure 1: Temperature variation of radiative energy losses of 10 GeV gluon, obtained from Refs. [14, 15, 16] scaled by that obtained from Ref. [12]

$$\begin{aligned}
\frac{dn_g}{d^2\vec{k}_\perp d\eta_g} &= \frac{C_A\alpha_s}{\pi^2} \frac{1}{k_\perp^2} \mathcal{D}^{(1)} \\
&\approx \frac{C_A\alpha_s}{\pi^2} \frac{q_\perp^2}{k_\perp^2 (\vec{k}_\perp - \vec{q}_\perp)^2} \mathcal{D}^{(1)} \quad (\text{in the limit } \vec{q}_\perp \gg \vec{k}_\perp) \\
&= \left[\frac{dn_g}{d^2\vec{k}_\perp d\eta_g} \right]_{GB} \mathcal{D}^{(1)} \tag{1}
\end{aligned}$$

where $\mathcal{D}^{(1)} = \left[\left(1 + \frac{t}{2s} + \frac{5t^2}{2s^2} - \frac{t^3}{s^3} \right) - \left(\frac{3}{2\sqrt{s}} + \frac{4t}{s\sqrt{s}} - \frac{3t^2}{2s^2\sqrt{s}} \right) k_\perp + \left(\frac{5}{2s} + \frac{t}{2s^2} + \frac{5t^2}{s^3} \right) k_\perp^2 \right]$, n_g is the number of gluons, k_\perp is the transverse momentum, η_g is the gluon rapidity, $t(\approx -q_\perp^2)$ and s are the Mandelstam variables, C_A is the Casimir factor and α_s is the strong coupling.

The radiative energy losses obtained by two earlier papers ([15, 16]) with non-eikonal corrections (but no $\mathcal{O}(k_\perp)$ corrections) have been compared with the present work (Fig.1) where the radiation depletion per collision beyond the first one has been calculated by the following formula:

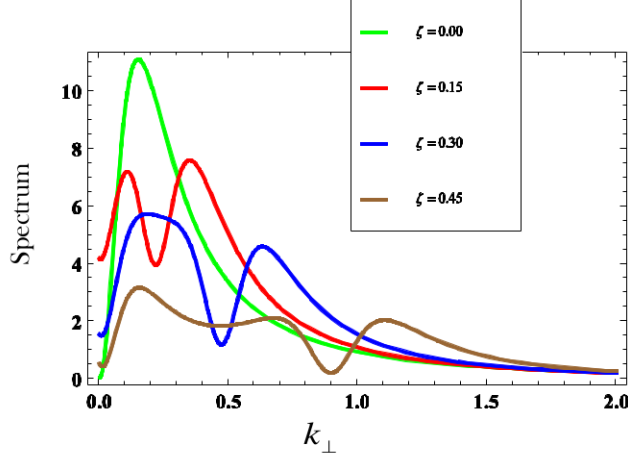


Figure 2: Emission spectrum versus k_{\perp} of gluon for varied non-eikonicity, ζ , for a 10 GeV Charm jet.

$$\Delta E_{rad} = \int d^2 k_{\perp} d\eta_g \frac{dn_g}{d^2 k_{\perp} d\eta} \omega \theta_1(\tau_m - \tau_F) \theta_2(E - k_{\perp} \cosh \eta) \quad (2)$$

where ω is the energy of the emitted gluon, the first θ -function constrains the phase space as a result of a radiative suppression due to interference of scattering amplitudes (the LPM effect) and the second θ -function is due to the fact that the energy of emitted gluon cannot be greater than that of its parent.

In the soft limit, the terms proportional to k_{\perp} approaches zero, but due to the presence of k_{\perp}^{-2} inside Gunion-Bertsch distribution formula, the terms inside $\mathcal{D}^{(1)}$ are $\mathcal{O}(k_{\perp}^{-2})$, $\mathcal{O}(k_{\perp}^{-1})$ and $\mathcal{O}(k_{\perp}^0)$ respectively. Hence the formula in Eq.1 is more general (compared to Refs.[15, 16]) correction to the Gunion-Bertsch formula within $\mathcal{O}(t^3/s^3)$.

Gluon radiation off heavy flavor jets

Effects of recoil due to scattering of heavy-flavours with the medium particles has been investigated in the thesis. Dokshitzer and Kharzeev in Ref. [17] find out the radiation distribution off heavy flavour (charm, bottom etc.) and show the presence of a radiation-free conical zone, the ‘dead-cone’, along and around the direction of propagation of the heavy quark. But that study considered all the three kinematic approximations *viz.* the *soft-eikonal-collinear* approximations.

The collinearity approximation has been removed in [10]. The present study [11] removes the eikonal approximation during scattering with the bath particles. Emission spectrum with respect to gluon emission angle is plotted in Fig.2 for varying non-eikonal $\zeta = q_{\perp}/\sqrt{s}$, where q_{\perp} is the transverse momentum transfer by the heavy quark and \sqrt{s} is the energy in the COM frame. Calculations in Refs.[10, 11] have shown a reduction of the respective modified distribution formulae to the Dokshitzer and Kharzeev formula for radiation distribution in proper limits.

Radiation distribution off a nearly on-shell parton

So far we have computed the Feynman amplitudes from pQCD to get the radiation distributions off energetic partons. But the calculations are all done for on-shell partons which obey Einstein’s energy-momentum relation. But the energetic partons, energy losses of which inside QGP medium is under discussion, may refrain from being on-shell even after QGP is formed [18] because it gains high virtuality from the momentum transfer owing to the heavy-ion collision. So is there any way to take into account this virtuality and calculate the radiation distribution? There is, if the virtuality of the particle is assumed to be sufficiently low so that the equation of motion for the field associated with the particle (the Dirac’s equation) is approximately valid. The radiation distribution off a slightly off-shell particle has been calculated in Ref.[19] and the calculation of energy loss using this distribution function (Fig.3) shows that slightly virtual

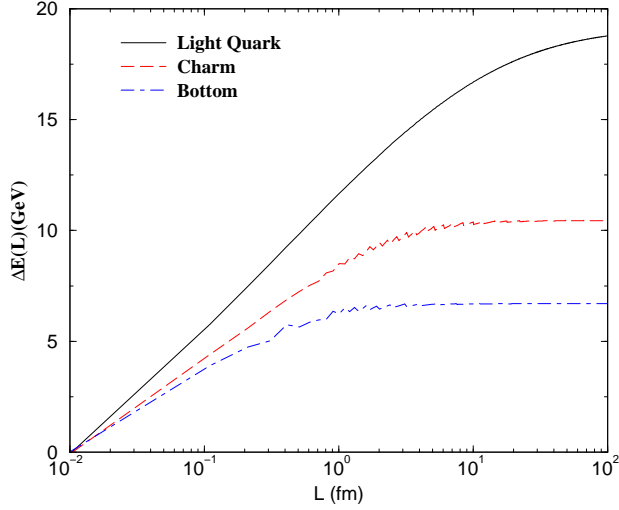


Figure 3: Variation of radiative energy loss off a nearly on-shell particle with length. The energy of the particle is taken to be 20 GeV.

partons, heavy or light, show similar radiative loss. Only after traversing a sufficient length, the energy losses between heavy and light partons become differentiable (see also [18]).

Summary and Outlook

In the present thesis, the radiative amplitudes for processes like gluon-gluon→gluon-gluon-gluon or quark-quark→quark-quark-gluon, where ‘quark’ stands for both heavy and light quarks, have been calculated from the methods of perturbative Quantum Chromodynamics. In the limit where the emitted radiation is of much less energy compared to that of the parent parton emitting the radiation, the radiative amplitude for two particles going to three particles can be written as that due to two particles going to two particles times the radiation distribution. The eikonal approximation (due to scattering) lingering inside the radiation distribution formula has been examined. An endeavour of removing the soft approximation may come afterwards.

Once the jet interacts with the medium, however, the possibility of multiple scattering can hardly be ruled out. The present thesis calculates the radiation distribution for single emission kernel in single scattering processes, $dn_g^{(1)}/(d^2\vec{k}_\perp d\eta_g)$. The multiple scattering has been introduced as a factor being multiplied with the single emission distribution.

So, given the fact that different approximations used in different energy loss models has been tried to be removed in single emission kernel scenario, the rigorous treatment of multiple scattering still awaits.

Bibliography

- [1] N. Itoh, Prog. Theor. Phys., 44, 291-292 (1970)
- [2] D. J. Gross and F. Wilczek, Phys. Rev. Lett **30**, 1343 (1973).
- [3] D. J. Gross and Frank Wilczek, Phys. Rev. D **8** , 3633 (1973).
- [4] H. D. Politzer, Phys. Rev. Lett **30**, 1346 (1973).
- [5] J. C. Collins and M. J. Perry, Phys. Rev. Lett **34**, 1353 (1975).
- [6] N. Cabibbo and G. Parisi, Phys. Lett. B **59**, 67 (1975).
- [7] K. Rajagopal and F. Wilczek, The frontier of particle physics **3** , 2061(2000)
- [8] J.D. Jackson, *Classical Electrodynamics*, Third edition,(John Wiley and Sons Pvt. Ltd. , New York 1998). Sections 11.10 and 15.4
- [9] F. Niedermayer, Phys. Rev. D **34**, 3494(1986)
- [10] R. Abir, C. Greiner, M. Martinez, M. G. Mustafa and J. Uphoff, Phys. Rev. D **85**, 054012(2012).
- [11] T. Bhattacharyya, S. Mazumder and R. Abir, e-print: arXiv: 1307.6931
- [12] J. F. Gunion and G. Bertsch, Phys. Rev. D **25**, 746(1982).
- [13] F. A. Berendes *et al.*, Phys. Lett. B **103**, 124(1981).

- [14] T. Bhattacharyya, S. Mazumder, J. Alam and S. K. Das, Phys. Rev. D **85**, 034033(2012).
- [15] S. K. Das and J. Alam, Phys. Rev. D **82**, 051502(R), (2010).
- [16] R. Abir, C. Greiner, M. Martinez, and M. G. Mustafa, Phys. Rev. D **83**, 011501 (R) (2011)
- [17] Y. L. Dokshitzer and D. E. Kharzeev, Phys. Lett. B **519**, 199(2001).
- [18] B. Z. Kopeliovich, I. K. Potashnikova, I. Schmidt, Phys. Rev. C **82**, 037901(2010).
- [19] T. Bhattacharyya and J. Alam, Int. J. of Mod. Phys. A **28**, 1350031(2013).

Contents

Synopsis	iii
List of Figures	xix
1 Introduction	1
1.1 From <i>Kanad</i> to <i>Quark-Gluon Plasma</i>	1
1.2 Creating Quark-Gluon Plasma: Critical values of Density and Temperature; and the evolution	5
1.3 Ways to know there is a medium	6
1.4 Discussion about Question 5, Section 1.1	8
1.5 Our aims and expectations	9
2 Radiation: ‘What’s and ‘How’s	13
2.1 Radiation: What do we mean?	14
2.2 Radiation: What do we mean and How ?	15
2.3 Calculating radiation loss: Count or Find Poynting’s Vector	17

3	Radiation Spectrum and energy loss due to scattering: A general perspective	22
3.1	Potential picture of single scattering	22
3.1.1	Advantage of being ‘soft’	23
3.1.2	Softness ‘burns’?	25
3.1.3	Potential picture of single scattering in a different gauge	27
3.2	Potential picture of multiple scattering: The energy loss model	28
3.2.1	Multiple scattering in potential model: the radiation distribution	29
3.2.2	Energy loss models: general considerations and approximations	31
3.2.3	Energy loss from the radiative distribution	33
3.3	‘Our aims and expectations’ revisited	34
4	Gluon Radiation off gluons	39
4.1	The radiation spectrum off a gluon in gluonic plasma	41
4.2	Reaction rate of $gg \rightarrow ggg$	44
4.3	Energy loss by energetic gluons	46
5	Scattering of heavy-quarks	50
5.1	The radiation intensity spectrum off a heavy particle: Classical approach	50
5.2	Elastic and radiative scattering cross-sections of a heavy quark : Perturbative QCD	53
5.2.1	Mass lifts collinear divergence in radiation spectrum	54

5.2.2	Divergence due to soft gluon exchange	54
5.3	Radiation distribution off heavy quarks recoiling due to scattering	57
5.3.1	Radiative matrix elements	61
5.3.2	Behaviour of non-eikonal heavy quark spectrum at different kinematic regions:	65
5.3.3	The non-eikonal radiation spectrum off Heavy Quarks	70
6	Gluon Radiation off slightly virtual quarks	75
6.1	Radiation spectrum off a slightly virtual quark	75
6.2	The radiation distribution off a virtual particle	81
6.3	The Energy loss by a virtual particle	83
7	Summary and Outlook	86
	Appendix A:	90
	Appendix B:	97

List of Figures

1	Temperature variation of radiative energy losses of 10 GeV gluon, obtained from Refs. [14, 15, 16] scaled by that obtained from Ref. [12]	vii
2	Emission spectrum versus k_{\perp} of gluon for varied non-eikonicity, ζ , for a 10 GeV Charm jet.	viii
3	Variation of radiative energy loss off a nearly on-shell particle with length. The energy of the particle is taken to be 20 GeV.	x
1.1	QCD Phase diagram [10].	4
1.2	Light-cone diagram of the longitudinal evolution [15].	6
2.1	Formation length	14
2.2	Explanation of radiation in terms of field lines. (adapted from [5])	16
2.3	Transverse and radial fields. (adapted from [5])	16
2.4	Particle of charge q moves with constant velocity v and passes P at a distance b	18
2.5	Variation of E_y with vt	19

3.1	Feynman diagrams of photon radiation off a charged particle scattered by a static source with interaction V	24
3.2	(a) Collisional and (b) radiative energy loss of high energy particles.	32
4.1	Variation of parton distribution function with x [10].	41
4.2	Temperature variation of the ratio of the equilibration rate obtained in Ref. [12] (solid line), Ref. [7] (dashed line), and [8] (dot-dashed) normalized by the corresponding value putting GB distribution for the process $gg \rightarrow ggg$	45
4.3	Temperature variation of the energy loss of 10 GeV gluon, obtained from Refs. [12] (solid line), [7](dashed), [8](dot-dashed) and scaled by that obtained from Ref. [14]. The ratio is denoted by ΔE_R ,	46
5.1	Polar plot of the power spectrum off a relativistic, heavy particle.	51
5.2	Tree level Feynman diagrams for Qg elastic scattering.	56
5.3	Tree level Feynman diagrams for $Qq \rightarrow Qqg$ scattering. The double line denotes the heavy quark.	58
5.4	Deviation from straight eikonal trajectory. Angle between incoming and outgoing momentum of heavy quark is θ_q and direction of emission of gluon with that of incoming momentum of heavy quark is θ_g	65
5.5	Variation of gluon spectrum off 10 GeV heavy quark with gluon transverse momentum with different extents of recoil of heavy quarks.	70
5.6	Polar plot of $\mathcal{W}(\theta, \omega)$ (at a typical ω) with $\zeta(= q_{\perp}/\sqrt{s}) = 0$ for a 10 GeV Charm jet.	72

5.7	Polar plot of $\mathcal{W}(\theta, \omega)$ (at a typical ω) with $\zeta(= q_{\perp}/\sqrt{s}) = 0.15$ for a 10 GeV Charm jet.	72
5.8	Polar plot of $\mathcal{W}(\theta, \omega)$ (at a typical ω) with $\zeta(= q_{\perp}/\sqrt{s}) = 0.30$ for a 10 GeV Charm jet.	72
5.9	Polar plot of $\mathcal{W}(\theta, \omega)$ (at a typical ω) with $\zeta(= q_{\perp}/\sqrt{s}) = 0.45$ for a 10 GeV Charm jet.	72
6.1	Tree-level Feynman diagram for gluon radiation by (a) quark and (b) anti-quark.	76
6.2	The variation of $F_{RH\theta}(E, \theta)$ with θ for $E = 1.5$ GeV.	82
6.3	The variation of F_{RHE} with E for $\theta = \pi/4$	82
6.4	The variation of $F_{RL\theta}(E, \theta)$ with θ for $E = 3$ GeV.	83
6.5	The variation of F_{RLE} with E for $\theta = \pi/4$	83
6.6	Variation of vacuum energy loss of a virtual particle with length.	84

Chapter 1

Introduction

1.1 From *Kanad* to *Quark-Gluon Plasma*

Two thousand years before, one day, Indian philosopher Kanad was walking with food in his hand. As he nibbled at the food throwing away some small pieces, it occurred to him, suddenly, that he could divide the food up to a certain extent only. Further division was not possible. This indivisible matter was called *anu* [1] by him. This story [2] how Kanad embarked upon the thought of a matter which cannot be divided any further may be fictitious; but is instructive. It shows the beginning of an incessant endeavor of humankind to find the building blocks of matter we are surrounded by or are constituted of. As a matter of fact, it won't be an exaggeration to state that one of the underlying philosophies of the modern Physics is to build more and more developed 'microscopes' which will be able to 'peek' inside the matter. Great men like Dalton, Einstein, Rutherford are the successors of Kanad who eventually have either talked of or have proven the existence of atoms, and in an even smaller scale, nuclei. Comes later the accelerators which tear apart the nuclei, too. Partons, the imaginative name coined by Richard P. Feynman, stands for quarks and gluons which make nuclei. We have now a zoo of fundamental particles, characterized by quarks, leptons, neutrinos and the gauge bosons.

Now, life would have been mundane without the talking terms among the particles. There are interactions like Gravity, Weak Interaction, Strong Interaction and Electromagnetism which strive hard to make things interesting. There are objects like vapour, water or ice which, apparently are different as far as their appearances are concerned. But we know that it all depends on the interplay of the potential energy and the kinetic energy of an individual atom. For solids, the kinetic energy is way behind the potential energy. For liquids, the situation is more liberal but unlike gas where the particles are violent and constantly jostle with others. The average kinetic energy per particle of a system is termed as the temperature (T) and when we can define such a temperature, the medium is told to have been thermalized¹ .

So far so good and we have come up to quarks, gluons (the gauge bosons of strong interaction) and we have mentioned about the nature of interactions among the particles. Let us imagine an overall charge neutral soup of quarks and gluons where the average kinetic energy per particle leaves the potential energy way behind. Such a soup of particles will be called Plasma². A plasma of quarks and gluons will be called Quark Gluon Plasma (QGP). As evident from the title we are going to study the energy loss of energetic particles inside QGP thereby trying to make out the nature of the medium formed. Now let us pose a string of questions:

- Q1: Why should we study QGP ?

Ans 1: 10^{-6} second after the big bang, the universe existed in the state of Quark Gluon Plasma. So by studying QGP we wish to access the micro-second old early universe.

- Q2: Can we create it now ?

Ans 2: Yes. That is one of the goals of Relativistic Heavy Ion Collision in LHC and RHIC. There two nuclei are collided with large energies (2.7 TeV/nucleon in LHC or 200

¹We can define something called *kinetic temperature* also if we don't assume thermalization. But in our context, temperature will imply thermalization.

²see [3] for the criteria satisfying which a medium will be called plasma

GeV/nucleon in RHIC) the resulting quarks and gluons interact and eventually evolve to QGP.

- Q3: Why so complicated ? We can take quarks, gluons and make merry !

Ans 3: That is difficult. Quarks and gluons are not freely available. The further they are, the stronger they bind. But that is an issue of ‘asymptotic freedom’ which also tells that they interact weakly when they are close together.

- Q4: How to make them close together ?

Ans 4: Let us imagine lots of bags of quarks, *i.e.* say nucleons in a box. We increase the number of nucleons per unit volume by compressing the box until the nucleons overlap. Then there will be a region in space where the quarks are unable to identify themselves as belonging to the nucleon which was bouncing around the corner or the one dancing at the centre of the box. Since they interact weakly when they are close, they form a Quark Gluon Plasma.

This is the way N. Itoh [4] thought of a quark matter. Just after the discovery of asymptotic freedom [5, 6, 7], Collins and Perry [8] also suggested that at very high density the degrees of freedom of the strongly interacting matters are not hadrons but quarks and gluons. In other words, when the vacuum is excited to high temperatures ([9]) new hadrons are produced and we observe overlap of them at a certain temperature. Such a phase of matter is called Quark Gluon Plasma (QGP). It is interesting to note that we are dealing with the hadronic as well as the partonic degrees of freedom and there is a relativistic system in which creation and annihilation of particles take place. So we are going to need Quantum Chromodynamics (QCD), the theory of strong interaction which is extremely successful in vacuum, to be applied in a thermal (also dense, if necessary) medium. Like the phase diagram of water, we can think of a ‘phase diagram’ of Quantum Chromodynamics where the ‘phases’ we are talking about

right now are the hadronic and the QGP phase (see Fig. 1.1). Depending on the temperature (T) and net-baryon density (n_B) different other phases of QCD exist.

The most important property of QCD is the ‘asymptotic freedom’ which tells how the QCD coupling evolves when we change the length scale between the interacting particles. The coupling is small at small distances (equivalently at large momentum transfer) and large at large distances (equivalently small momentum transfer). The general treatment of the ‘flow’ of the coupling is treated by the Renormalization Group (RG) Equation. The RG equation is a differential equation which dictates the evolution of the coupling with length scale. The differential change in the coupling is given by the ‘ β -function’ and unlike Quantum Electrodynamics (QED), the QCD β -function is negative [11], a fact which is responsible for the asymptotic freedom which, in turn, is the *raison d’être* of Quark Gluon Plasma. Obviously, the medium sets another scale, temperature of bath, in the consideration; and hence the strong coupling now runs with temperature, too.

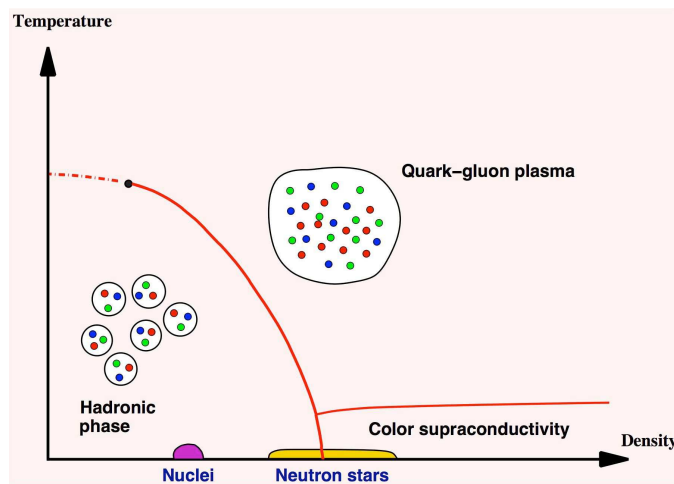


Figure 1.1: QCD Phase diagram [10].

- Q5: So, by making QGP in Relativistic HIC can we really study early universe ? Is there no difference ?

Ans 5: We will be addressing this question and some related aspects at length in Sec.1.4.

1.2 Creating Quark-Gluon Plasma: Critical values of Density and Temperature; and the evolution

Once we have motivated the creation of a state of matter called QGP, we may ask, what may be the external parameters which will help creating this state. There are certain recipes:

- As we have already pointed out, we can go on compressing the box containing nucleons until they overlap. The critical density needed for the creation of QGP is $\rho_c \sim (3 - 4) \times \rho_{NM}$, where ρ_{NM} is normal nuclear matter density ($\sim 0.16 \text{ fm}^{-3}$).
- An alternative way of making nucleons overlap is to thermally generate the nucleons by exciting the QCD vacuum. An interesting study which tells us at what temperature nucleons overlap may be made by seeing the variation of the inter-nucleon distance with temperature. If $n(T)$ is the number density of nucleons at temperature T , the average inter-particle distance r_{av} (at temperature T) is given by $\sim n^{-1/3}$. As $n \sim T^3$, $r_{av} \sim T^{-1}$. The temperature at which the inter-particle distance³ becomes less than the nucleon diameter, the QGP is said to have formed.

As, for relativistic systems, the energy density is proportional to the fourth power of temperature, the energy density for creation of QGP can also be estimated ($\sim 1 \text{ GeV}/\text{fm}^3$) knowing the temperature for hadron to quark phase transition⁴. This high energy density or temperature (100 MeV temperature is equivalent to 10^{12} Kelvin, 10^6 times hotter than the centre of sun !) can be attained by relativistic collision of two heavy nuclei (like lead or gold).

³Actually the average separation can be shown to be $0.55396 n^{-1/3}$ assuming random distribution of particles [12]

⁴it is doubted whether this phase transition, temperature of which is $\sim 170 \text{ MeV}$, is a phase transition in proper sense [13]. Transformation of hadrons to QGP is, rather, identified as a cross-over, *i.e.* just like ionization.

However, the state just after the quarks and gluons are liberated is the out of equilibrium state as the liberated particles are to interact in order to get thermalized⁵. So, this pre-equilibrium state evolves to a (locally) equilibrated QGP phase within ~ 1 fm and freezes-out to hadrons within ~ 10 fm (in Pb-Pb collision in RHIC, for example). The space-time diagram of the evolution of the liberated matter can be summarized in the Fig. 1.2.

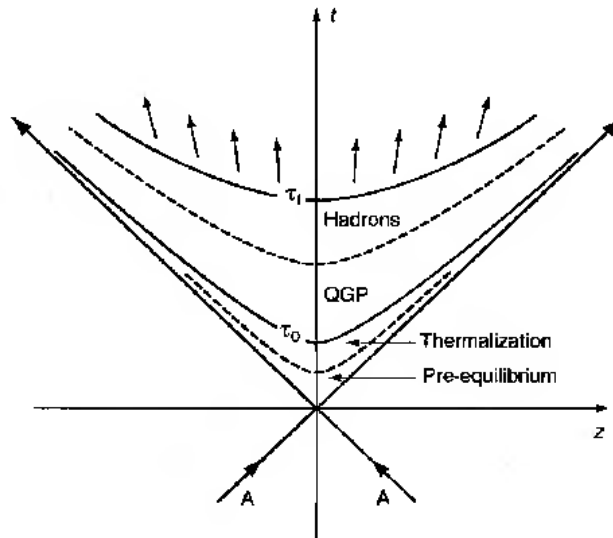


Figure 1.2: Light-cone diagram of the longitudinal evolution [15].

1.3 Ways to know there is a medium

In heavy ion-collision, once we have the recipes to create QGP, how do we know that it has been created after following those ? There are, in fact, different indirect proofs which will be able to detect and characterize the formed QGP medium. The most important probe as far as the relevance of the present thesis is concerned, is the high-energy particles produced very early just after the collision between two heavy-ions with energies hundreds of GeVs per nucleon. This is worth mentioning at this point that the life time of QGP is roughly ~ 10 fm and hence we cannot

⁵how the particles thermalize is addressed by the classical field theory techniques [14]

employ an external probe for investigation. So we rely on the internal probe like collimated beam of high-energy particles generated just after the collision of two nuclei (crashing which we intend to liberate the quarks and gluons). Moreover we know that one whose de Broglie wavelength is much greater compared to the matter intended for investigation can barely act as a probe. Hence we must compare the characteristic wavelength of those high-energy particles with that of the QGP medium. Now, we have the scale $\Lambda_{QCD} \sim 200$ MeV which corresponds to a length scale of 1 fm — the length scale corresponding to the QGP medium. So particles with energies much higher than 200 MeV will act as good probes. Energy loss of high-energy particles inside QGP hence can act as a good proof that there exists a medium created due to collisions of two heavy nuclei. Now, jet quenching is only a proof that there is a medium. The energy loss of a quark (heavy or light) can be due to electromagnetic interaction, too. So the corresponding inference is: we cannot tell unambiguously that energy loss of a quark jet is the proof for the existence of a colored medium. But the energy loss of gluon jet tells this without doubt.

Quarkonium (bound states of heavy quark and anti-quark) is a probe which, if it melts, is the proof that it is residing in a color ambience because Quarkonia melting is due to the color screening effect of the colored medium produced. J/ψ , a bound state of charm (c) and anti-charm (\bar{c}) quarks, for example, melts due to color charge screening present in a color medium. In this case also, the radius of J/ψ is 0.25 fm, much smaller than the QGP length scale. Had it not been so, melting of J/ψ would not be possible and it would not act as probe. This instance re-emphasizes the importance of the length scale in choosing a probe to QGP.

Photons and dileptons serve as the cleanest probes of QGP as they decouple immediately from the space-time point at which they are formed. So there is no distortion in their energy-momentum. Electromagnetic probes are emitted from the whole volume of QGP. The only problem with this probe is the large background due to hadrons decaying to photons (the

Dalitz decay, for example). Several experimental processes have been devised to subtract the background photons.

1.4 Discussion about Question 5, Section 1.1

Once we are done with the discussion on how to create QGP in HIC and what the possible signals are, we may ask, naturally, how this QGP is similar to the early universe QGP; or, is the evolution of the QGP fireball similar to that created after the big bang? This question is already put forward in a previous section and the answer was promised. The QGPs produced at the two cases, albeit being plasmas of quarks and gluons, are different as far as their nature of evolutions are concerned. While the early universe evolves quasi-statically, *i.e.*, at every instant the plasma temperature deviates infinitesimally from the equilibrium, the QGP produced in heavy-ion collision is not like that.

In case of an evolving fireball, this quasi-static evolution is guaranteed if the expansion rate (R_{exp}) of QGP is comparable with the interaction rate (R_{int}). In other words, we can say, if R_{exp} is not so high so that it refrains the particles from interacting, we may safely use the quasi-static approximation. Since interaction gives birth to momentum exchange, the medium can maintain the thermal equilibrium during arbitrarily small scale of time slices. This assumption is called the *local thermal equilibrium*.

So far, we constrained ourselves within the evolution of medium created. But how do the quantum mechanical states evolve inside an evolving plasma? We can take the example of an open heavy quark or heavy quark-antiquark (quarkonia) bound states evolving inside QGP. This question will be of importance while one intends to study the evolution of probe particles inside plasma and relates the modification of the distribution of probes with some experimental observable. We may here find out two characteristic time-scales involved in this problem: the internal time scale, T_{int} , and the time scale over which the thermodynamic parameters of the

plasma change appreciably, T_p . If $T_p \gg T_{\text{int}}$, the ‘smoothness’ in motion is guaranteed. The gradual change in external conditions defines an adiabatic process. From quantum mechanics point of view also, this means, if a system is in i th eigenstate of a (time-evolving) Hamiltonian $\mathcal{H}(t_1)$ at time t_1 , then the system remains to be the i th eigenstate of the Hamiltonian $\mathcal{H}(t_2)$. This consideration is the essential content about the *adiabatic approximation* [16] in quantum mechanics.

For all practical purposes, the medium is assumed to be evolving quasi-statically. Whereas the QCD phase transition in early universe QGP takes place over micro-seconds, HIC QGP is a much more violently expanding system than the early universe QGP having the QCD phase transition time-duration roughly ~ 10 fm. So the assumption of quasi-static evolution of HIC QGP is questionable. Also, there are very recent proofs from the basic Quantum Mechanical conditions [10] that the adiabatic evolution of heavy-quarkonia in QGP is not a valid approximation. So, a dynamic theory without the assumption of quasi-static evolution is necessary at this moment.

1.5 Our aims and expectations

The present dissertation takes up high-energy particles as investigators of the colored plasma. More specifically, the energy loss of the energetic particles will be studied. Once we declare in the title of the thesis that we have studied the energy loss phenomenon of high energy particles inside the QGP medium to see what changes do the particles undergo, we must think about the interaction of the high energy particles with the medium particles. There may be two types of interactions, the collisional (elastic) and the radiative. The radiation loss dominates when the energy is high (*i.e.* momentum > 2 GeV roughly). The present thesis is about the radiative energy loss of high energy particles with the medium. To be more precise, we have counted the number of gluons radiated from the highly energetic partons.

This counting is termed as the distribution of the radiation, which is calculated from the perturbative Quantum Chromodynamics (pQCD). We focus on the kinematic approximation like the eikonal approximation lingering inside the radiation distribution at the level of single scattering processes and we find out the non-eikonal corrections to the widely used Gunion-Bertsch formula (chapter 4). Also the non-eikonal radiation distribution off heavy-quarks have been calculated (chapter 5). The radiation distribution off highly virtual quarks has been calculated in chapter 6. Multiplying the radiation distribution with the energy per quantum of radiation we get the radiative energy loss in a single scattering.

This concludes the discussion on what QGP is and what are the physical considerations we must have while creating and/or studying QGP. We have briefly discussed what we aim to achieve or calculate during the course of our discussion. The next two chapters (chapters 2 and 3) will be devoted to clarify, in a greater detail, our objective and the motivations behind the present study. We will return to the same discussion again in chapter 3 and we hope that during this journey we will be in a better niche to appreciate the goals and the techniques used to achieve them.

Bibliography

- [1] Space, Time and Anu in Vaisheshika, R. Narayan,
<http://citeseerx.ist.psu.edu/viewdoc/summary?doi=10.1.1.69.7655>
- [2] <http://en.wikipedia.org/wiki/Kanad>
- [3] Introduction to Plasma Physics R. Fitzpatrick, course homepage:
<http://farside.ph.utexas.edu/teaching/plasma/plasma.html>
- [4] N. Itoh, Prog. Theor. Phys., 44, 291-292 (1970)
- [5] D. J. Gross and F. Wilczek, Phys. Rev. Lett **30**, 1343 (1973).
- [6] D. J. Gross and Frank Wilczek, Phys. Rev. D **8** , 3633 (1973).
- [7] H. D. Politzer, Phys. Rev. Lett **30**, 1346 (1973).
- [8] J. C. Collins and M. J. Perry, Phys. Rev. Lett **34**, 1353 (1975).
- [9] N. Cabibbo and G. Parisi, Phys. Lett. B **59**, 67 (1975).
- [10] *Heavy Quarkonia in Quark Gluon Plasma as Open Quantum Systems*, Ph. D. Thesis by Nirupam Dutta, University of Bielefeld.
- [11] M. E. Peskin and D. V. Schroeder, *An Introduction to Quantum Field Theory*, (Levant Books, Kolkata, India 2005)

- [12] S. Chandrasekhar, Stochastic Problems in Physics and Astronomy, Rev. Mod. Phys **15**, 1 (1943)
- [13] T. D. Lee and C. N. Yang, Phys. Rev. **87**, 404 (1952)
- [14] F. Gelis, hep-ph/arXiv:1211.3327
- [15] *QUARK GLUON PLASMA From Big Bang to Little Bang*, K. Yagi, T. Hatsuda and Y. Miake, (Cambridge University Press, Cambridge CB2 2RU, UK, 2005)
- [16] *Introduction to Quantum Mechanics*, David J. Griffiths, (Pearson Prentice Hall, Upper Saddle River, NJ 07458)

Chapter 2

Radiation: ‘What’s and ‘How’s

In the previous chapter we gave a general introduction on the physical considerations we must have before studying the QGP Physics. Once the QGP fluid is created, we will try to know the properties of it; and we have discussed that we need internal probes for looking into such a short lived (life-time ~ 10 fm) medium. The internal probes being used in the present discussion are the high energy particles produced very early, just after the collision takes place. They lose energy inside the medium and for a very high energy particle the radiative energy loss dominates. Radiative energy loss of high energy internal probes being the subject matter of the present dissertation, in this chapter we will emphasize on the physical considerations which ensure the radiation. Later, the phenomenon of radiation will be discussed from a very general perspective, mostly adapted from the Classical Electrodynamics¹ textbooks, to understand the basic assumptions and analogies one use in calculating the radiation loss.

¹Why do we expect that this adaptation from electrodynamics will work in chromodynamics? We will discuss it in the long run.

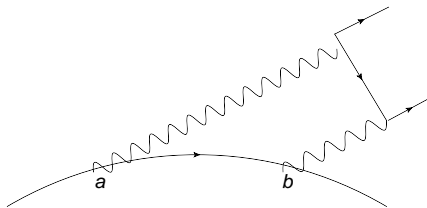


Figure 2.1: Formation length

2.1 Radiation: What do we mean?

When can we tell that radiation is given off by a particle? First of all, radiation means photons/gluons oozed out from a parent parton. That means, the emitted particle is ‘well separated’ from its parent particle. As long as the radiation is in coherence with the parent particle, it is not radiated. The time needed for the radiation to be well-separated (by, say, one Compton length) from its parent parton is called the *formation time*. Similarly, for pair-production the required distance of separation between the pairs is two Compton wavelength for the pair to be ‘seen’ as a collection of two distinct particles. Quantitative estimate [1] of the formation time, l_0 shows (in natural unit) that

$$l_0 = \frac{2E(E - k)}{m^2k} \quad (2.1)$$

where E and k are the energies of the radiating and the radiated particle respectively and m is the mass of the emitting particle. Formation length actually comes due to uncertainty in momentum transfer [2] which blurs the information at which point of the trajectory of the radiating particle the radiation has taken place. Hence, formation length is also an extended region in space anywhere within which the radiation might have taken place. Apparently, there are different ways one can explain the formation length as far as different physical contexts are concerned [1].

The concept of formation length plays a very important role in case of determining the radiation distribution off a particle undergoing multiple scattering inside a medium. Fig. 2.1 may help

understand the effect it may have on the spectrum. Formation length is the maximum distance within which two radiations, if emitted, will not be resolved by the detector. So, according to Fig. 2.1, ab is the formation length. Now, emissions are results of scattering events (as free particles cannot radiate). As a result, the above scenario translates into the fact that, two scatterings, if take place within the formation time, can reduce the counting of number of radiation quanta emitted. This phenomenon of suppression is, clearly, an interplay of two time-scales (or equivalently, lengths), the formation time (τ_f) and the mean free time (τ_m) and is the famous Landau-Pomeranchuk-Migdal suppression[3].

2.2 Radiation: What do we mean and How ?

Radiation means dissipation of power even at infinite distance. It is calculated by integrating the *Poynting's vector* $\vec{\mathcal{S}}$ over a large surface. We know,

$$\vec{\mathcal{S}} \sim \vec{E} \times \vec{B} \quad (2.2)$$

where $\vec{E}(\vec{B})$ is the electric (magnetic) field. The power radiated (over area a) is given by:

$$\mathcal{P}(r) = \oint \vec{\mathcal{S}} \cdot d\vec{a} \quad (2.3)$$

If $\lim_{r \rightarrow \infty} \mathcal{P}(r) \neq 0$, then we get radiation. This is the way we calculate the radiated power of an electric dipole or a point charge [4].

But we can examine the idea of radiation in a more intuitive picture with the help of Ref. [5]. We assume a particle travelling right and bouncing off a wall at the point 'e' (see Fig. 2.2). Its present position is 'g'; and 'f' would be its position at present had there been no wall. Since, the message that the particle has bounced off travels with a finite speed c (the velocity of light in

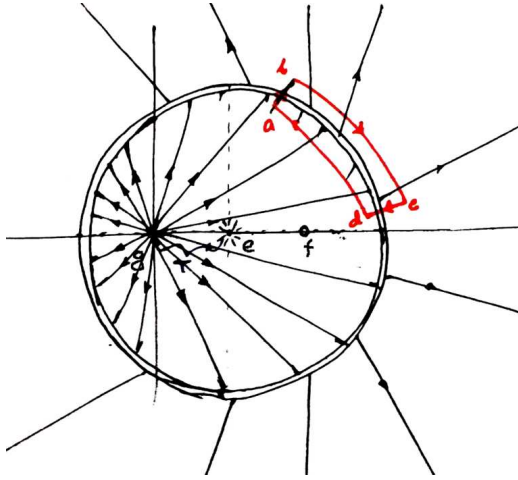


Figure 2.2: Explanation of radiation in terms of field lines. (adapted from [5])

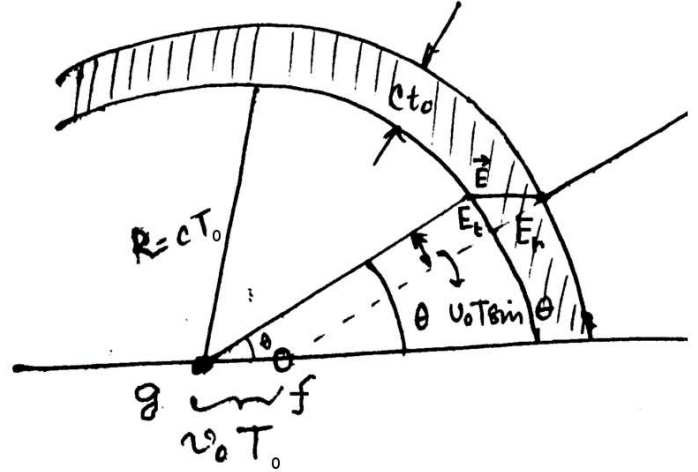


Figure 2.3: Transverse and radial fields. (adapted from [5])

vacuum), the lines of force within a circle of radius ct_0 , where T_0 is the time difference between the points e and g , will reorient themselves according to the new position of the particle (Fig. 2.2). The field lines outside radius ct_0 will point towards the ‘would-have-been’ present position of the particle. Now, if we consider the surface encompassed by the lines $abcd$, we see that there is an imbalance in the density² of lines of forces (LOFs) penetrating the surface ad and surface bc . The density ratio corresponding to the surfaces is 2:3. According to the Gauss’s law, which tells that the net number of lines of forces penetrating a surface must be zero, we must have transverse field entering across ad or bc . Now, if the acceleration (bounce) of the particle occurs for a time $t_0 \ll T_0$, we have a ring of width ct_0 (see Fig. 2.3) which connects the field lines oriented according to the present position of the particle and those oriented according to the position ‘f’ of the particle .

Now, we want to find out the field inside the ring (the shaded region in Fig. 2.3). The field has two components, the transverse component, E_t and the radial component E_r . From Fig. 2.3,

²As there are infinite number of LOFs passing through any surface, we can talk of density and not the numbers of them.

$$\frac{E_t}{E_r} = \frac{v_0 T_0 \sin\theta}{ct_o} = \frac{f' T_0 \sin\theta}{c} \quad (2.4)$$

where $f' = v_0/t_0$ is the acceleration. We can find out the radial field from the Gauss's law considering a Gaussian pillbox across the inner radius of the ring . Since the sides of the pillbox are of vanishing width, the radial component of field is almost same on the each side of the shell's inner surface. If we remember $E_r \sim 1/R^2$, the transverse field is given by,

$$E_t \propto \frac{f' \sin\theta}{R} \quad (2.5)$$

and since $E_t \sim 1/R$ (hence electric energy density $\sim 1/R^2$), the integral over infinitely large surface will give constant value of power dissipation. Hence the transverse field will be responsible for radiation. We notice from Eq. 2.5 that E_t is dependent on θ . It is maximum at $\theta = 90^\circ$ and minimum at $\theta = 0^\circ, 180^\circ$. Hence density of 'kinks' will be greater along the perpendicular direction of motion, and it decreases as θ approaches 0 or 180. Also, the transverse (or *radiation*) field depends on the magnitude of acceleration. Greater the acceleration (or deceleration, because the magnitude matters, anyway) greater the radiation.

2.3 Calculating radiation loss: Count or Find Poynting's Vector

So, we learn that an accelerated charge radiates. The radiated power is calculated by integrating the Poynting's vector over an infinitely large surface. But, in section 1.5 we demand that we have 'counted' the 'number' of emitted quanta given off by an accelerated charge. Are the two approaches equivalent ? In next few paragraphs we will endeavour to bridge the gap between

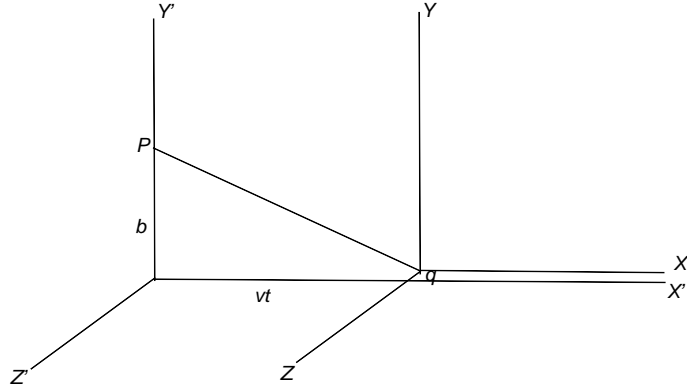


Figure 2.4: Particle of charge q moves with constant velocity v and passes P at a distance b

them. For that, we need to study fields of a uniformly moving charge and the fate of it when acceleration occurs.

The fields of a uniformly moving charge are given in [6]. Our aim is to extract some ideas which will help us understand how we can find radiation loss by ‘counting’ the number of emitted quanta. If a particle of charge q is moving along X-axis with velocity v and passes an observation point P on Y-axis with the closest distance of approach b (see Fig. 2.4), the fields in the observer’s frame (*i.e. laboratory frame*) are given by [6],

$$\begin{aligned}
 E_x &= -\frac{q\gamma vt}{(b^2 + \gamma^2 v^2 t^2)^{3/2}} \\
 E_y &= \frac{\gamma qb}{(b^2 + \gamma^2 v^2 t^2)^{3/2}} \\
 B_z &= vE_y
 \end{aligned} \tag{2.6}$$

where $\gamma = (1 - v^2)^{-1/2}$, vt is the X distance at which the charge is (as observed by P) after a time t . It will be interesting if we study the variation of the fields E_x and E_y with vt . We see

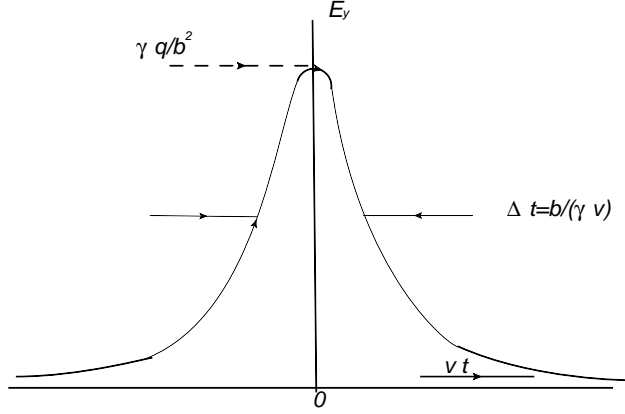


Figure 2.5: Variation of E_y with vt

$$E_y = \frac{\gamma q}{b^2} \frac{1}{\left(1 + \frac{\gamma^2 v^2 t^2}{b^2}\right)^{3/2}} \quad (2.7)$$

We observe that E_y is maximum at $vt = 0$ and decays along the $\pm vt$ axes. The maximum value of E_y is $E_{y,max} = \gamma q/b^2$ and the time duration within which the field assumes an appreciable value is (see Fig. 2.5).

$$\Delta t \sim b(\gamma v)^{-1} \quad (2.8)$$

Similarly, the longitudinal field rapidly varies from $+ve$ to $-ve$ values. So the observer observes a pulse of plane polarized radiation. This observation leads us to picturize that a rapidly moving charge, when Lorentz boosted, acquires virtual quanta (up to frequency $\omega_{max} \sim 1/\Delta t$ [7]), called Weizsäcker-Williams (WW) quanta [6]. A violent collision of particles results in acceleration imparted to the moving charges. While the fast Fourier components of the field (or equivalently, WW quanta), whose transverse momenta $k \geq a_0$, where a_0 is the inverse acceleration time, can manage to follow the charge, the softer part is 'left behind' [8]. The WW quanta which are now detached from the charge are regenerated along a new direction. So, there is radiation — the

radiation off accelerated charge particles in the form of real particles. So it makes no harm if we start counting the number of such quanta emitted (which can be done by the help of quantum field theory techniques) in stead of finding out the Poynting's vector and integrating it over a large surface. But, we must remember one thing, we use the word 'count' in a sense that we want to find out the number of quanta emitted within certain range of variables. It should better be called the *radiation distribution* which means, probability of finding a particle with certain values of some physical quantities (like momentum or the angle of emission) is always zero. So what we will 'count' is the number of particles emitted within a range of momentum and angle the emission makes with the parent parton.

Before the curtain down of this chapter, let us be familiar with the jargons which are popularly used in stead of the terms used in the discussion so far. Hence, the high-energy (*i.e* at an energy where the mass difference between heavy and light particles becomes irrelevant), collimated beam of internal probes along with the WW gluons (a jargon which we have already discussed) is called a *jet shower* (loosely *jet*). The probe particle around which hovers the WW cloud is called the leading particle³; and the energy loss phenomenon of jets is called *jet quenching*.

³with which the medium interacts. The WW gluons become noticeable only after they metamorphose as radiations.

Bibliography

- [1] S. Klein, *Rev. Mod. Phys.*, **71**, 1501(1999).
- [2] *Ultra-relativistic particles in matter*, Ph. D. Thesis, Ulrik I Uggerhøj (2011), Department of Physics and Astronomy, University of Aarhus, Denmark
- [3] L.D. Landau and I.Ya. Pomeranchuk, *Dokl. Akad. Nauk SSSR* 92 **535**, 735(1953); A.B. Migdal, *Phys. Rev.* **103**, 1811(1956).
- [4] *Introduction to Electrodynamics*, David J. Griffiths, Pearson Education Pte. Ltd. (2003)
- [5] <http://physics.weber.edu/schroeder/mrr/MRRtalk.html>
- [6] J.D. Jackson, *Classical Electrodynamics*, Third edition,(John Wiley and Sons Pvt. Ltd. , New York 1998). Sections 11.10 and 15.4
- [7] M. S. Zoloterov and K. S. McDonald, arxiv: physics/0003096
- [8] F. Niedermayer, *Phys. Rev. D* **34**, 3494(1986)

Chapter 3

Radiation Spectrum and energy loss due to scattering: A general perspective

3.1 Potential picture of single scattering

In the previous chapter we have established that finding out the radiation distribution off an energetic particle will enable us calculate the radiative dissipation. Since the degrees of freedom in the present case are the fundamental coloured objects like quarks and gluons, the dynamics will be dictated by the perturbative techniques for dynamics of colours—perturbative Quantum Chromodynamics (pQCD). The basic process we are going to study is the QCD gluon *bremstrahlung* (means ‘*breaking radiation*’). But the gluon *bremstrahlung* off coloured particles is not much different, under certain approximation, from the photon emission off (electrically) charged particles. We can see [1] that the approximated radiation four-current has nothing to do with the underlying process it has been formed through. The current depends,

in stead, on the four momenta. The four current has a classical nature and is derivable from the classical electrodynamics by considering the potential induced by charge of an electromagnetic current due to scattering. So, often we will be able to draw the analogies between the radiation spectrum obtained for particles moving with different kinematic constraints in electrodynamics with those in QCD. We will also notice that these kinematic constraints are going to play a major role in deciding the shape of the emission spectrum.

3.1.1 Advantage of being ‘soft’

We have mentioned that ‘under certain approximation’, the electrodynamic radiation current resembles colour radiation¹. That approximation is the ‘soft radiation approximation’. To see how this approximation really helps draw the analogy, let us consider the photon bremsstrahlung off a charged particle (mass m) induced by a static electromagnetic source. If we write down the quantum amplitudes for the two Feynman diagrams (see Fig. 3.1) representing the scattering, we see that in the soft approximation, *i.e.* when the energy of the emitted radiation ω is much less than that of the parent partons E , we can write the radiation amplitude in terms of a product of elastic part times the soft radiation current. Writing down the Feynman amplitudes from Fig. 3.1,

$$\begin{aligned}\mathcal{M}_{pre}^\mu &= e\bar{u}(k_3)V\frac{m+k'_\alpha-k}{m^2-(k_1-k)^2}\gamma^\mu u(k_1) \\ \mathcal{M}_{post}^\mu &= e\bar{u}(k_3)\gamma^\mu V\frac{m+k'_\beta+k}{m^2-(k_3+k)^2}u(k_1)\end{aligned}\tag{3.1}$$

¹Then why do we need to do ‘soft radiation QCD’ in stead of classical calculations ? We discuss it in Sec. 3.3

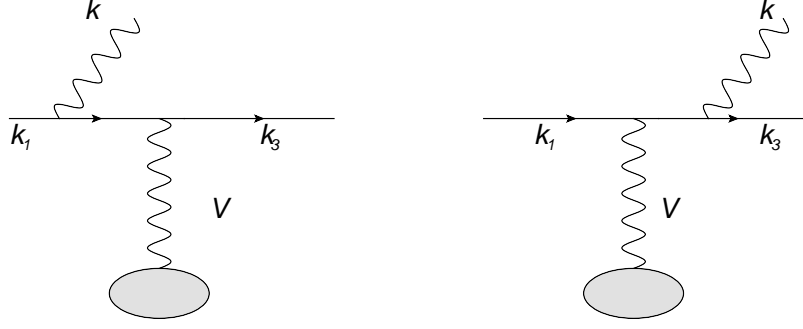


Figure 3.1: Feynman diagrams of photon radiation off a charged particle scattered by a static source with interaction V

where ‘pre’ and ‘post’ denote the pre-emission (*i.e.* emission from k_1) and post-emission (*i.e.* emission from k_3) respectively. Neglecting \not{k} with respect to $k_1^\not{\alpha}$, $k_3^\not{\beta}$ and putting $k_i^\not{\alpha}\gamma^\rho = -\gamma^\rho k_i^\not{\alpha} + 2k_i^\rho$ we get,

$$\begin{aligned} (m + k_1^\not{\alpha})\gamma^\alpha u(k_1) &= (\gamma^\alpha[m - k_1^\not{\alpha}] + 2k_1^\alpha)u(k_1) = 2k_1^\alpha u(k_1) \\ \bar{u}(k_3)\gamma^\beta(m + k_3^\not{\beta}) &= \bar{u}(k_3)([m - k_3^\not{\beta}]\gamma^\beta + 2k_3^\beta) = 2k_3^\beta \bar{u}(k_3) \end{aligned} \quad (3.2)$$

with the help of Dirac’s equation for fermions. Considering on-shell ($k^2 = 0$) gluon emission we obtain the total amplitude as:

$$\mathcal{M}_{rad} = e j^\mu \times \mathcal{M}_{el}, \text{ where } j^\mu = \frac{k_1^\mu}{k_1 \cdot k} - \frac{k_3^\mu}{k_3 \cdot k} \quad (3.3)$$

and e is the coupling. The radiation current j^μ is exactly that obtained from the classical calculations also. This clearly shows an universality in the radiation current which, upon squaring, yields the radiation distribution. So, to find out the radiation distribution, we may proceed by calculating the radiative amplitude from which the elastic part is separable by virtue of the soft approximation. Then the remaining part will yield the desired spectrum. The soft approximation is, thus, a very convenient one which implies inability of the emitted gluon to

probe the elastic part of the process. Also, the form of radiation current j^μ in Eq. 3.3 shows that the radiation current is dependent only on the momenta of the particles. No reference to the process they undergo in the elastic part is necessary. So, in the same spirit of discussion about the classical nature of the soft radiation, it will really be interesting to see (in chapter 5) how the soft radiation spectrum off a heavy quark takes after that of a heavy classical charged particle or dipole under certain kinematic constraints.

3.1.2 Softness ‘burns’?

We have already discussed that the square of the radiation current provides us the radiation spectrum. The radiation probability can be written multiplying the (Lorentz invariant) phase space factor as below:

$$d\mathcal{W}_{rad} = \sum_{\beta=1,2} |\epsilon_\mu^\beta j^\mu|^2 \frac{d^3k}{2\omega(2\pi)^3} d\mathcal{W}_{el} \quad (3.4)$$

where ϵ_μ^β is the polarization of the emitted radiation. Using the Feynman gauge², for which $\sum_{\beta=1,2} \epsilon_\mu^\beta \epsilon_\nu^\beta \Rightarrow -g_{\mu\nu}$, we get

$$\begin{aligned} d\mathcal{N} &= \frac{d\mathcal{W}_{rad}}{d\mathcal{W}_{el}} \sim (j^\mu)^2 \frac{d^3k}{2\omega(2\pi)^3} \\ &\sim \frac{d\omega d\Omega}{\omega 2\pi} \frac{(1 - \cos\theta_{13})}{(1 - \cos\theta_1)(1 - \cos\theta_3)} \end{aligned} \quad (3.5)$$

from Eq. 3.3, where θ_{13} stands for the angle between incoming and the scattered particle, *i.e.* the angle between k_1 and k_3 . $\theta_1(\theta_3)$ is the angle the emission, with momentum k , makes with the particle with momentum $k_1(k_3)$. We also neglect the term $(m/E)^2$ (energy of parent

²In the next section, we will repeat the same calculation in a different gauge, called the light cone gauge, for some added advantages.

particles are $\sim E$) with respect to the terms involving angles. Now let us assume that the emitted gluon is almost collinear with the incoming particle so that $\theta_{13} \approx \theta_3$, then

$$\begin{aligned} d\mathcal{N} &= \frac{d\mathcal{W}_{rad}}{d\mathcal{W}_{el}} \\ &\sim \frac{d\omega d\Omega}{\omega 2\pi} \frac{1}{(1 - \cos\theta_1)} \end{aligned} \quad (3.6)$$

assuming the z direction to be along that of the incoming particle, we get, for $\theta_1 \rightarrow 0$,

$$\begin{aligned} d\mathcal{N} &\sim \frac{d\omega}{\omega} \frac{\sin\theta_1 d\theta_1}{(1 - \cos\theta_1)} \\ &\sim \frac{d\omega}{\omega} \frac{d\theta_1^2}{\theta_1^2} \end{aligned} \quad (3.7)$$

Treating the emission to be i) soft ii) collinear (with incoming particle) and iii) treating $m^2 \ll E^2$, we get a *double logarithm* [2] distribution for emission spectrum. For $\omega, \theta \rightarrow 0$ there exists divergences (called *soft* and *collinear* divergence respectively). The soft divergence exists if we consider the radiative bremsstrahlung processes only³. However, for the physical scenarios, these divergences are not present because there the radiative process cannot be separated. The collinear divergence, *i.e.* emission of huge number of photons/gluons almost grazing the trajectory of the parent quark, is regulated once we consider mass of emitting particles. It can also be shown from the classical electrodynamics [4] that there exists a conical region around the direction of motion of a massive particle, whose velocity is parallel to acceleration, where radiation is negligible. This region is called the ‘dead cone’ region and is a classical phenomenon.

³for regularization of soft divergence see [3]

3.1.3 Potential picture of single scattering in a different gauge

Single scattering is the building block for a multiple-scattering scenario; and so we must understand how single radiative scattering amplitudes can be calculated. But, we have done so just in the last section, and what makes us redo the same calculation ? As hinted in the footnote [2], light cone gauge is preferred to the Feynman gauge, used for treating the single scattering and for understanding the divergences therein, because the light cone gauge calculations allow one to neglect the Feynman diagrams arising due to the radiation off the target partons as the amplitudes corresponding to the said diagrams are kinematically suppressed. So, much complexities (*i.e.* number of diagrams) can be avoided while treating the multiple scattering with the help of the single scattering.

Now, let us consider the quark(q)-quark radiative (*i.e.* radiation of gluons (g)) scattering in scalar QCD (*i.e.* spin neglected). The scattering amplitudes, however, are calculated [5] in the soft-eikonal limit and the radiation distribution, *i.e.* number of gluons (n_g) per unit transverse momentum of emission (k_\perp) and per unit rapidity (η) is obtained as below:

$$\left[\frac{dn_g}{d^2k_\perp d\eta} \right]_{GB} = \frac{C_A \alpha_s}{\pi^2} \frac{q_\perp^2}{k_\perp^2 (\vec{k}_\perp - \vec{q}_\perp)^2} \quad (3.8)$$

where q_\perp is the transverse momentum transfer, C_A is the Casimir factor and α_s is the strong coupling. The above result is the celebrated Gunion-Bertsch formula which was derived by the authors of [6] who found out the Eq. 3.8 for the emitted gluon emitted making a substantial angle ($\sim \pi/2$, *i.e.* the gluon mid-rapidity, $\eta \sim 0$) with the incoming or the scattered particle. Now, there are two singularities in the formula – the noted soft singularity for the radiative processes and the singularity at $\vec{k}_\perp = \vec{q}_\perp$. It can be shown [7] that for $\vec{k}_\perp \ll \vec{q}_\perp$, the contribution from the diagrams with three-gluon ($3g$) vertices can be neglected compared to that of the other diagrams. The corresponding radiative matrix element can be written as:

$$\mathcal{M}_{rad}^\mu = \frac{\vec{k}_\perp}{k_\perp^2} \mathcal{M}_{el} + (\text{a term, constant as } k_\perp \rightarrow 0) \quad (3.9)$$

So we have the Gribov's bremsstrahlung theorem which states that there exists a factorization of elastic and radiation current provided $k_\perp \ll q_\perp$. The corresponding limit is called the Gribov limit [1].

But the inequality $k_\perp \geq q_\perp$ makes the diagrams with $3g$ vertices important. So while considering the corresponding amplitude, we must shield the $k_\perp = q_\perp$ singularity by the thermal mass of gluon.

3.2 Potential picture of multiple scattering: The energy loss model

After a brief introduction to the single particle scattering by a potential, we encounter a very similar situation where multiple scatterings off static centres occur in a colour neutral ensemble. The medium partons are considered to be static at the positions $x_i = (z_i, \vec{x}_{\perp i})$ such that $z_{i+1} > z_i$ and the inter-scatterer longitudinal distance is much larger compared to the color screening length. Then we can model the potential offered by the scatterer as a static Debye screening potential:

$$V_{i,AA'}^a(\vec{q}) = \frac{gT_{i,AA'}^a}{\vec{q}^2 + \mu^2} \quad (3.10)$$

for the i th scatterer with colors A, A' and T_i is the d_i dimensional generator of the representation corresponding to the target parton at the i th position. In each scattering the amount of the transferred momentum is, on the average small compared to the incident parton energy, E . Also, in the high temperature limit (*i.e.* $g \ll 1$), it can be shown [8] that the energy transfer

is g times smaller than the transverse momentum transfer, thereby providing a justification of the use of the potential model in which energy transfer must be negligible. The Born amplitudes, neglecting the spin of the particles are written down with the *soft, eikonal and collinear approximations*, where soft approximation enables to neglect the energy of the emission with respect to the incident particle, eikonality allows to neglect the transverse momenta of the scattered/radiated particles with respect to the energies of the scattered/radiating particle; and collinearity makes us assume that radiation almost grazes the parent particle. With these three assumptions, the multiple scattering and hence the jet energy loss model calculations are done. It may be a good opportunity to discuss the physical scenarios, though general, of the Gyulassy-Wang Potential Model (GWPM) with which we have computed the energy loss for a gluonic jet in a gluonic plasma in the next chapter.

3.2.1 Multiple scattering in potential model: the radiation distribution

So, the question we may ask is: ‘is multiple scattering just like adding the probabilities of the single scatterings or we have to add the amplitudes, not the probabilities?’ This is a general concern of basic quantum mechanics where we add the probabilities when we know that two processes are independent whereas we add the amplitudes when the processes are not independent. In the present scenario what we mean by this is: the answer of the question, just asked, depends on how frequently the scatterings are taking place and how much time does the radiation take to form, the formation time (see section 2.1 for a discussion on the formation time). Actually, when the scattering centres are well separated so that the radiation gets ample time to be formed, then the single scattering amplitudes are independent and it suffices to add the squared amplitudes or the probabilities (the cross-sections). But, because of a scattering which has taken place before the radiation is formed, the amplitudes interfere and then the basic quantum mechanics tells us to add the quantum mechanical amplitudes and

not the probabilities. This is, as already mentioned in the previous chapter, the famous issue of Landau-Pomeranchuk-Migdal (LPM) suppression where the two time scales, the formation time τ_f and the time between two scatterings τ_m become important. $\tau_f \gg \tau_m$ gives the factorization limit where the resulting radiation distribution is not just the addition of all the single scattering radiation distribution patterns. The other limit dictated by $\tau_f \ll \tau_m$ is the Bethe-Heitler (BH) limit in which the scattering centres act independently. We may write down a relation between the multiple collision differential radiation distribution and the corresponding single scattering one as below:

$$\frac{dn_g^{(m)}}{d^2k_\perp d\eta} = C_m(k) \frac{dn_g^{(1)}}{d^2k_\perp d\eta}, \quad (3.11)$$

where ‘1’ stands for single scattering and ‘ m ’ stands for multiple scattering. C_m is called radiation formation factor characterizing the interference pattern due to multiple scattering. η is the gluon rapidity related with its emission angle θ with respect to the emitting particle as:

$$\eta = -\ln \left(\tan \frac{\theta}{2} \right) \quad (3.12)$$

Naturally, in the BH limit, $C_m \approx m$, *i.e.* the scatterings add up to give the resultant intensity with no interference pattern. On the other hand, the factorization limit gives [7, 8],

$$\begin{aligned} C_m(k) &\approx \frac{8}{9} [1 - (-1/8)^m] \quad \text{for quarks} \\ &\approx 2(1 - 1/2^m) \quad \text{for gluons} \end{aligned} \quad (3.13)$$

Eq. 3.13 shows that the interference effect due to many multiple scatterings for quarks leaves corresponding radiation spectrum a factor of $\sim 8/9$ of that due to single scattering. It can also be checked that the gluon intensity radiated by gluon jet is $9/4$ times higher than that

radiated by quark jets in multiple scattering. Thus, the LPM effect in QCD depends on colour representation due to non-abelian nature of the problem under discussion.

3.2.2 Energy loss models: general considerations and approximations

We have already discussed about the radiation distribution due to multiple scattering off an energetic particle inside a thermal bath considered to be consisting of static scattering centres. But for ‘not-so-high’ momenta (*i.e.* ~ 2 GeV) there is collisional loss also and the partonic energy loss in QGP Considering elastic partonic interaction with thermal quarks and gluons (see Fig. 3.2a) was estimated by Bjorken [9]. The energy loss per unit length can be shown to be:

$$\frac{dE}{dx} = \frac{g^4}{6\pi} \left(1 + \frac{N_f}{6}\right) T^2 \ln \left(\frac{q_{\max}}{q_{\min}}\right) \quad (3.14)$$

where g is the strong coupling, $q_{\max}(q_{\min})$ is the maximum(minimum) momentum transfer, T is the bath temperature and N_f is the number of quark flavors. The energy loss taking into account the plasma effects has also been calculated in Ref. [10] and is shown to be:

$$\frac{dE}{dx} = \frac{g^4}{12\pi} \left(1 + \frac{N_f}{6}\right) T^2 \ln \left(a \frac{ET}{m_D^2}\right) \quad (3.15)$$

where m_D is the Debye screening mass and a is a constant ($\mathcal{O}(1)$). Also, Ref. [11] calculates the partonic energy loss for both hard and soft momentum exchange for two-body going to two-body ($2 \rightarrow 2$) scattering. Cancellation of the intermediate energy scale q^* below(above) which the momentum transfer is considered to be soft(hard) while summing the energy dissipation from two sectors is also shown. They exhibit the existence of a cut-off energy E_c below which the collisional energy loss dominates. The closed form of the energy loss is given by:

$$\frac{dE}{dx} = \frac{\nu g^2}{48\pi} \omega_p^2 \ln\left(\frac{E}{g^2 T}\right) \quad (3.16)$$

where ν is the statistical degeneracy factor and ω_p is the plasma frequency.

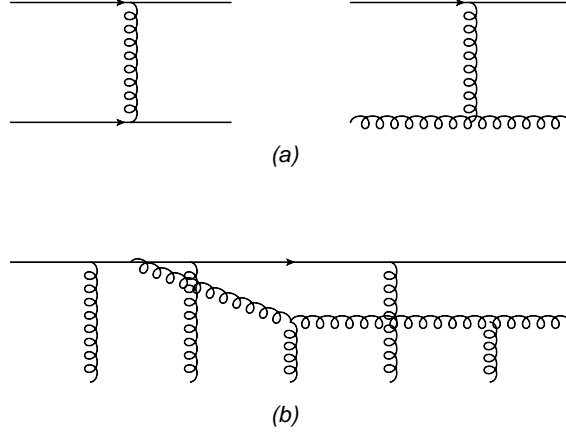


Figure 3.2: (a) Collisional and (b) radiative energy loss of high energy particles.

However, as already depicted in Fig. 3.2b, the multiple scattering of the incident particle with the soft (*i.e.* energy $\sim T$) medium particles has to be incorporated and to meet that end there are a handful of other energy loss models⁴ like those by Baier-Dokshitzer-Mueller-Peigne-Schiff (the BDMPS formalism)[13], Gyulassy-Levai-Vitev (the GLV formalism) [14], Armesto, Salgado, Wiedemann (the ASW formalism) [15], Arnold, Moore and Yaffe (AMY) (the thermal perturbative approach) [16], Higher twist approach [17] etc. The energy loss models make use of the following three approximations:

- soft *i.e.* energy of radiation, ω , is much smaller compared to that of the parent parton, E . Only AMY formalism, however, refrains from using this limit.
- eikonal *i.e.* no recoil of the leading parton due to scattering and radiation *i.e.* if q_\perp is the transverse momentum transfer and k_\perp is the transverse momentum of radiation, then, $k_\perp, q_\perp \ll E$, where E is the order of energy values of the radiating/ scattered particle;

⁴For a detailed comparison of all the energy loss models see [12]

and

- collinear *i.e.* gluons/photons almost graze the trajectory of the parent particle. From the on shell condition for the radiated particle,

$$\begin{aligned}k^2 = 0, & \Rightarrow \omega^2 - k_{\perp}^2 - k_z^2 = 0 \\ \Rightarrow \omega &= k_{\perp} \sin\theta, \quad k_z = k_{\perp} \cos\theta\end{aligned}\tag{3.17}$$

if we parametrize ω and k_z in terms of the radiation emission angle θ . Hence $\omega/k_{\perp} \ll 1$ implies the emission angle is very small. Hence the condition for collinearity boils down to $\omega \ll k_{\perp}$.

3.2.3 Energy loss from the radiative distribution

All the above kinematic constraints are generally imposed while obtaining the radiation distribution and once we have the radiation distribution, the radiative energy loss can be obtained by integrating the distribution function multiplied by the energy of each gluon (ω) over the transverse momentum (k_{\perp}) and the rapidity (η) of the gluon. Hence we can write the additive energy loss for each collision after the first one as:

$$\begin{aligned}
\Delta E_{rad} &= \frac{E_{m+1} - E_m}{m+1 - m} \\
&= \int d^2 k_{\perp} d\eta \frac{dn_g}{d^2 k_{\perp} d\eta} \omega \frac{C_{m+1} - C_m}{m+1 - m} \theta(E - k_{\perp} \cosh \eta) \\
&= \int d^2 k_{\perp} d\eta \frac{dn_g}{d^2 k_{\perp} d\eta} \omega \frac{dC_m}{dm} \theta(E - k_{\perp} \cosh \eta) \\
&\sim \int d^2 k_{\perp} d\eta \frac{dn_g}{d^2 k_{\perp} d\eta} \omega \theta(\tau_m - \tau_F) \theta(E - k_{\perp} \cosh \eta)
\end{aligned} \tag{3.18}$$

where $\frac{dC_m}{dm}$ has been approximated as a θ -function following [7] and the second θ -function imposes the constraint that the emission cannot have energy more than that of the emitting particle. The differential energy loss per unit length can be obtained by multiplying the energy loss per collision ΔE_{rad} with the scattering rate Λ .

3.3 ‘Our aims and expectations’ revisited

Now, as pledged in the section 1.5, after general discussion on energy loss phenomenon and its estimation in the radiative domain, we return to review our ‘aims and expectations’ again and we can modify the statement made there that the present thesis is about counting the number of emitted radiation. The reason is, we have already established that counting is same as finding out the radiation distribution. The two issues related to calculating the distribution which have been addressed are:

- Keeping in mind the kinematic approximations used in the energy loss models we endeavour to calculate the radiation distribution off energetic particles like gluon or heavy quark relaxing them (the eikonal approximation due to scattering, to be specific) at the level of single scattering. During this course we have calculated the non-eikonal gluon distribution off gluon jets and expect to find out non-eikonal corrections to the Gunion-Bertsch

distribution. Non-eikonal corrections to the heavy quark radiation distribution has also been found out with a view to re-explore the noted ‘dead-cone’ spectrum off heavy quarks which we have mentioned about in the beginning of this chapter.

The important messages we will get from these parts are:

- The non-eikonal corrections to the Gunion-Bertsch distribution create significant differences in the energy loss of gluons specifically in the lower temperature region. The non-eikonal corrections become important while considering the chemical equilibration of the gluons in thermal bath, too.
 - The non-eikonal corrections to the heavy quark radiation spectrum helps display the absence of the ‘dead-cone’ region along the direction of propagation of the heavy quark.
- The second issue is a bit different because this problem deals with the radiation distribution off quarks whose virtuality due to the acceleration received in heavy-ion collision is taken in to account.

We have already discussed the Weizsäcker-Williams (WW) picture of the energy loss where the WW gluons associated with a parton are detached from its parent due to acceleration and there is radiation in the form of these detached quanta. Now, along with the acceleration received by an incoming particle by the medium particles, there exists already a huge acceleration imparted upon them at the beginning when we collide two heavy nuclei to produce these jet particles, and, much later, the QGP. When comes the context of radiation distribution due to scattering inside medium, there is also a question whether the radiation is same as the radiation due to off-shellness, or a mix. A rigorous field theoretic technique of their interplay is necessary. The radiation off virtual quarks has been addressed and distribution of radiation given off by them has been calculated.

This part of thesis infers that the radiation distribution off virtual quarks, heavy or light, are similar and it is only after they become real that the difference between their spectra become distinguishable.

In all these calculations just mentioned above, it is not surprising to see the radiation distributions resembling with those obtained from the Classical Electrodynamics. We will see it most vividly in chapter 5 while dealing with the radiation distribution off the heavy quarks. But we should keep in mind that the dynamics is after all dictated by QCD and while calculating the energy loss we have the asymptotically free strong coupling in our calculation. So, though the radiation current is same as the classical current, the QCD plays its part in the radiation distribution where the property of asymptotic freedom becomes important.

Bibliography

- [1] QCD for beginners, Y. L. Dokshitzer, http://www.lpthe.jussieu.fr/~yuri/reviews/yd_cr.pdf
- [2] M. E. Peskin, D. V. Schroeder, *An Introduction to Quantum Field Theory*, Perseus Books, 1995
- [3] QCD and Jets, George Sterman, arXiv:hep-ph/0412013v1
- [4] J. D. Jackson, *Classical Electrodynamics* (John Wiley and Sons Pvt. Ltd. , New York 1998).
- [5] Energy Loss of Quarks by Gluon Radiation in Deconfined Matter, R. Thomas Ph. D. Thesis, Institut für Theoretische Physik 2003.
- [6] J. F. Gunion and G. Bertsch, *Phys. Rev. D* **25**, 746(1982).
- [7] X.N. Wang, M. Gyulassy, M. Plümer, *Phys. Rev. D* **51**, 3436(1995).
- [8] M. Gyulassy, X.N. Wang, *Nucl. Phys. B* **420**, 583(1994).
- [9] J. D. Bjorken, Fermilab Report No. Fermilab-Pub-82/59- THY, 1982 and Erratum (unpublished).
- [10] *Quark Gluon Plasma 2*, Ed. R. C. Hwa, (World Scientific, Singapore 1995)
- [11] A. K. Dutt-Mazumder, J. Alam, P. Roy and B. Sinha *Phys. Rev. D* **71**, 094016 (2005)

- [12] N. Armesto *et. al.*, Phys. Rev. C **86** 064904 (2012).
- [13] R. Baier, Y. L. Dokshitzer, A. H. Mueller, S. Peigne and D. Schiff, Nucl. Phys. B **483**, 291 (1997)
- [14] M. Gyulassy, P. Levai, and I. Vitev, Nucl. Phys. B **571**, 197(2000).
- [15] N. Armesto, C. A. Salgado, and U. A. Wiedemann, Phys. Rev. D **69**, 114003 (2004).
- [16] P. B. Arnold, G. D. Moore, and L. G. Yaffe, J. High Energy Phys. **12** (2001) 009.
- [17] X.-N. Wang and X.-F. Guo, Nucl. Phys. A **696**, 788 (2001).

Chapter 4

Gluon Radiation off gluons

So far, we have been engaged into the general discussion on radiation and the corresponding energy loss. We have tried to relate the facts that we can either calculate the Poynting's vector or can find out the radiation distribution in order to estimate the power dissipation. The latter is the approach taken in our calculations (and in many other pQCD calculations) to find out the radiation distribution.

The present chapter will discuss about the non-eikonal correction to the Gunion-Bertsch radiation distribution formula obtained from the $gg \rightarrow ggg$ scattering. This process is nothing but the radiative energy loss of high energy gluons in gluonic plasma.

First of all, is purely gluonic plasma an idealization ? It may be opportune to discuss the point here. We have already discussed that a charge, when Lorentz boosted, becomes dressed by Weizsäcker-Williams (WW) virtual quanta. After the head-on encounter of two nuclei in heavy-ion collision, the virtual quanta are excited and after some time, they become real quarks and gluons. Now, the WW virtual quanta are also known as 'sea' partons¹ and from the variation of the distribution of sea-partons with the momentum fraction x of the nucleon they carry, we

¹and the Lorentz boosted charge is nothing but the valence parton, which we termed as the *leading parton* in section 2.3

see that the sea quanta distribution becomes larger and larger as $x \rightarrow 0$. In addition to that, gluon distribution dominates over the sea quarks at very small x (see Fig. 4.1). So, the gluons outnumber the quarks for low- x (equivalently, high energy transfer) region which is the case for, at least, the heavy-ion collision experiments at Large Hadron Collider (LHC) at CERN and Relativistic Heavy-Ion Collider (RHIC) at BNL. Hence, we may very well treat the matter produced in the central rapidity region as dominantly gluonic.

It will be interesting to take the help of Eq. 2.8 which might be able to provide an alternative explanation to the increase of parton distribution with energy. We observe that with increasing energy (equivalently, γ), the upper limit of energy in frequency spectrum of virtual particles associated with the charge ($\omega_{max} \sim 1/\Delta t$) increases. So, the number of associated particles increase and hence the density of them goes up with increasing energy. Also, there are possibilities of gluons fluctuating into quark-antiquark pairs which contribute to the sea-quark distribution coupled with three-gluon as well as four-gluon vertices. But due to gluon-gluon color factor, the sea-gluons are expected to dominate.

After all these, why $gg \rightarrow ggg$? First of all, it is more important process than other similar (*i.e.* 2 \rightarrow 3) processes involving one or more quarks. Second of all, inelastic, number non-conserving processes help maintain the chemical equilibrium of the system. In the present discussion we will employ the 2-gluon \rightarrow 3-gluon process for revisiting the Gunion-Bertsch (GB) distribution formula widely used in transport models [1, 2, 3, 4, 5, 6] keeping in mind the recent trend of the similar efforts observed in Refs. [7, 8, 9].

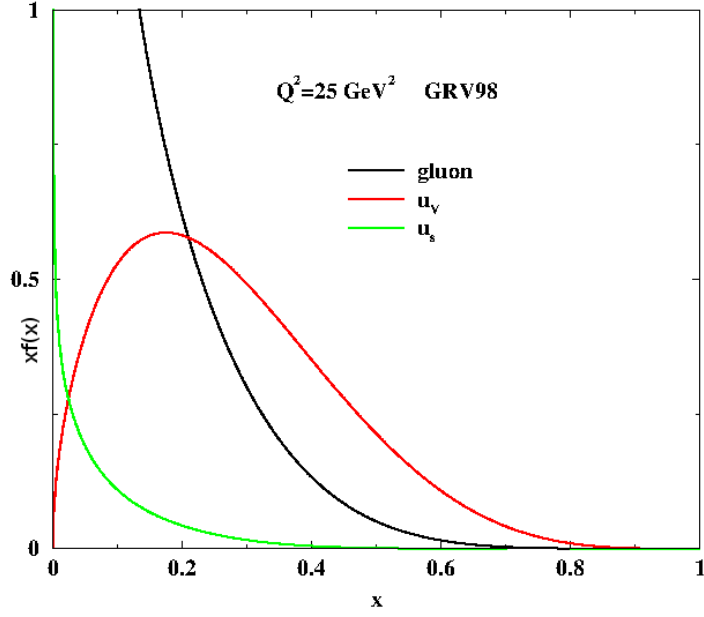


Figure 4.1: Variation of parton distribution function with x [10].

4.1 The radiation spectrum off a gluon in gluonic plasma

The square of the invariant amplitude for the process $g(k_1) + g(k_2) \rightarrow g(k_3) + g(k_4) + g(k_5)$ can be written elegantly as [11]:

$$\begin{aligned}
 |M_{gg \rightarrow ggg}|^2 &= \frac{1}{2} g^6 \frac{N_c^3}{N_c^2 - 1} \frac{\mathcal{N}}{\mathcal{D}} \times [(12345) + (12354) + (12435) + (12453) + (12534) \\
 &+ (12543) + (13245) + (13254) + (13425) + (13524) + (14235) \\
 &+ (14325)]
 \end{aligned} \tag{4.1}$$

where

$$\begin{aligned} \mathcal{N} &= (k_1.k_2)^4 + (k_1.k_3)^4 + (k_1.k_4)^4 + (k_1.k_5)^4 + (k_2.k_3)^4 + (k_2.k_4)^4 + (k_2.k_5)^4 \\ &+ (k_3.k_4)^4 + (k_3.k_5)^4 + (k_4.k_5)^4 \end{aligned} \quad (4.2)$$

$$\mathcal{D} = (k_1.k_2)(k_1.k_3)(k_1.k_4)(k_1.k_5)(k_2.k_3)(k_2.k_4)(k_2.k_5)(k_3.k_4)(k_3.k_5)(k_4.k_5) \quad (4.3)$$

and

$$(ijklm) = (k_i.k_j)(k_j.k_k)(k_k.k_l)(k_l.k_m)(k_m.k_i) \quad (4.4)$$

$N_c(=3)$ is the number of colors, $g = \sqrt{4\pi\alpha_s}$ is the color charge, and α_s is the strong coupling.

The quantity, $|M_{gg \rightarrow ggg}|^2$ after simplifying up to $\mathcal{O}(t^3/s^3)$ and $\mathcal{O}(1/k_\perp^2)$ can be written as[12] (calculation given in Appendix A also):

$$\begin{aligned} \frac{|M_{gg \rightarrow ggg}|^2}{|M_{gg \rightarrow gg}|^2} = \\ 12g^2 \frac{1}{k_\perp^2} \underbrace{\left[\left(1 + \frac{t}{2s} + \frac{5t^2}{2s^2} - \frac{t^3}{s^3}\right) - \left(\frac{3}{2\sqrt{s}} + \frac{4t}{s\sqrt{s}} - \frac{3t^2}{2s^2\sqrt{s}}\right) k_\perp + \left(\frac{5}{2s} + \frac{t}{2s^2} + \frac{5t^2}{s^3}\right) k_\perp^2 \right]}_{\mathcal{D}^{(1)}} \end{aligned} \quad (4.5)$$

where $|M_{gg \rightarrow gg}|^2 = (9/2)g^4s^2/t^2$, Mandelstam variables: $s = (k_1 + k_2)^2$, $t = (k_1 - k_3)^2$, $u = (k_1 - k_4)^2$, k_\perp is the magnitude of the transverse momentum of the radiated gluon.

The Mandelstam variable $t \approx -q_\perp^2$ and q_\perp^2 , the square of the transverse momentum transfer, is replaced by the corresponding average value:

$$\langle q_\perp^2 \rangle = \frac{1}{\sigma_{el}} \int_{m_D^2}^{\frac{s}{4}} dq_\perp^2 \frac{d\sigma_{el}}{dq_\perp^2} q_\perp^2 \quad (4.6)$$

where

$$\sigma_{el} = \int_{m_D^2}^{\frac{s}{4}} dq_{\perp}^2 \frac{d\sigma_{el}}{dq_{\perp}^2} \quad (4.7)$$

For dominant small-angle scattering ($t \rightarrow 0$),

$$\frac{d\sigma_{el}}{dq_{\perp}^2} = C_i \frac{2\pi\alpha_s^2}{q_{\perp}^4} \quad (4.8)$$

C_i is 9/4, 1 and 4/9 for gg, qg, and qq scattering. $\langle q_{\perp}^2 \rangle$ is then obtained as,

$$\langle q_{\perp}^2 \rangle = \frac{sm_D^2}{s - 4m_D^2} \ln \left(\frac{s}{4m_D^2} \right) \quad (4.9)$$

$m_D = \sqrt{2\pi\alpha_s(T)(C_A + \frac{N_F}{2})/3} T$, is the thermal mass of the gluon [13], N_F is the number of flavors contributing in the gluon self-energy loop, $C_A = 3$ is the Casimir invariant for the SU(3) adjoint representation. With the replacement as in Eq. 4.9, the emission distribution can be obtained by the following steps [14]:

$$\begin{aligned} \int dn_g &= \int \frac{d^4k}{(2\pi)^4} 2\pi\delta(k^2) \frac{|M_{gg \rightarrow ggg}|^2}{|M_{gg \rightarrow gg}|^2} \\ &= \int \frac{d^3\vec{k}}{(2\pi)^3} dk_0 \delta(k_0^2 - |\vec{k}|^2) \frac{|M_{gg \rightarrow ggg}|^2}{|M_{gg \rightarrow gg}|^2} \\ &= \int \frac{d^3\vec{k}}{(2\pi)^3} dk_0 \delta(k_0^2 - k_{\perp}^2 - k_z^2) \frac{|M_{gg \rightarrow ggg}|^2}{|M_{gg \rightarrow gg}|^2} \end{aligned} \quad (4.10)$$

Where $k_0(k_z)$ is the energy(longitudinal momentum) of the emitted gluon. But if we parametrize $k_0 = k_{\perp} \cosh \eta$ and $k_z = k_{\perp} \sinh \eta$ in terms of the gluon rapidity η , then $k_z = 0$ at $\eta = 0$. So, we can write Eq. 4.10 as,

$$\begin{aligned}
\int dn_g &= \frac{12g^2}{2(2\pi)^3} \int \frac{1}{k_\perp^2} d^2\vec{k}_\perp d\eta \mathcal{D}^{(1)} \\
\frac{dn_g}{d^2\vec{k}_\perp d\eta} &= \frac{C_A \alpha_s}{\pi^2} \frac{1}{k_\perp^2} \mathcal{D}^{(1)} \\
&\approx \frac{C_A \alpha_s}{\pi^2} \frac{q_\perp^2}{k_\perp^2 (\vec{k}_\perp - \vec{q}_\perp)^2} \mathcal{D}^{(1)} \\
&= \left[\frac{dn_g}{d^2\vec{k}_\perp d\eta} \right]_{GB} \mathcal{D}^{(1)} \tag{4.11}
\end{aligned}$$

in the limit, transverse momentum transfer $q_\perp \gg k_\perp$ (see Eq. 3.8 and the discussions thereafter). In the light of the discussion of Sec. 3.2.2 about the eikonal approximation due to scattering where $q_\perp \ll \sqrt{s}$, we identify Eq. 4.5 as the non-eikonal correction to the noted GB radiation distribution. Though it seems that $\mathcal{O}(k_\perp^n)$, $n = 0, 1, 2$ terms introduce corrections beyond the ‘soft approximation’, they are actually divided by the factor $1/k_\perp^2$ in front, and hence are the most dominant terms in the soft approximation limit. Other terms for $n > 2$ will have a k_\perp in the numerator and so those will tend to zero in the soft limit. So Eq. 4.5 refers to the more general modification (compared to those in Refs.[7, 8]) to the Gunion-Bertsch distribution within $\mathcal{O}(t^3/s^3)$.

4.2 Reaction rate of $gg \rightarrow ggg$

Why are we interested to know the rate of this reaction ? The rate is important because the number/particle identity non-conserving processes are important maintain the chemical equilibration of the plasma medium. So processes like $gg \rightarrow ggg$ (number non-conserving) or $gg \rightarrow q\bar{q}$ (particle identity non-conserving) coupled with the reverse processes will significantly contribute to the chemical equilibrium. When the inelastic processes cease, the medium restrains from being chemically equilibrated and the number of gluons gets fixed.

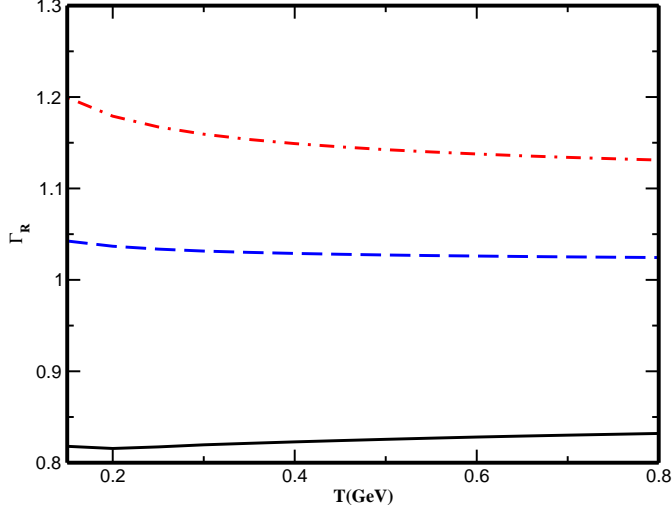


Figure 4.2: Temperature variation of the ratio of the equilibration rate obtained in Ref. [12] (solid line), Ref. [7] (dashed line), and [8] (dot-dashed) normalized by the corresponding value putting GB distribution for the process $gg \rightarrow ggg$.

The reaction rate of $gg \rightarrow ggg$, R_3 , has been estimated by finding out $\sigma^{gg \rightarrow ggg}$, the corresponding cross-section, and multiplying it with the gluon density $\rho_g \sim T^3$, where T is the bath temperature. The $\sigma^{gg \rightarrow ggg}$ can be found out by integrating the triple differential cross-section

$$\frac{d\sigma^{gg \rightarrow ggg}}{d^2\vec{q}_\perp d\eta d^2\vec{k}_\perp} \approx \frac{d\sigma^{gg \rightarrow gg}}{d^2\vec{q}_\perp} \left[\frac{dn_g}{d^2\vec{k}_\perp d\eta} \right] \quad (4.12)$$

over q_\perp and the emitted gluon phase space. We find out $2 \rightarrow 3$ reaction rate putting the corrections to the GB distribution obtained in Refs. [7, 8, 12] in Eq. 4.12 and compare their respective ratios to the reaction rate putting GB distribution in Fig. 4.2. We see that the non-eikonal correction has significant contribution to the equilibration rate of gluon.

4.3 Energy loss by energetic gluons

Energy loss of energetic gluon in a gluonic plasma can be obtained with the help of Eq. 3.18. As long as we are in the additive (Bethe-Heitler) region, the energy loss for each collision beyond the first one is given by the formula. Hence the energy loss obtained by Eq. 3.18 yields that over the distance of mean free path of plasma. The mean free path of the plasma is obtainable from the inverse interaction rate which can be evaluated using pQCD in the same way as [15]. The θ -functions in the formula constrain the phase space of emitted gluon because the energy loss formula demands $\tau_m > \tau_F$ as well as $E > k_\perp \cosh \eta$. We put mean free path $\tau_m \sim \Lambda^{-1}$, where Λ is the interaction rate obtained from [15] and $\tau_F \sim \cosh \eta / k_\perp$ is the formation time of gluon. So we get $E / \cosh \eta > k_\perp > \Lambda \cosh \eta$.

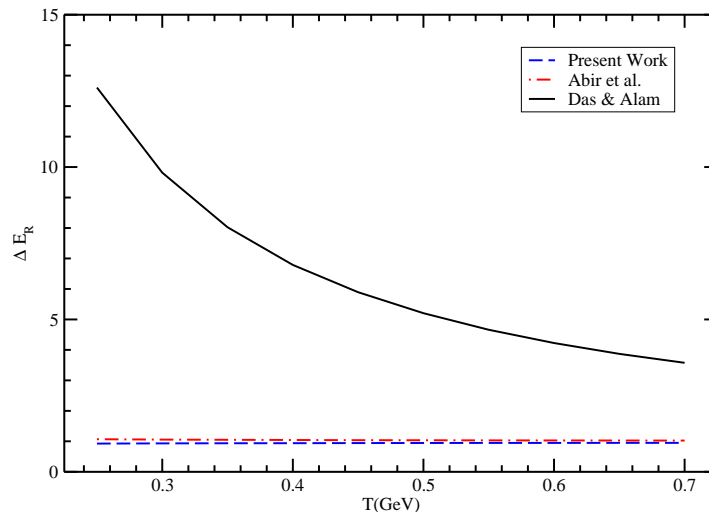


Figure 4.3: Temperature variation of the energy loss of 10 GeV gluon, obtained from Refs. [12] (solid line), [7](dashed), [8](dot-dashed) and scaled by that obtained from Ref. [14]. The ratio is denoted by ΔE_R ,

Keeping the above considerations in mind, we find out the energy losses obtained using the distributions of Refs. [7, 8, 12] and scaled by the corresponding value obtained from Ref. [14]. The difference in the scaled energy loss obtained from Ref [12] with those from Refs. [7, 8]

is more prominent in the lower temperature region than the upper temperature realm. So it is expected that the distribution function will have considerable effect in case of energy loss calculations around the RHIC energy (see Fig. 4.3).

The qualitative difference of the ΔE_R in different cases can be attributed to the fact that while the correction terms in [7, 8] contain terms like $(t/s)^n$ only, the present calculation shows the existence of (at $\mathcal{O}(k_\perp^{-2,-1})$) terms like $s^{-1/2,-1}$ (see Eq. 4.5). Given $s = 18T^2$ in the COM frame of the colliding particles, the temperature variation of $\frac{t}{k_\perp^2 s}$ is negligible in comparison with $\frac{1}{k_\perp \sqrt{s}}$ (for a given k_\perp) or $1/s$ — a fact which results in the qualitative difference in the present radiation distribution formula, and hence, in energy loss. So, in conclusion, we can tell that the qualitative difference in the energy loss using modified Gunion-Bertsch formula will compel us rethink the radiation distribution to be used in phenomenological models; as also, this may be seen as a step towards the continuous endeavour of removing the approximations prevailing inside the energy loss calculations.

Bibliography

- [1] T. S. Biró, E. Van Doorn, B. Müller, M. H. Thoma and X. N. Wang, Phys. Rev. C **48**, 1275 (1993).
- [2] L. Xiong and E. V. Shuryak, Phys.Rev. C **49**, 2203(1994).
- [3] S. M. H. Wong, Nucl. Phys. A **607**, 442(1996).
- [4] D. K. Srivastava, M. G. Mustafa, and B. Muller, Phys.Rev. C **56**, 1064(1997).
- [5] Z. Xu and C. Greiner, Phys. Rev. C **71**, 064901 (2005).
- [6] J.-W. Chen, J. Deng, H. Dong, and Q. Wang, Phys.Rev. D **83**, 034031(2011).
- [7] S. K. Das and J. Alam, Phys. Rev. D **82**, 051502(R), (2010).
- [8] R. Abir, C. Greiner, M. Martinez, and M. G. Mustafa, Phys. Rev. D **83**, 011501 (R) (2011)
- [9] O. Fochler, J. Uphoff, Z. XU and C. Greiner, Phys. Rev. D **88**, 014018(2013)
- [10] Taken from a lecture by Prof. Jan-e Alam
- [11] F. A. Berendes *et al.*, Phys. Lett. B **103**, 124(1981).
- [12] T. Bhattacharyya, S. Mazumder, S. K Das and J. -e Alam, Phys. Rev. D **85**, 034033 (2012),
- [13] M. Le Bellac, Thermal Field Theory, Cambridge University Press, Cambridge 1996.

[14] J. F. Gunion and G. Bertsch, Phys. Rev. D **25**, 746(1982).

[15] M. H. Thoma, Phys. Rev. D **49**, 451(1994)

Chapter 5

Scattering of heavy-quarks

5.1 The radiation intensity spectrum off a heavy particle: Classical approach

Let us begin our discussion with the reference to the computation of radiation spectrum off heavy particles from classical electrodynamics. Why classical electrodynamics ? Because, we have already discussed, in chapter 3 that, there is nothing ‘quantum’ in soft radiation current (Eq. 3.3). At this point, it may be worthwhile compare the radiation spectra off heavy, relativistic particles obtained with the help of classical electrodynamics and the Quantum field theory.

The power spectrum off a non-relativistic heavy particle is given by Ref. [1],

$$\frac{dP}{d\Omega} \sim |\dot{\vec{\beta}}|^2 \sin^2\theta \quad (5.1)$$

where $\vec{\beta}$ is the velocity of the particle, Ω is the solid angle the observer makes with the direction of motion of the particle. We observe that the power spectrum dips at $\theta = 0, 180^\circ$ and shows

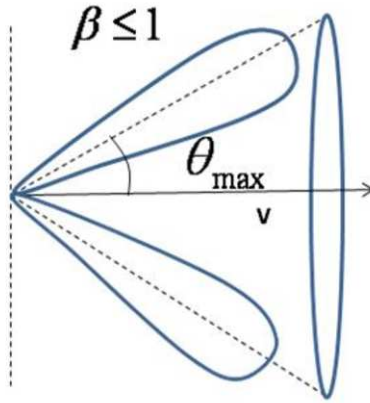


Figure 5.1: Polar plot of the power spectrum off a relativistic, heavy particle.

a peak at $\theta = 90^\circ$. The radiation free zone around $\theta = 0$, which signifies the direction of propagation of the heavy particle, is called the ‘dead-cone’ region. The use of the term ‘cone’ will be apparent if we study the angular distribution of power emitted by a heavy, relativistic particle with acceleration parallel to its velocity (*i.e.*, no bending. See Fig. 5.1). The angular dependence of the power spectrum looks like,

$$\frac{dP}{d\Omega} \sim |\dot{\beta}|^2 \frac{\sin^2\theta}{(1 - \beta\cos\theta)^5} \quad (5.2)$$

Now, a natural question which may arise at this point is how the power spectrum $dP/d\Omega$ in classical electrodynamics is related to the radiation spectrum $dn_g/(d^2k_\perp d\eta)$. They cannot be equivalent in a sense that though the small angle behaviours of both of them are similar, they hardly resemble in large angles. Second of all, dimensionally they are not same. So there is a hint that we must look for some other β quantity for establishing the correspondence. Let us search for it.

If we consider a time-dependent function $\vec{A}(t)$ which is related to the retarded acceleration field (see Ref. [1] for details) then the power spectrum can be written as

$$\frac{dP}{d\Omega} = |\vec{A}(t)|^2 \quad (5.3)$$

The total energy (W) radiated per unit solid angle is the integration of the r.h.s. of Eq. 5.3

$$\frac{dW}{d\Omega} = \int |\vec{A}(t)|^2 dt \quad (5.4)$$

which in the Fourier domain can be written as

$$\frac{dW}{d\Omega} = \int |\vec{A}(\omega)|^2 d\omega \quad (5.5)$$

by dint of the Parseval's theorem, where ω is the frequency of radiation. From Eq. 5.5 we identify

$$|\vec{A}(\omega)|^2 = \frac{dI}{d\omega d\Omega} \quad (5.6)$$

Now, if we can show that the angular dependence in $dI/(d\omega d\Omega)$, the intensity spectrum, is same as that in $dn_g/(d^2k_{\perp} d\eta)$ (for small angle, say), then we can find out the correspondence between the intensity spectrum in classical field theory and the radiation spectrum in quantum field theory. As expected, we can show that the said angular dependences are same, at least, for small angle emissions.

5.2 Elastic and radiative scattering cross-sections of a heavy quark : Perturbative QCD

So far we have emphasized on finding out the radiation distribution off an energetic parton so that we can find out the radiative dissipation of the particle. But the radiative dissipation is not the only energy loss mechanism of a fast particle inside the QGP medium. The elastic loss has to be incorporated, too. Transport coefficients like drag and diffusion can be estimated [2] from the elastic and/or radiative scattering amplitudes in case of heavy quarks(Q) scattering with light quarks(q) or gluons(g). The drag and diffusion coefficients act as inputs to the Fokker-Planck equation (FPE) (an approximation of the Boltzmann Transport Equation (BTE)), which dictates the evolution of the heavy quark distribution in the background of the evolving QGP medium. The distribution the FPE spits out is divided by the initial distribution fed to it to obtain the nuclear suppression factor (R_{AA}) [3, 4] which is experimentally measured by the relative value of the hadronic multiplicity distribution (in terms of their transverse momentum p_T and rapidity y) in HIC (Pb-Pb or Au-Au collision) with respect to that in proton-proton collision and is scaled by the number of collisions (N_{coll}). Hence,

$$R_{AA} = \frac{\left(\frac{dN}{d^2p_T dy}\right)^{AA}}{N_{\text{coll}} \left(\frac{dN}{d^2p_T dy}\right)^{PP}} \quad (5.7)$$

Essentially, with the help of the Feynman amplitudes we have to find out the values for some experimental observables which will not entertain infinite results, anyway. So, let us review various infinities playing their parts in the heavy quark scattering amplitudes and possible measures to shield them.

5.2.1 Mass lifts collinear divergence in radiation spectrum

The number of gluons emitted off a light particle, its radiation distribution, is characterized by the soft and the collinear divergence (see chapter 3 for discussion). But unlike light particles, the collinear divergence in the emission spectrum of a heavy particle is regulated by the mass of the particles and the shielding of collinear divergence for heavy quarks is manifested in the form of the existence of dead-cone. The radiation distribution of soft gluons (energy ω , transverse momentum k_{\perp}) off a heavy quark (of mass m and energy E) is given by Ref. [5].

$$d\mathcal{N} \sim \frac{d\omega}{\omega} \frac{k_{\perp}^2 dk_{\perp}^2}{k_{\perp}^2 + \omega^2 \theta_0^2} \quad (\theta_0 = \frac{m}{E}) \quad (5.8)$$

which with the help of Eq. 3.17 and in small angle approximation can be written as

$$d\mathcal{N} \sim \frac{d\omega}{\omega} \frac{\theta^2 d\theta^2}{(\theta^2 + \theta_0^2)^2} \rightarrow \frac{d\omega}{\omega} \frac{d\theta^2}{\theta^2}, \text{ when } E \gg m \quad (5.9)$$

So the presence of mass shields the collinear divergence. But this shielding works only when the energy of heavy quark is comparable to its mass. Otherwise, in the limit $E \gg m$, θ_0 becomes very small and the collinear divergence starts to become prominent again.

5.2.2 Divergence due to soft gluon exchange

This divergence is termed as the ‘ t -channel divergence’ as the softness in exchanged gluon (*i.e.* its energy and momentum is much less than those of the the other particles) is manifested through a small value of the Mandelstam variable t in the elastic heavy quark scattering amplitudes. In centre of momentum frame, small t translates into small angle scattering. So the corresponding cross-section of the $Qq \rightarrow Qq$ and/or $Qg \rightarrow Qg$ processes are dominated by the t -channel diagrams and hence $d\sigma^{Qq \rightarrow Qq}/dt \sim 1/t^2$. Since the radiative cross section is given by

the product of elastic cross-section and the radiation distribution, the radiative part encounters the same divergence, too. This divergence can be shielded in an ad hoc manner just by putting a cut-off of thermal mass (m_D) of gluons inside thermal bath *i.e.* by replacing $1/t$ terms by $1/(t - m_D^2)$.

For a more rigorous shielding, however, one may use thermally modified gluon propagators, the Hard Thermal Loop (HTL) resummed propagators in calculating the Feynman amplitudes. Resummation in propagator is necessary when quantum corrections to it are of same magnitude as that of the uncorrected part. Actually, in thermal bath, the existence of the scales¹, the ‘hard’ scale (when momenta $\sim T$, temperature of the bath) and the ‘soft’ scale ($\sim gT$, where g is the coupling), may lead to quantum corrections with magnitudes same as that of the uncorrected value. The loop integrals which are of less importance (*i.e.* of higher order in g where $g \ll 1$) in comparison with tree level calculations in vacuum field theory, may become, in thermal field theory, as important as the tree-level diagrams.

Matrix elements for the processes $Qq \rightarrow Qq$ and $Qg \rightarrow Qg$ in large angle scattering limit has been calculated using resummed (HTL) propagators in Ref. [6](see Ref. [7] for small angle scattering calculations for light quarks). The details of the calculations and the comparison between the values of drag and diffusion coefficients obtained using thermal mass shielding and that using HTL propagator can be obtained in Ref. [8]. The Feynman diagrams calculated for Qg elastic scattering are given in Fig. 5.2. Replacing gluons by quarks in the t -channel diagram, one can get the diagram for the Qq scattering. The solid black dot on the propagator line denotes the HTL resummation. It is noteworthy that the heavy quark lines (solid) in Fig. 5.2, even when they appear as propagators, are never resummed. This is due to the fact that the heavy quarks are not assumed to be thermalized, and hence bare propagators for them suffice.

¹Actually the scale gT is called the *electric scale* and that corresponding to g^2T is called *magnetic scale*

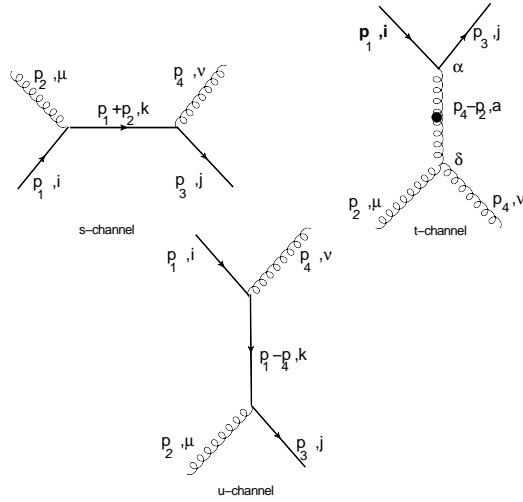


Figure 5.2: Tree level Feynman diagrams for Qg elastic scattering.

Now, generically speaking, HTL approximation and resummation needs examination of correlation functions in high temperature limit and the $\sim T^2$ contributions of them are known to give rise to the HTLs. But the ‘correlation function’ does not mean ‘two-point correlation functions’, *i.e.* propagators only. Though the ϕ^4 field theory yields HTL in the propagator only, the situation is far more complicated in case of a non-abelian gauge theory like QCD, where three-point and even four point correlation functions can yield HTLs. So what about HTL three-gluon/quark-gluon vertex correction? From Ref. [9] we can compare the contributions of the 1-loop vertex corrections to N -gluon vertex or two-quark $N - 2$ gluon vertex with their bare counterparts in terms of powers of g (coupling) and T (temperature). Assuming $g \ll 1$, if the corrections become sub-leading to the bare values, we can neglect the vertex corrections. Putting $N = 3$ in the present case, and for hard external momenta ($\sim T$) for heavy quarks, light quarks and gluons we can easily verify that vertex corrections are not necessary for this tree-level calculations.

5.3 Radiation distribution off heavy quarks recoiling due to scattering

The radiation distribution off heavy quarks as obtained in Ref. [5] considers the soft-eikonal-collinear kinematic approximations (see Eq. 5.8 and Sec. 3.2.2). The factor $\theta^2/(\theta^2 + \theta_0^2)$ in Eq. 5.8 is called the heavy quark dead-cone factor and is extensively used in finding out the drag, diffusion, and hence the R_{AA} [3, 4]. There are some recent attempts to relax the kinematic approximations like collinearity and eikonal approximation due to scattering (henceforth to be called eikonal 1 approximation) in calculating heavy quark radiation distribution. While Ref. [10] calls off the collinearity assumption, the present dissertation will concentrate on the removal of the eikonal 1 approximation.

The motivations behind these revisions are, first of all, an ad hoc use of the modified dead cone factor $\sin^2\theta/(\sin^2\theta + \theta_0^2)$ (which becomes $\theta^2/(\theta^2 + \theta_0^2)$ at small angles) for large angles of emitted gluons (with the heavy quark) may not be accurate. Second of all, removal of the eikonal 1 approximation will be of importance in case of heavy quarks with moderate energies [11] because the effect of recoil will come into play.

In general, the radiation spectrum for heavy quarks can be obtained with the help of Feynman diagram techniques of pQCD. For the present discussion, we will consider heavy quarks scattering with light quarks (q) and there exists recoil due to this scattering (no eikonal 1 approximation). The tree level Feynman diagrams for the $Qq \rightarrow Qqg$ scattering are given in Fig. 5.3. As discussed in Sec. 3.1.1, we have to find out the soft radiation current by separating the $Qq \rightarrow Qq$ amplitude from the radiative part. Squaring the radiation current gives the radiation distribution.

The dynamics of the process is obtained once we find out the amplitudes from the pQCD. For sake of finding out energy loss we need to incorporate the kinematic approximations. Generally

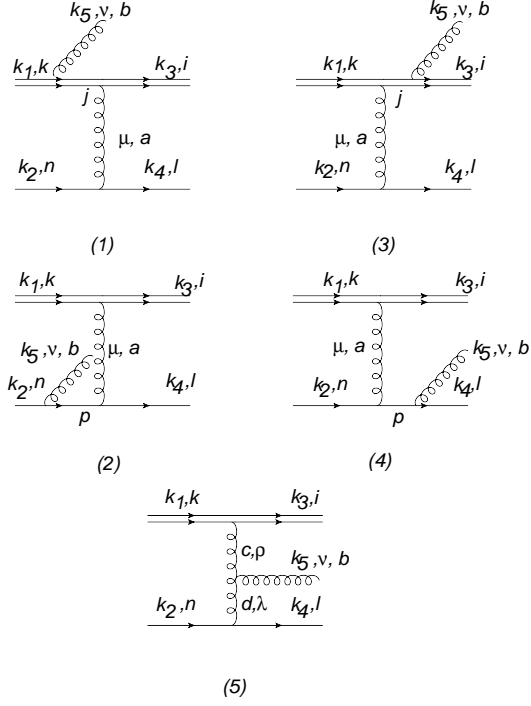


Figure 5.3: Tree level Feynman diagrams for $Qq \rightarrow Qqg$ scattering. The double line denotes the heavy quark.

the calculations are done in centre of momentum (COM) frame. We begin with the process $Q(k_1)q(k_2) \rightarrow Q(k_3)q(k_4)g(k_5)$, where the four momenta of the particles are indicated inside the brackets. For the $2 \rightarrow 3$ process obeying the four momentum conservation relation $k_1 + k_2 = k_3 + k_4 + k_5$, we have six Mandelstam variables s, s', t, t', u, u' where

$$\begin{aligned}
 s &= (k_1 + k_2)^2, & t &= (k_1 - k_3)^2 \\
 u &= (k_1 - k_4)^2, & s' &= (k_3 + k_4)^2 \\
 t' &= (k_2 - k_4)^2, & u' &= (k_2 - k_3)^2,
 \end{aligned} \tag{5.10}$$

subject to the constraint equation,

$$s + t + u + s' + t' + u' = 4m^2. \tag{5.11}$$

Hence, we need five kinematic variables for 3-body phase space. At this point, we may assume the four-momentum of the emitted gluon, k_5 , to be small enough so that the corresponding kinematics reduces to one due to $2 \rightarrow 2$ scattering. This approximation is called the ‘soft gluon emission approximation’. In $k_5 \rightarrow 0$ approximation, $s \rightarrow s'$, $t \rightarrow t'$ and $u \rightarrow u'$ which lead to

$$s + t + u \rightarrow 2m^2 \quad (5.12)$$

Hence, the kinematics we are dealing with, is similar to, as already said, two-body kinematics which need two Mandelstam variables, s and t (say), square of COM scattering energy and COM scattering angle respectively, to be specified. We may write down s in the following way,

$$\begin{aligned} s &= (k_1 + k_2)^2 = k_1^2 + k_2^2 + 2k_1 \cdot k_2 = m^2 + 2(E_1 E_2 - \vec{k}_1 \cdot \vec{k}_2) \\ &= m^2 + 2E_1 |\vec{k}_2| + 2|\vec{k}_1|^2 = m^2 + 2E_1 |\vec{k}_2| + 2E_1^2 - 2m^2 \quad (\text{COM frame}) \\ &= 2E_1 |\vec{k}_1| + 2E_1^2 - m^2 = 2E_1^2 - m^2 + 2E_1 \sqrt{E_1^2 - m^2}, \end{aligned} \quad (5.13)$$

in COM frame in terms of mass (m) and energy (E_1) of incoming heavy quark. Similarly, t can be written as

$$\begin{aligned} t &= (k_1 - k_3)^2 = 2m^2 - 2k_1 \cdot k_3 = 2m^2 - 2E_1 E_3 + 2\vec{p}_1 \cdot \vec{p}_3 \\ &= 2m^2 - 2E_1^2 + 2|\vec{p}_1|^2 \cos \theta_{13,CM} = -2|\vec{p}_1|^2 + 2|\vec{p}_1|^2 \cos \theta_{13,CM} \\ &= -\frac{(s - m^2)^2}{2s} (1 - \cos \theta_{13,CM}), \end{aligned} \quad (5.14)$$

where $\theta_{13,CM}$ is the COM scattering angle between incoming HQ (momentum k_1) and the scattered HQ (momentum k_3). We can form, for 2-body scattering processes, two dimensionless variables from the available quantities of our present problem. One is m/\sqrt{s} and another is t/s .

Besides, there may be another set of four, k_5/\sqrt{s} , which remind us of the fact that we are dealing with a 3-body phase space, in reality. Now, $k_5 = (\omega, \vec{k}_\perp, k_z)$; and from Sec. 3.2.2 we know that $|\vec{k}_\perp| = k_\perp = \omega \sin \theta$, where θ is the angle the radiation makes with the parent quark. If we note that $k_z = \sqrt{\omega^2 - k_\perp^2}$ for on-shell radiated gluon, then $k_z = \omega \cos \theta$. Consequently, all the components of k_5 are now expressible in terms of ω and θ ; and the third dimensionless quantity k_5/\sqrt{s} becomes ω/\sqrt{s} . We consider $\omega \rightarrow 0$ as the soft approximation limit. Or, we may tell that we are assuming $\omega/\sqrt{s} \rightarrow 0$ when we speak about soft limit of emitted gluon. Under this approximation, we explore the effect of $\mathcal{O}(t/s)$ terms and higher in Feynman amplitude (\mathcal{M}). $\mathcal{O}(t/s)$ terms will exist if we remove the eikonal 1 approximation. To be precise, we look for terms only $\mathcal{O}(1/\omega^2)$ as well as terms $\mathcal{O}(t/s)$ and higher in our calculation of radiative matrix element of $Qq \rightarrow Qqg$ process. We can also see that, as shown in Ref. [10], with the choice of four momenta as given in Eq. 5.15 one may be able to call off the collinearity approximation of the emitted gluon, too. So the amplitude we are going to find out will be free from collinearity and the eikonal 1 approximation. The heavy quark scattering amplitude, thus obtained, in the present dissertation will generalize the soft, non-eikonal, mid rapidity amplitude for light quarks calculated in Ref. [11], will be reduced to the soft, eikonal (but not collinear) matrix element of Ref. [10] and reproduces the soft, eikonal, collinear amplitude as obtained in Ref. [5] (the kinematic regions I, II and IV respectively in Sec. 5.3.2).

We hereby specify our choice of four momenta (k_i , $i = 1 \rightarrow 5$) of interacting particles in COM frame assuming that the incoming particles have no transverse momentum, *i.e.* they are travelling along the z-axis, say.

$$\begin{aligned}
k_1 &\equiv (E_1, \vec{0}_\perp, k_{1z}), & k_2 &\equiv (E_2, \vec{0}_\perp, -k_{1z}), \\
k_3 &\equiv (E_3, \vec{q}_\perp, k_{3z}), & k_4 &\equiv (E_4, -\vec{q}_\perp, -k_{3z}) \\
k_5 &\equiv (\omega, \omega \sin \theta \hat{k}_\perp, \omega \cos \theta)
\end{aligned} \tag{5.15}$$

The scattered particles are assumed to acquire a transverse momentum q_\perp . Since we are working in COM frame in the soft gluon radiation limit, we may approximately assume $E_{1(2),CM} \approx E_{3(4),CM}$ and $|\vec{p}_{1(2),CM}| \approx |\vec{p}_{3(4),CM}|$, where approximation sign is replaced by equality for $2 \rightarrow 2$ case.

5.3.1 Radiative matrix elements

There are five Feynman diagrams pertaining to the process under discussion, $Qq \rightarrow Qqg$. We denote a generic matrix element by,

$$\mathcal{M}_{ij} = \mathcal{M}_i \mathcal{M}_j^\dagger; \quad i, j = 1 \rightarrow 5 \quad \forall i \leq j \quad (5.16)$$

Clearly, i (or j) denotes the Feynman diagram being indicated among five of them (fig. 5.3). Below, we list down the matrix elements, \mathcal{M}_{ij} , up to terms $\mathcal{O}(1/\omega^2)$ with all large t corrections in \mathcal{M} . The detailed derivation is deferred to the Appendix B. $\forall i \leq j$, we list down \mathcal{M}_{ij} and \mathcal{M}_{ij}^S , where $\mathcal{M}_{ij}^S = \mathcal{M}_{ij} + \mathcal{M}_{ji}$. $\mathcal{M}_{ij} = \mathcal{M}_{ji}$, in point of fact, and hence $\mathcal{M}_{ij}^S = 2\mathcal{M}_{ij}$.

$$\begin{aligned}
\mathcal{M}_{11} &= \frac{128}{27} g^6 \frac{s^2}{t^2} \frac{1}{\omega^2} \frac{1}{\sin^2 \theta} \left(\frac{-1}{\tan^2 \frac{\theta}{2}} \right) \mathcal{J}^2 \left(\Delta_M^2 + \frac{f_1}{(1 - \Delta_M^2)^2} \right) \\
\mathcal{M}_{33} &= \frac{128}{27} g^6 \frac{s^2}{t^2} \frac{1}{\omega^2} \frac{1}{\sin^2 \theta} \left(\frac{-1}{\tan^2 \frac{\theta}{2}} \right) \mathcal{J}^2 \left(\frac{\Delta_M^2 + \frac{f_1}{(1 - \Delta_M^2)^2}}{\mathcal{F}_{35}^2} \right) \\
\mathcal{M}_{13}^S &= \frac{128}{27} g^6 \frac{s^2}{t^2} \frac{1}{\omega^2} \frac{1}{\sin^2 \theta} \frac{1}{4} \left(\frac{-1}{\tan^2 \frac{\theta}{2}} \right) \mathcal{J}^2 \left(\frac{\Delta_M^2 - \frac{f_2}{(1 - \Delta_M^2)^2}}{\mathcal{F}_{35}} \right) \\
\mathcal{M}_{12}^S &= \frac{128}{27} g^6 \frac{s^2}{t^2} \frac{1}{\omega^2} \frac{1}{\sin^2 \theta} \frac{1}{4} (1 - \Delta_M^2) \mathcal{J} \left(1 - \frac{f_3}{(1 - \Delta_M^2)^3} \right) \\
\mathcal{M}_{34}^S &= \frac{128}{27} g^6 \frac{s^2}{t^2} \frac{1}{\omega^2} \frac{1}{\sin^2 \theta} \frac{1}{4} (1 - \Delta_M^2) \mathcal{J} \left(\frac{1 - \frac{f_3}{(1 - \Delta_M^2)^3}}{\mathcal{F}_{35} \mathcal{F}_{45}} \right) \\
\mathcal{M}_{14}^S &= \frac{128}{27} g^6 \frac{s^2}{t^2} \frac{1}{\omega^2} \frac{1}{\sin^2 \theta} \frac{7}{8} (1 - \Delta_M^2) \mathcal{J} \left(\frac{1 + \frac{f_4}{(1 - \Delta_M^2)^3}}{\mathcal{F}_{45}} \right) \\
\mathcal{M}_{23}^S &= \frac{128}{27} g^6 \frac{s^2}{t^2} \frac{1}{\omega^2} \frac{1}{\sin^2 \theta} \frac{7}{8} (1 - \Delta_M^2) \mathcal{J} \left(\frac{1 + \frac{f_4}{(1 - \Delta_M^2)^3}}{\mathcal{F}_{35}} \right) \\
\mathcal{M}_{24}^S &= \frac{128}{27} g^6 \frac{s^2}{t^2} \frac{1}{\omega^2} \frac{1}{\sin^2 \theta} \frac{1}{8} \frac{t}{s} \tan^2 \frac{\theta}{2} \left(\frac{1 + \frac{\frac{t}{s}(1 + \frac{t}{2s})}{(1 - \Delta_M^2)^2}}{\mathcal{F}_{45}} \right),
\end{aligned} \tag{5.17}$$

$\mathcal{M}_{22} = \mathcal{M}_{44} = 0$; and \mathcal{M}_{i5} , $\forall i = 1 \rightarrow 5$ do not contribute in $\mathcal{O}(1/\omega^2)$. The definitions of the quantities used in describing the matrix elements in Eq. 5.17 are written below:

$$\begin{aligned}
\Delta_M &= \frac{m}{\sqrt{s}}; \quad \mathcal{J} = \frac{1 - \Delta_M^2}{1 + \frac{\Delta_M^2}{\tan^2 \frac{\theta}{2}}}; \\
f_1 &= \Delta_M^2 \frac{t}{s} \left(1 + \frac{t}{2s}\right); \quad f_2 = \frac{\Delta_M^4 t}{2s} - 2 \frac{\Delta_M^2 t}{s} + \frac{t}{2s} - \frac{\Delta_M^2 t^2}{2s^2} + \frac{t^2}{2s^2} + \frac{t^3}{4s^3}; \\
f_3 &= \Delta_M^2 \frac{t}{s} - \frac{t}{s} - \frac{t^2}{2s^2} + \frac{\Delta_M^2 t^2}{2s^2}; \quad f_4 = \Delta_M^4 \frac{t}{s} - 3 \Delta_M^2 \frac{t}{s} + 2 \frac{t}{s} - \frac{\Delta_M^2 t^2}{2s^2} + \frac{3t^2}{2s^2} + \frac{t^3}{2s^3}; \\
\mathcal{F}_{35} &= 1 + \frac{\left[\cot \theta \left(1 - \sqrt{1 - \frac{4 \left(\frac{q_\perp}{\sqrt{s}}\right)^2}{(1 - \Delta_M^2)^2}}\right) - \frac{2 \left(\frac{q_\perp}{\sqrt{s}}\right)}{(1 - \Delta_M^2)} \right] (1 - \Delta_M^2)}{\tan \frac{\theta}{2} \left(1 + \frac{\Delta_M^2}{\tan^2 \frac{\theta}{2}}\right)} \\
\mathcal{F}_{45} &= 1 - \frac{\left[\cot \theta \left(1 - \sqrt{1 - \frac{4 \left(\frac{q_\perp}{\sqrt{s}}\right)^2}{(1 - \Delta_M^2)^2}}\right) - \frac{2 \left(\frac{q_\perp}{\sqrt{s}}\right)}{(1 - \Delta_M^2)} \right] (1 - \Delta_M^2)}{\cot \frac{\theta}{2}} \quad (5.18)
\end{aligned}$$

However, that $\frac{q_\perp}{\sqrt{s}}$ is related to $\frac{t}{s}$ can be seen from the following few steps:

$$\begin{aligned}
t &= (k_1 - k_3)^2 \\
&= (E_1 - E_3)^2 - q_\perp^2 - (k_{1z} - k_{3z})^2 \\
&= -q_\perp^2 - (k_{1z} - k_{3z})^2 \\
&= -q_\perp^2 - k_{1z}^2 \left(1 - \sqrt{1 - \frac{q_\perp^2}{k_{1z}^2}}\right)^2 \\
&= -q_\perp^2 - \frac{(s - m^2)^2}{4s} \left(1 - \sqrt{1 - \frac{4sq_\perp^2}{(s - m^2)^2}}\right)^2 \\
\therefore \frac{t}{s} &= -\frac{q_\perp^2}{s} - \frac{1}{4} (1 - \Delta_M^2)^2 \left(1 - \sqrt{1 - \frac{4q_\perp^2}{(1 - \Delta_M^2)^2}}\right)^2 \quad (5.19)
\end{aligned}$$

Now, to define the total matrix element, $\mathcal{M}_{Q_q \rightarrow Q_{qg}}$, we need the following functions obtainable from Eq. 5.18,

$$\begin{aligned}
A &= \Delta_M^2 + \frac{f_1}{(1 - \Delta_M^2)^2} ; \quad B = \Delta_M^2 - \frac{f_2}{(1 - \Delta_M^2)^2} \quad C = 1 - \frac{f_3}{(1 - \Delta_M^2)^3} ; \\
D &= 1 + \frac{f_4}{(1 - \Delta_M^2)^3}
\end{aligned} \tag{5.20}$$

With the help of Eqs. 5.18 and 5.20 we can write,

$$\begin{aligned}
|\mathcal{M}_{\text{Qq} \rightarrow \text{Qqg}}|^2 &= \frac{128}{27} g^6 \frac{s^2}{t^2} \frac{1}{\omega^2 \sin^2 \theta} \\
&\times \left[\frac{\mathcal{C}_1 (1 - \Delta_M^2)^2}{\left(1 + \frac{\Delta_M^2}{\tan^2 \frac{\theta}{2}}\right)} + \frac{\mathcal{C}_2 (1 - \Delta_M^2)^2}{\tan^2 \frac{\theta}{2} \left(1 + \frac{\Delta_M^2}{\tan^2 \frac{\theta}{2}}\right)^2} + (1 - \Delta_M^2)^2 \mathcal{C}_0 \tan^2 \frac{\theta}{2} \right]
\end{aligned} \tag{5.21}$$

where \mathcal{C}_1 , \mathcal{C}_2 and \mathcal{C}_0 are given by,

$$\begin{aligned}
\mathcal{C}_2 &= - \left(A + \frac{A}{\mathcal{F}_{35}^2} + \frac{B}{4\mathcal{F}_{35}} \right) ; \\
\mathcal{C}_1 &= \frac{C}{4} \left(1 + \frac{1}{\mathcal{F}_{35}\mathcal{F}_{45}} \right) + \frac{7}{8} D \left(\frac{1}{\mathcal{F}_{45}} + \frac{1}{\mathcal{F}_{35}} \right) ; \\
\mathcal{C}_0 &= \frac{1}{8\mathcal{F}_{45}(1 - \Delta_M^2)^4} \left[(1 - \Delta_M^2)^2 z^2 + z^4 + \frac{1}{2} z^6 \right] ;
\end{aligned} \tag{5.22}$$

Using gluon rapidity $\eta = -\ln(\tan \frac{\theta}{2})$ and the light cone variable $x = k_\perp e^\eta / \sqrt{s}$, we can get

$$|\mathcal{M}_{Qq \rightarrow Qqg}|^2 = \frac{16}{3} g^2 |\mathcal{M}_{Qq \rightarrow Qq}|^2 \frac{1}{\omega^2} \frac{1}{\sin^2 \theta} \underbrace{\left[\sum_{n=2,1,0} \mathcal{C}_n e^{2(n-1)\eta} \left(\frac{k_{\perp}^2}{k_{\perp}^2 + x^2 M^2} \right)^n \right]}_{\mathcal{W}(x, k_{\perp}^2)} \quad (5.23)$$

Where we use,

$$|\mathcal{M}_{Qq \rightarrow Qq}|^2 = \frac{8}{9} g^4 \frac{s^2}{t^2} (1 - \Delta_M^2)^2 \quad (5.24)$$

5.3.2 Behaviour of non-eikonal heavy quark spectrum at different kinematic regions:

While treating different kinematic regions, we keep in mind the following cartoon depicting the angles θ_g which the gluons make with the parent heavy quark and θ_q , the heavy quark scattering angle. According to this figure (Fig. 5.4), the eikonal approximation implies $\theta_q = 0$ and the collinearity implies $\theta_g = 0$.

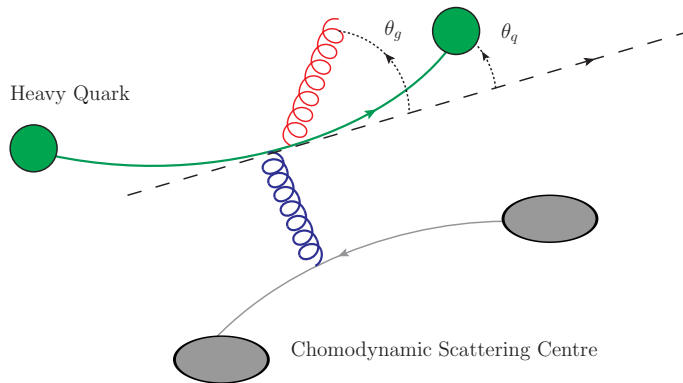


Figure 5.4: Deviation from straight eikonal trajectory. Angle between incoming and outgoing momentum of heavy quark is θ_q and direction of emission of gluon with that of incoming momentum of heavy quark is θ_g .

Region I: Massless quark with non-eikonal trajectory

We may obtain the non-eikonal gluon radiation spectrum of light quarks from Eq. 5.21 if we take its masses limit. Below we jot down the forms of the functions $f_i, \forall i = 1 \rightarrow 5, A \rightarrow D$ and $\mathcal{C}_1, \mathcal{C}_2, \mathcal{C}_0$ when we take massless limit, *i.e.* $m \rightarrow 0 \Rightarrow \Delta_M \rightarrow 0$,

$$\begin{aligned}
& \text{(i)} \mathcal{J} \rightarrow 1 \\
& \text{(ii)} f_1 \rightarrow 0 ; f_2 \rightarrow \frac{t}{2s} + \frac{t^2}{2s^2} + \frac{t^3}{4s^3} ; \\
& f_3 \rightarrow -\frac{t}{s} - \frac{t^2}{2s^2} ; f_4 \rightarrow \frac{2t}{s} + \frac{3t^2}{2s^2} + \frac{t^3}{2s^3} \\
& \text{(iii)} \mathcal{F}_{35} \rightarrow \mathcal{F}_{35}^0 = 1 + \left[\cot \theta \left(1 - \sqrt{1 - 4\frac{q_{\perp}^2}{s}} \right) - \frac{2q_{\perp}}{\sqrt{s}} \right] \cot \frac{\theta}{2} ; \\
& \mathcal{F}_{45} \rightarrow \mathcal{F}_{45}^0 = 1 + \left[\cot \theta \left(1 - \sqrt{1 - 4\frac{q_{\perp}^2}{s}} \right) - \frac{2q_{\perp}}{\sqrt{s}} \right] \tan \frac{\theta}{2} \\
& \text{(iv)} A \rightarrow 0 ; B \rightarrow B^0 = -\frac{t}{2s} - \frac{t^2}{2s^2} - \frac{t^3}{4s^3} ; \\
& C \rightarrow C^0 = 1 + \frac{t}{s} + \frac{t^2}{2s^2} ; D \rightarrow D^0 = 1 + \frac{2t}{s} + \frac{3t^2}{2s^2} + \frac{t^3}{2s^3} \\
& \text{(v)} \mathcal{C}_1 \rightarrow \mathcal{C}_1^0 = \frac{C^0}{4} + \frac{C^0}{4\mathcal{F}_{35}^0\mathcal{F}_{45}^0} + \frac{7D^0}{8\mathcal{F}_{35}^0} + \frac{7D^0}{8\mathcal{F}_{45}^0} ; \\
& \mathcal{C}_2 \rightarrow \mathcal{C}_2^0 = -\frac{B^0}{4\mathcal{F}_{35}^0} \\
& \mathcal{C}_0 \rightarrow \mathcal{C}_0^0 = \frac{1}{8\mathcal{F}_{45}^0} \frac{t}{s} \left(1 + \frac{t}{s} \left(1 + \frac{t}{2s} \right) \right) \tag{5.25}
\end{aligned}$$

Hence,

$$|\mathcal{M}_{\text{qq}' \rightarrow \text{qq}'\text{g}}|^2 = 12g^2 \frac{s^2}{t^2} \frac{1}{k_{\perp}^2} |M_{\text{qq}' \rightarrow \text{qq}'}|^2 \left\{ \mathcal{C}_1^0 + \frac{\mathcal{C}_2^0}{\tan^2 \frac{\theta}{2}} + \mathcal{C}_0^0 \tan^2 \frac{\theta}{2} \right\} \tag{5.26}$$

Keeping up to $\mathcal{O}(\frac{t}{s})$ of B^0, C^0, D^0 and putting $\mathcal{F}_{35} = 1 = \mathcal{F}_{45}$ we get

$$\begin{aligned}
|\mathcal{M}_{\text{qq}' \rightarrow \text{qq}'\text{g}}|^2 &= \frac{128}{27} g^6 \frac{s^2}{t^2} \frac{1}{k_{\perp}^2} \left\{ 2 \frac{1}{4} \left(1 + \frac{t}{s} \right) + 2 \frac{7}{8} \left(1 + \frac{2t}{s} \right) + \frac{t}{8s} \frac{1}{\tan^2 \frac{\theta}{2}} + \frac{t}{8s} \tan^2 \frac{\theta}{2} \right\} \\
&= 12g^2 \left\{ \frac{8}{9} g^4 \frac{s^2}{t^2} \right\} \frac{1}{k_{\perp}^2} \left(1 + \frac{16t}{9s} + \frac{t}{9s} \cosh 2\eta \right)
\end{aligned} \tag{5.27}$$

In the limit $\eta \rightarrow 0$ Eq. 5.27 boils down to the light quark non-eikonal (up to $\mathcal{O}(t/s)$) matrix element obtained in Ref. [11].

Region II: Massive quark with eikonal trajectory

This region considers

$$\frac{q_{\perp}}{\sqrt{s}} \rightarrow 0 \Rightarrow \frac{t}{s} \rightarrow 0 \tag{5.28}$$

Hence, from Eq. 5.18,

$$f_i = 0 \quad \forall i = 1 \rightarrow 5 ; \quad \mathcal{F}_{35} = \mathcal{F}_{45} = 1 \tag{5.29}$$

From Eq. 5.20 we get, in the same limit,

$$A = B = \Delta_M^2 ; \quad C = D = 1 ; \quad \mathcal{F}_{35} = \mathcal{F}_{45} = 1 \tag{5.30}$$

Hence

$$\mathcal{C}_1 = \frac{9}{4} ; \quad \mathcal{C}_2 = -\frac{9\Delta_M^2}{4} ; \quad \mathcal{C}_0 = 0 \tag{5.31}$$

In Eq. 5.22.

With the help of Eqs. 5.29, 5.30, 5.31 we can write Eq. 5.21 as,

$$\begin{aligned}
|\mathcal{M}_{Qq \rightarrow Qqg}|^2 &= \frac{128}{27} g^6 \frac{s^2}{t^2} \frac{1}{k_\perp^2} \frac{9}{4} \mathcal{J}^2 \\
&= \frac{128}{27} g^6 \frac{s^2}{t^2} \frac{1}{k_\perp^2} (1 - \Delta_M^2)^2 \frac{9}{4} \frac{1}{\left(1 + \frac{\Delta_M^2}{\tan^2 \frac{\theta}{2}}\right)^2} \\
&= 12g^2 \left[\frac{8}{9} g^4 \frac{s^2}{t^2} (1 - \Delta_M^2)^2 \right] \frac{1}{k_\perp^2} \frac{1}{\left(1 + \frac{\Delta_M^2}{\tan^2 \frac{\theta}{2}}\right)^2} \\
&= 12g^2 |\mathcal{M}_{Qq \rightarrow Qq}|^2 \left\{ \frac{1}{k_\perp^2} \left(1 + \frac{m^2}{s} e^{2\eta}\right)^{-2} \right\} \tag{5.32}
\end{aligned}$$

with $\eta = -\ln(\tan \frac{\theta}{2})$; and the expression embraced by the curly braces is the radiated gluon spectrum ($\sim |\mathcal{M}_{Qq \rightarrow Qqg}|^2 / |\mathcal{M}_{Qq \rightarrow Qq}|^2$) for this case. Evidently, the present calculation yields the calculation in Ref. [10] in the small angle scattering limit (Eq. 5.32).

Region III: Massless quark with eikonal trajectory

Now we explore the behaviour of the radiation spectrum in the following limits,

$$\begin{aligned}
\text{(i)} \quad & \frac{q_\perp}{\sqrt{s}} \rightarrow 0 \Rightarrow \frac{t}{s} \rightarrow 0 \\
\text{(ii)} \quad & m = 0 \Rightarrow \Delta_M = 0 \Rightarrow \mathcal{J} \rightarrow 1
\end{aligned} \tag{5.33}$$

The above limits force Eq. 5.32 to take the form given below,

$$|\mathcal{M}_{Qq \rightarrow Qqg}|^2 = 12g^2 |\mathcal{M}_{Qq \rightarrow Qq}|^2 \frac{1}{k_\perp^2} \tag{5.34}$$

which in the limit $q_\perp \gg k_\perp$ can be written as,

$$|\mathcal{M}_{qq' \rightarrow qq'g}|^2 \approx 12g^2 |\mathcal{M}_{qq' \rightarrow qq'}|^2 \left[\frac{q_\perp^2}{k_\perp^2 (\vec{k}_\perp - \vec{q}_\perp)^2} \right], \quad (5.35)$$

where q, q' are two different light quark flavors. The part within the square braces can very well be identified with the celebrated Gunion-Bertsch gluon spectrum [12] emitted from light quarks.

Region IV: Massive quark with eikonal trajectory emitting collinear gluons

This region considers the following limits

$$\begin{aligned} \text{(i)} \quad & m \ll \sqrt{s} \Rightarrow s \approx 4E_1^2 \\ \text{(ii)} \quad & \frac{q_\perp}{\sqrt{s}} \rightarrow 0 \quad \text{and} \\ \text{(iii)} \quad & \theta \rightarrow 0 \Rightarrow \tan \frac{\theta}{2} \approx \frac{\theta}{2} \end{aligned} \quad (5.36)$$

In the above limit Eq. 5.21 yields the dead-cone factor of Ref. [5],

$$|\mathcal{M}_{Qq \rightarrow Qqg}|^2 = 12g^2 |\mathcal{M}_{Qq \rightarrow Qq}|^2 \frac{1}{k_\perp^2} \left(1 + \frac{\theta_0^2}{\theta^2} \right)^{-2}, \quad (5.37)$$

with $\theta_0 = \frac{m}{E_1}$.

5.3.3 The non-eikonal radiation spectrum off Heavy Quarks

In Fig. 5.5 we plot the radiation spectrum off heavy quarks with varying k_{\perp} of gluons for different ζ values. $\zeta = q_{\perp}/\sqrt{s}$ signifies the extent of transverse momentum transferred to the heavy quark due to scattering with light quarks. Hence, ζ can be treated as the non-eikonality parameter in our calculation.

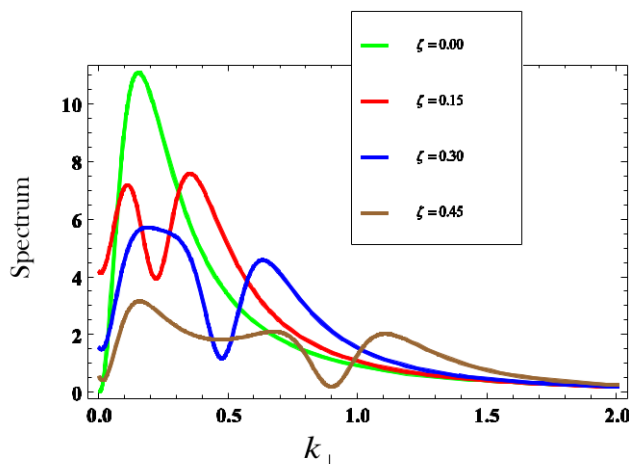


Figure 5.5: Variation of gluon spectrum off 10 GeV heavy quark with gluon transverse momentum with different extents of recoil of heavy quarks.

The polar plots of the radiation distribution for different ζ values are really interesting. Fig. 5.6 is the QCD counterpart of the polar plot of the intensity spectrum off a heavy, relativistic particle in Fig. 5.1. Figs. 5.7-5.9 are analogous to the generalization of the emission spectrum for instantaneous circular motion of the heavy particle with different radii of curvature. The magnitude of the radius vector of any point on the polar plot (joined by red lines) gives the number of gluons emitted at the angle the radius vector makes with the direction of propagation of heavy quark (denoted by the arrow). It is noteworthy that the dead cone present along and around the direction of propagation of heavy quark exists no more when it recoils. This may be understood if we think the polar plots as composed of two parts, the spectrum before collision and the spectrum after the collision. For the eikonal case (*i.e.* no recoil, $\zeta = 0$) the spectra are

along the same direction. When the heavy quark bends, the spectra before and after scattering make an angle and hence the composition results in non-zero radiation even along the direction of propagation of the scattered heavy quark.

If we want to calculate the energy loss and its effect on the nuclear suppression factor we have to consider the $Qg \rightarrow Qgg$ scattering which will have more cross-section than the $Qq \rightarrow Qqg$, too. While in the eikonal case [10], the $Qg \rightarrow Qgg$ matrix element differs from that of $Qq \rightarrow Qqg$ just by a number due to color factor, the non-eikonal case is not going to be so simple and we have to calculate the Feynman amplitudes of a lot more diagrams. The present calculation may, in principle, be useful when quarks dominate in the medium, *i.e.* in case of Compressed Baryonic Matter experiment energies, for example². But that needs a consistent treatment of the multiple scattering process. Once that is done, we can easily find out the effect of non-eikonicity in energy loss.

²There may be some questions about the abundance of heavy-quarks and about the possibility of its radiation at this energy.

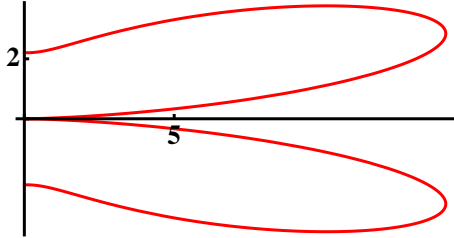


Figure 5.6: Polar plot of $\mathcal{W}(\theta, \omega)$ (at a typical ω) with $\zeta(= q_{\perp}/\sqrt{s}) = 0$ for a 10 GeV Charm jet.

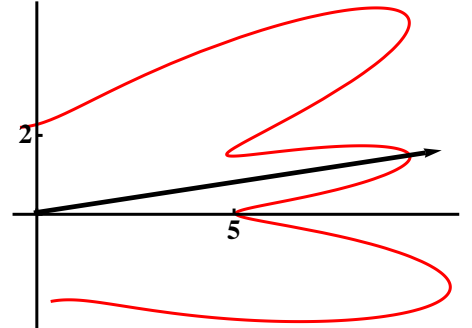


Figure 5.7: Polar plot of $\mathcal{W}(\theta, \omega)$ (at a typical ω) with $\zeta(= q_{\perp}/\sqrt{s}) = 0.15$ for a 10 GeV Charm jet.

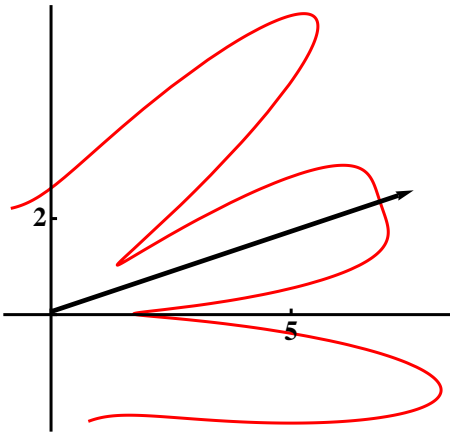


Figure 5.8: Polar plot of $\mathcal{W}(\theta, \omega)$ (at a typical ω) with $\zeta(= q_{\perp}/\sqrt{s}) = 0.30$ for a 10 GeV Charm jet.

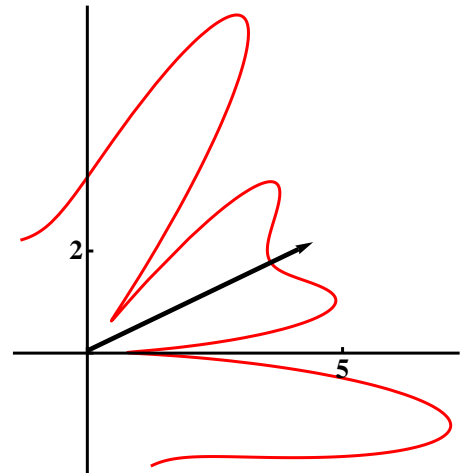


Figure 5.9: Polar plot of $\mathcal{W}(\theta, \omega)$ (at a typical ω) with $\zeta(= q_{\perp}/\sqrt{s}) = 0.45$ for a 10 GeV Charm jet.

Bibliography

- [1] J. D. Jackson, *Classical Electrodynamics* (John Wiley and Sons Pvt. Ltd. , New York 1998).
- [2] B. Svetitsky, Phys. Rev. D **37**, 2484(1988).
- [3] S. K. Das, J. Alam and P. Mohanty, Phys. Rev. C **82**, 014908(2010).
- [4] S. Mazumder, T. Bhattacharyya, J. Alam and S. K. Das, Phys. Rev. C **84**, 044901(2011).
- [5] Y. L. Dokshitzer and D. E. Kharzeev, Phys. Lett. B **519**, 199(2001).
- [6] S. Mazumder, T. Bhattacharyya and S. K. Das, Advances in High Energy Physics(2013), 136587
- [7] H. Heiselberg and Xin-Nian Wang, Nucl. Phys. B **462**, 389(1996).
- [8] Transport of Heavy Quarks in Quark Gluon Plasma, Ph. D. Thesis, Surasree Mazumder, Homi Bhabha National Institute, Variable Energy Cyclotron Centre, Kolkata, India (2014).
- [9] M. Le Bellac, *Thermal Field Theory*, (Cambridge University Press, Cambridge 1996).
- [10] R. Abir, C. Greiner, M. Martinez, M. G. Mustafa and J. Uphoff, Phys. Rev. D **85**, 054012(2012).
- [11] R. Abir, Phys. Rev. D **87**, 034036(2013).

[12] J. F. Gunion and G. Bertsch, Phys. Rev. D **25**, 746(1982)

Chapter 6

Gluon Radiation off slightly virtual quarks

6.1 Radiation spectrum off a slightly virtual quark

We have already discussed the Weizsäcker-Williams (WW) picture of the energy loss where the WW gluons associated with a parton are detached from its parent due to acceleration and there is radiation in the form of these detached quanta. Now, along with the acceleration received by an incoming particle by the medium particles, there exists already a huge acceleration imparted upon them at the beginning when we collide two heavy nuclei to produce these high energy particles, and, much later, the QGP. So the high energy particles whose interaction with the QGP bath particles is under study, are highly virtual.

The present study endeavors to find out the radiation distribution off slightly off-shell particles. We take $e^+e^- \rightarrow Q\bar{Q}g$ process where Q stands for heavy quark and radiates gluons. The assumption of very small off-shellness (or virtuality) enables us to use Dirac's equation in our calculation as an approximate equation of motion for the fermionic fields associated with

the quarks. We will follow the line of arguments proposed in Ref. [1] to give a formula for the radiation distribution off slightly virtual heavy quarks. It will be argued that for non-zero virtuality the distribution is independent of the current mass of quark. The absence of virtuality in heavy quarks results in a behaviour similar to that obtained in [2]; we will also verify the absence of ‘conventional’ dead-cone suppression for on-shell light quarks from the same formula. Lastly, The radiation distribution off the virtual particles will be employed to find out the energy loss inside QGP.

The tree-level Feynman diagrams for gluon radiation by quarks/anti-quarks in the process $e^+e^- \rightarrow Q\bar{Q}g$ are depicted in Fig. 6.1. The amplitude for the process shown in Fig. 6.1a can

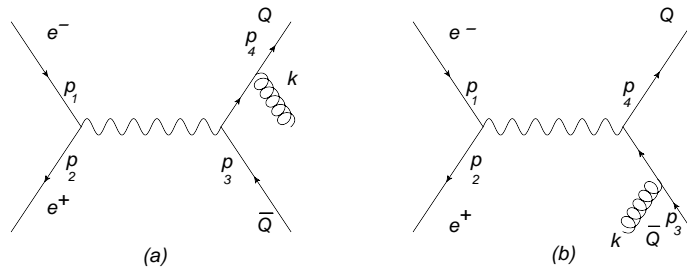


Figure 6.1: Tree-level Feynman diagram for gluon radiation by (a) quark and (b) anti-quark.

be written as:

$$\mathcal{M}_a = \frac{g_s e_Q e^2}{s} (t^a)_j^i [\bar{v}(p_2) \gamma_\mu u(p_1)] [\bar{u}_i(p_4) \not{\epsilon}^{a*}(k) \frac{(\not{p}_4 + \not{k} + m)}{((p_4 + k)^2 - m^2)} \gamma^\mu v^j(p_3)] \quad (6.1)$$

where g_s is the colour coupling, e_Q is the quark electric charge, e is electric charge, a, i, j are the color indices and $s = (p_1 + p_2)^2$. We assume that $p_3^2 = p_4^2 \neq m^2$. For off-shell particles the virtuality can be defined through the parameter V as:

$$V^2 = q^2 - m^2, \quad (6.2)$$

where q^2 is four-momentum square of external virtual particles, $q^2 = m^2$ implies $V = 0$, i.e. the particle becomes on-shell. We build our calculation on very small value of V so that the off-shell external quarks are at the vicinity of being on-shell. Under such approximations we can use the Dirac's equation for quark and anti-quark.

The denominator of Eq. 6.1 can be expanded in terms of V to get,

$$\begin{aligned} (p_4 + k)^2 - m^2 &= p_4^2 + 2p_4 \cdot k + k^2 - m^2 \\ &= V^2 + 2p_4 \cdot k \end{aligned} \quad (6.3)$$

with $k^2 = 0$ for on-shell radiated gluon. The numerator of Eq. 6.1 can be simplified by using the anti-commutator, $\{\not{p}_i, \not{p}_j\} = 2p_i \cdot p_j$ and Dirac equation $\bar{u}(p)(\not{p} - m) = 0$ as follows:

$$\begin{aligned} \bar{u}_i(p_4)\not{\epsilon}^{a*}(k)(\not{p}_4 + \not{k} + m) &= \bar{u}_i(p_4)\not{\epsilon}^{a*}(k)(\not{p}_4 + m) + \bar{u}_i(p_4)\not{\epsilon}^{a*}(k)\not{k} \\ &= \bar{u}_i(p_4)(-\not{p}_4 + m)\not{\epsilon}^{a*}(k) + 2p_4 \cdot \epsilon^{a*}(k)\bar{u}_i(p_4) \\ &\quad + \bar{u}_i(p_4)\not{\epsilon}^{a*}(k)\not{k} \\ &= 2p_4 \cdot \epsilon^{a*}(k)\bar{u}_i(p_4) + \bar{u}_i(p_4)\not{\epsilon}^{a*}(k)\not{k} \end{aligned} \quad (6.4)$$

The first term of Eq. 6.4 which is proportional to $p_4 \cdot \epsilon^{a*}(k)$ can be defined as the soft part of amplitude [1] which dominates in the soft radiation limit. Using similar arguments for the process depicted in Fig. 6.1b, we get the total soft amplitude given by:

$$[\mathcal{M}_{soft}]_{a+b} \sim 2 \left(\frac{p_4 \cdot \epsilon^{a*}(k)}{V^2 + 2p_4 \cdot k} - \frac{p_3 \cdot \epsilon^{a*}(k)}{V^2 + 2p_3 \cdot k} \right) \quad (6.5)$$

This part of the amplitude originates from the gluon radiation. We call it the ‘radiation factor’ R . To obtain the cross-section of the process we square the amplitude and sum over the relevant colour and spin degrees of freedom. In the limit $V = 0$, algebraic manipulation of $|R|^2$ gives rise to the conventional dead-cone suppression of on-shell massive quarks. Now, with our assumption of low virtuality of quarks, R is, again, expected to lead us to a quantitative understanding of the radiation distribution off off-shell quarks.

The radiation factor R , when squared and summed over spin, gives

$$\begin{aligned}
\sum_{\text{spin}} |R|^2 &= \left(\frac{p_4^\alpha}{V^2 + 2p_4 \cdot k} - \frac{p_3^\alpha}{V^2 + 2p_3 \cdot k} \right) \left(\frac{p_4^\beta}{V^2 + 2p_4 \cdot k} - \frac{p_3^\beta}{V^2 + 2p_3 \cdot k} \right) \sum \epsilon_\alpha^{a*}(k) \epsilon_\beta^{a'}(k) \\
&= \left(\frac{p_4^\alpha}{V^2 + 2p_4 \cdot k} - \frac{p_3^\alpha}{V^2 + 2p_3 \cdot k} \right) \left(\frac{p_4^\beta}{V^2 + 2p_4 \cdot k} - \frac{p_3^\beta}{V^2 + 2p_3 \cdot k} \right) (-g_{\alpha\beta}(k) \delta^{aa'}) \\
&= - \left| \frac{p_4}{V^2 + 2p_4 \cdot k} - \frac{p_3}{V^2 + 2p_3 \cdot k} \right|^2 \delta^{aa'} \\
&= \left(\frac{2p_4 \cdot p_3}{(V^2 + 2p_4 \cdot k)(V^2 + 2p_3 \cdot k)} - \frac{p_4^2}{(V^2 + 2p_4 \cdot k)^2} - \frac{p_3^2}{(V^2 + 2p_3 \cdot k)^2} \right) \delta^{aa'} \\
&= (2R_{43} - R_{44} - R_{33}) \delta^{aa'} \tag{6.6}
\end{aligned}$$

modulo the color factor, where $g_{\alpha\beta}$ is the metric. Our problem now boils down to simplify the quantity, $2R_{43} - R_{44} - R_{33}$ to get the necessary distribution.

To proceed further, we take the following form of the four-momenta for the radiating and the radiated particles:

$$\begin{aligned}
p_4 &= E_4(1, \vec{\beta}_4) \\
p_3 &= E_3(1, \vec{\beta}_3) \\
k &= \omega(1, \vec{n}) \tag{6.7}
\end{aligned}$$

where $\vec{\beta}_i$ is the velocity of the quark carrying a momentum \vec{p}_i and energy E_i and the gluon is emitted along direction \vec{n} with energy ω . If the radiating quark and antiquark were on-shell then one could write, for quark, say,

$$\begin{aligned} p_4^2 &= m^2 = E_4^2(1 - \beta_4^2) \\ \Rightarrow (1 - \beta_4^2) &= \frac{m^2}{E_4^2} = \frac{1}{\gamma_4^2} \end{aligned} \quad (6.8)$$

where γ is the Lorentz factor. But, for our present purpose we define,

$$(1 - \beta_4^2) = \frac{q^2}{E_4^2} = \frac{1}{\gamma_4^2}; \quad \text{and} \quad \beta_4 = \frac{p_4}{E_4} = \frac{p_4}{\sqrt{p_4^2 + p^2}} \quad (6.9)$$

Here γ_4 is almost but not exactly the Lorentz factor as we have considered small off-shellness of the partons here. Had β been that for an on-shell quark, it would have been

$$\beta_4 = \frac{p_4}{E_4} = \frac{p_4}{\sqrt{p_4^2 + m^2}} \quad (6.10)$$

But $p^2 \neq m^2$ for the present case and in that respect the relation in Eq. 6.9 becomes understandable.

The factor $\omega^2 R_{43}$ can be written as:

$$\omega^2 R_{43} = \frac{\omega^2 E_3 E_4 (1 - \beta_3 \beta_4 \cos \theta_{34})}{(V^2 + 2E_4 \omega (1 - \beta_4 \cos \theta_4))(V^2 + 2E_3 \omega (1 - \beta_3 \cos \theta_3))} \quad (6.11)$$

In the equal- β frame, where both particles have equal velocities back to back such that $\beta_3 = \beta_4$; $\theta \equiv \theta_3 = \theta_4 - \pi$; and $\theta_{34} = \theta_4 - \theta_3 = \pi$, we have $E_3 = E_4 = E$. In this frame we can write [3],

$$\begin{aligned}
\omega^2 R_{43} &= \frac{(1 + \beta^2)}{\left(\frac{V^2}{\omega E} + 2(1 - \beta \cos \theta)\right) \left(\frac{V^2}{\omega E} + 2(1 + \beta \cos \theta)\right)} \\
\omega^2 R_{33} &= \frac{(1 - \beta^2)}{\left(\frac{V^2}{\omega E} + 2(1 + \beta \cos \theta)\right)^2} \\
\omega^2 R_{44} &= \frac{(1 - \beta^2)}{\left(\frac{V^2}{\omega E} + 2(1 - \beta \cos \theta)\right)^2}
\end{aligned} \tag{6.12}$$

Hence the radiation factor reads:

$$\begin{aligned}
F &= \omega^2(2R_{43} - R_{44} - R_{33}) \\
&= 4\beta^2 \left(\frac{\frac{V^4}{\omega^2 E^2} + \frac{4V^2}{\omega E} + 4 \sin^2 \theta}{\left(\frac{V^4}{\omega^2 E^2} + \frac{4V^2}{\omega E} + 4(1 - \beta^2 \cos^2 \theta)\right)^2} \right)
\end{aligned} \tag{6.13}$$

The full radiation distribution, considering the color factors, can, however, be obtained from $|\mathcal{M}_{e^+e^- \rightarrow Q\bar{Q}g}|^2/|\mathcal{M}_{e^+e^- \rightarrow Q\bar{Q}}|^2$ using Eq. 4.10. So, the radiation distribution off virtual quarks heavy or light can be written as:

$$\begin{aligned}
\frac{dn_g}{d^2\vec{k}_\perp d\eta} &= \frac{64g^2\beta^2}{2(2\pi)^3} \frac{\chi^2 + 4\chi\omega + 4\omega^2 \sin^2 \theta}{(\chi^2 + 4\chi\omega + 4\omega^2(1 - \beta^2 \cos^2 \theta))^2} \\
&= \frac{16\alpha_s\beta^2}{\pi^2} \frac{\chi^2 + 4\chi\omega + 4\omega^2 \sin^2 \theta}{(\chi^2 + 4\chi\omega + 4\omega^2(1 - \beta^2 \cos^2 \theta))^2}
\end{aligned} \tag{6.14}$$

, where $\chi = V^2/E$ and $g^2 = 4\pi\alpha_s$ (α_s :strong coupling).

Next we explore different limits of F given in Eq. 6.13.

- For zero virtuality ($V = 0$) of the massive quark, Eq. 6.13 reduces to the conventional dead cone factor:

$$F = \omega^2(2R_{43} - R_{44} - R_{33}) \longrightarrow \frac{\beta^2 \sin^2 \theta}{(1 - \beta^2 \cos^2 \theta)^2} \quad (6.15)$$

This is the well-known conventional dead cone for a gluon emitted by a massive quark. The divergence of the factor is shielded by the quark mass or virtuality through $\beta (< 1)$. In fact, for on-shell quarks with small θ one can show that Eq. 6.15 (see [2]) boils down to:

$$F = \frac{1}{\theta^2} \frac{1}{(1 + \theta_0^2/\theta^2)^2}, \quad \theta_0 = m/E \quad (6.16)$$

- Now we investigate the light quark limit ($\beta = 1$). For $V = 0$, $\beta = 1$,

$$F \sim \frac{1}{\sin^2 \theta} \quad (6.17)$$

For light quarks Eq. 6.17 ensures the absence of dead-cone suppression at $\theta = 0$ and π for vanishing virtuality.

6.2 The radiation distribution off a virtual particle

For quantitative variation of F with energy E of the radiating partons, and angle θ between the radiating and radiated partons, we replace the virtuality by $V = \sqrt{q^2 - m^2} = \sqrt{E^2 - p^2 - m^2}$. The emitted gluon carry a fraction of parent parton energy. The variation of $F_{RH\theta} = F(E = 1.5\text{GeV}, \theta)/F(E = 1.5\text{GeV}, \theta = 0)$ with θ is depicted in Fig. 6.2. In Fig. 6.3 the variation of $F_{RHE} = F(E, \theta = \pi/4)/F(E = 100\text{GeV}, \theta = \pi/4)$ with E is displayed for heavy quarks. The results displayed in Figs. 6.2, 6.3 are evaluated for heavy quark mass, $m = 1.27$ GeV, emitted

gluon energy, $\omega = 20$ MeV, $\beta = 0.5$ and $V^2 = E^2 - \beta^2 E^2 - m^2$. It is interesting to note in Fig. 6.2 that for vanishingly small virtuality ($V^2 = 0.0746$ GeV²), the θ variation of the scaled spectrum shows the conventional dead cone that appears for massive on-shell quarks. In Fig. 6.3, larger the virtuality¹ is (which increases with parton energy, E) smaller the F_{RHE} becomes.

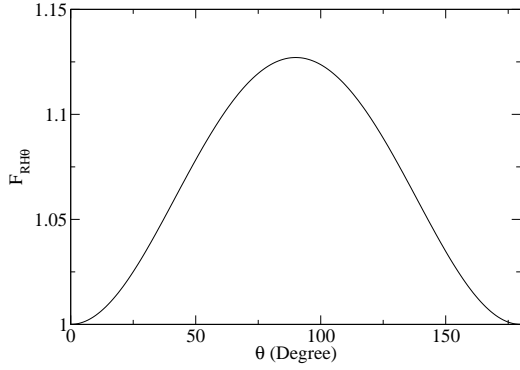


Figure 6.2: The variation of $F_{RH\theta}(E, \theta)$ with θ for $E = 1.5$ GeV.

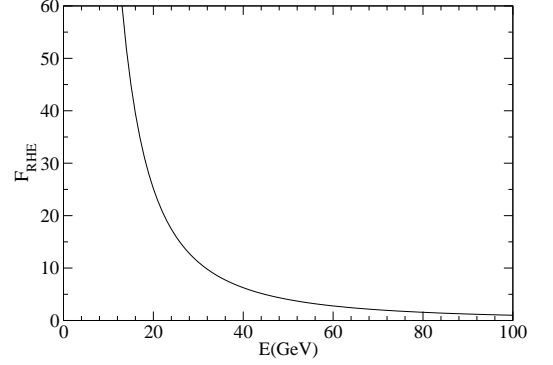


Figure 6.3: The variation of F_{RHE} with E for $\theta = \pi/4$.

In Fig. 6.4 the variation of $F_{RL\theta} = F(E = 3\text{GeV}, \theta)/F(E = 3\text{GeV}, \theta = 0)$ with θ is shown for light partons. In Fig. 6.5 the variation of $F_{RLE} = F(E, \theta = \pi/4)/F(E = 100\text{GeV}, \theta = \pi/4)$ with E is depicted. The results displayed in Figs. 6.4, 6.5 are evaluated for light quark mass $m = 0$ GeV, emitted gluon energy, $\omega = 30$ MeV, $\beta = 0.98$ and $V^2 = E^2 - \beta^2 E^2$. It is important to note in Fig. 6.4 that the variation of $F_{RL\theta}$ with θ for light quark with low virtuality ($V^2 = 0.36$ GeV²) is drastically different from the corresponding quantity, $F_{RH\theta}$ for heavy quark. This is obvious because for $V \rightarrow 0$ the light partons are not subjected to any dead cone suppression at $\theta = 0$ and π unlike heavy quarks. Moreover, the $\sin^{-2}\theta$ behaviour for light quarks (Eq. 6.17) ensures a minimum at $\theta = \pi/2$ as opposed to a maximum at the same θ for heavy quarks. However, for Fig. 6.5 we note that the behaviour of F_{RLE} with E is similar to that of F_{RHE} which indicates that the suppression due to virtuality overwhelm the effects due to the conventional dead cone.

¹If we take the liberty to extrapolate our calculation for large virtuality at all

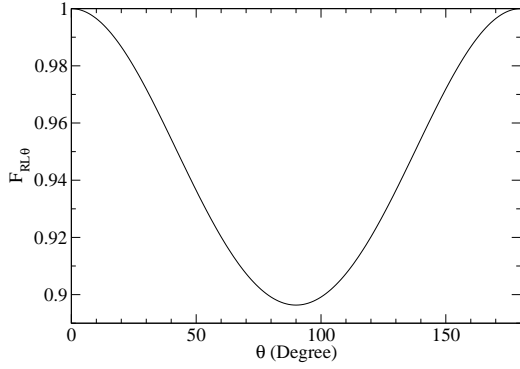


Figure 6.4: The variation of $F_{RL\theta}(E, \theta)$ with θ for $E = 3$ GeV.

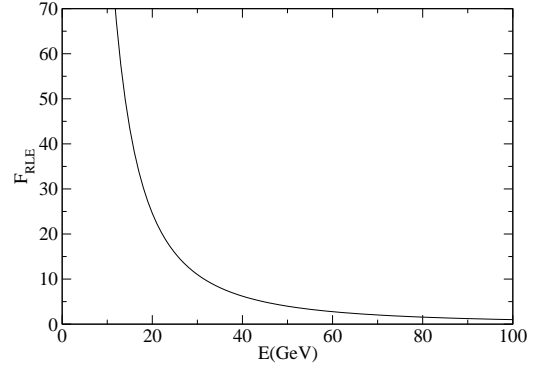


Figure 6.5: The variation of F_{RLE} with E for $\theta = \pi/4$

6.3 The Energy loss by a virtual particle

The high virtuality of a particle is an effect of large amount of momentum transferred to it due to nucleus-nucleus scattering. From the field line viewpoint, the lines of forces of an accelerated particle is highly tampered and since lines of forces are infinitely extended, all of its parts cannot reorient themselves according to the acceleration given to it (see chapter 2 for detailed discussion about this issue). Essentially, the produced high momentum parton is lacking the part of field which does not follow it. The charged particle will try to get back its old configuration of lines of forces by radiating and this radiation stops as soon as the particle regains it [4]. So when a virtual particle scatters and gives off some radiation before it has regained its old configuration, the emitted radiation spectrum can only have the high frequency part of the field which could follow it. More the energy (equivalently, virtuality) of the particle is, less and less portion of the field associated with the charge particle becomes available for energy loss; and hence the radiation spectrum off virtual particles decreases with increasing energy. This phenomenon is reflected in Figs. 6.3 and 6.5. The spectrum of heavy and light virtual particles are similarly suppressed when subjected to the similarly high virtuality (Figs. 6.3 and 6.5). Consequently, they will lose similar energy [5].

We can estimate the energy loss by a virtual particle after the traversal of a path length L due to gluons which have lost coherence during this time following [5] but using the radiation

spectrum of Eq. 6.14. When we plot energy loss with respect to the path length, as in Fig. 6.6, we see that up to the length $0.1 - 1$ fm, which is of the order of the lifetime of QGP, the heavy and light partons lose similar energy. This finding is similar to that of Ref. [5]. Only after the said length, the dead-cone of heavy quark starts playing its part and heavy partons lose less energy. For a charm, quark, for example, of energy 10 GeV, the length after which the heavy quark energy loss will be less than the light partons, is $\sim 1/p_g$ fm [5], where p_g is the momentum fraction of the emitted gluon. Since the radiation spectrum is dominated by very small p_g gluons, there exists a likelihood that the virtual particles do not get back their ‘on-shellness’ before hadronization.

So, our message is, the energy loss of energetic partons, which enter QGP as probes, must be treated with caution as the virtuality of quarks is seen to play an important part. On that note, the present work may throw some light on the similar suppression of electrons from heavy and light quarks in RHIC experiments ([6]).

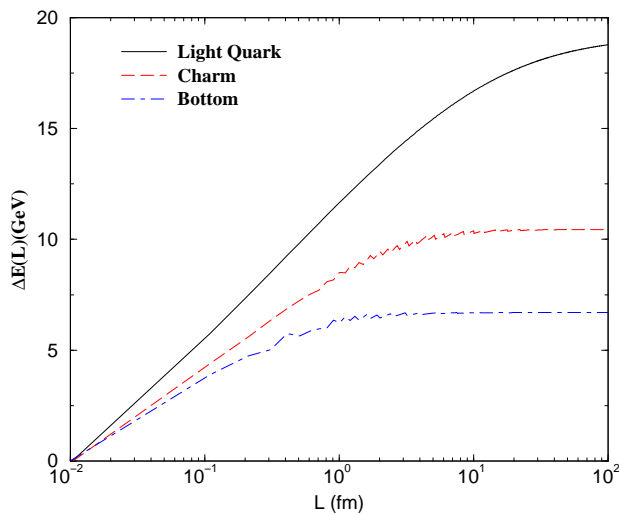


Figure 6.6: Variation of vacuum energy loss of a virtual particle with length.

Bibliography

- [1] K. M. Paul Ph. D. Thesis, University of Illinois at Urbana-Champaign, 2002
- [2] Y. L. Dokshitzer and D. E. Kharzeev, Phys. Lett. B **519**, 199 (2001)
- [3] T. Bhattacharyya and J. Alam, Int. Jour. of Mod. Phys. A **28**, 1350031(2013)
- [4] F. Niedermayer, Phys. Rev. D **34**, 3494(1986)
- [5] B. Z. Kopeliovich, I. K. Potashnikova, I. Schmidt, Phys. Rev. C **82**, 037901(2010)
- [6] A. Adare *et al.* (PHENIX Collaboration), Phys. Rev. Lett. **98**, 172301 (2007); B. I. Abelev *et al.* (STAR Collaboration), Phys. Rev. Lett. **98**, 192301 (2007)

Chapter 7

Summary and Outlook

We wrap up our discussion with the summary of the works presented in this dissertation and we will try to explore where the present works may lead to. Any work is, by no means, complete and there will always be scopes of improvements over the existing formalism. The summary and future scopes will thus be an intertwined platform of discussion where, at places, after summarizing some part of our work we will indicate the future scopes of generalizations.

As far as the subject matter of this dissertation, the study of energy loss of energetic particles, is concerned, it is an age-old topic where we have tried to make a continuous transition from the calculation of Classical Electrodynamics to that of the Quantum Electro(and/or Chromo)dynamics. Given all that, we find it an opportunity to learn the physical (sometimes philosophical) niceties of this beautiful phenomenon of nature. We concentrated on explaining the meaning of radiation *i.e* what physical situations will compel one to tell that there is radiation at all. We have defined the formation length of radiation — the length the radiated photons/gluons take to be separated from the parent particle by one Compton length. We have also calculated the electric field off a moving charge and argued that a (colour or electric) charge, when Lorentz boosted, acquire sea of virtual particles, the Weizsäcker-Williams particles and have discussed how they can metamorphose into radiation once there is acceleration.

In conclusion, we commented that to find the Poynting's vector and integrating it over a surface, large enough, is equivalent to calculating the number of gluons emitted from the Feynman diagram technique of Quantum Field Theory. We hope that by dint of these discussions, we are able to show how the classical theory can have a smooth voyage towards the quantum calculations (chapter 2).

We have emphasized on a strange fact that when the radiation is soft *i.e.* its energy is much smaller than that of the emitting particle, the distribution of radiation is independent of what type of process the emitting particle has undergone in the collisional or elastic part of the diagram. Based on this we are able to factorize the square of the radiation current, the radiation distribution, from the elastic part. We must remember that the situation becomes complicated when there is medium. Not only that the mass and life-time of the propagating particle change, it undergoes multiple scattering also. When there is radiation in multiple scattering, there are possibilities of quantum interference among the scattering amplitudes, the LPM effect as opposed to the Bethe-Heitler case where the scattering processes add up and hence the total energy loss adds up with increasing number of scatterings. As far as the title goes, our main aim is to estimate the energy loss of an energetic particle inside QGP. What we mean by energetic particle is a particle whose energy is so high that the radiative loss will dominate. The potential model (the Gyulassy-Wang potential model, GWPM, to be precise) for multiple scattering has been discussed where the calculations are done in a frame where motion of the bath particles (average momentum $\sim T$, T : temperature) is neglected compared to that of the incoming particle having energies of several GeVs. In the potential model calculations, the radiation distribution off fast particles can be calculated and the multiple scattering scenario can be introduced. Due to negligible motion of the bath particles in comparison with the fast incoming particles, the Feynman diagrams with the bath particles radiating are kinetically suppressed (chapter 3).

When we calculate the radiation distributions off either gluons or quarks in Chapters 4, 5 and 6 respectively, relaxing kinematic approximations like non-eikonicity or considerations of on-shellness, we calculate it for the single scattering. We see in chapter 4 that the non-eikonal correction to the widely used Gunion-Bertsch formula significantly modifies the energy loss and the gluon thermalization rate inside QGP obtainable from Refs. [1, 2]. In chapter 5, the non-eikonal radiation distribution off moderately energetic heavy quarks has been calculated and the ‘dead cone’ region is seen to vanish. The proper limits of the formula of Eq. 5.23 generalizes the main results of Refs. [3, 4]. In chapter 7 we wanted to find out the radiation distribution off quarks whose off-shellness due to huge acceleration received from collision is taken in to account. We derived a formula for the corresponding radiation distribution and showed that with vanishing virtuality the formula reproduces those for the on-shell quarks.

Now, the distribution due to multiple scattering is what energy loss models primarily talk about. If we announce that we are going to relax the kinematic approximations in energy loss models, we must find a way to incorporate the multiple scattering, too. The computation of multiple scattering has so far been done in scalar QCD approach (potential model), thermal QCD approach (AMY) etc. The potential picture helps reduce the number of Feynman diagrams to a considerable extent because one, then, neglects the diagrams containing the radiation from the bath particles. But the single scattering amplitudes calculated in the present dissertation is done in the Feynman gauge and then the distribution is multiplied with the factor due to multiple scattering appearing in the GWPM in an ad hoc way. So, if we are to find a consistent way to incorporate multiple scattering in Feynman gauge, we are going to meet with larger number of diagrams than that in light cone gauge calculations in potential model. So, it remains to find out how we can tackle this problem of large number of diagrams in multiple scattering.

All the calculations of radiation distributions in the present dissertation assumes the Gribov’s limit (see Sec. 3.1.3). We must find out how to remove the Gribov limit approximation in the

calculation; and this leads to considering the diagrams with non-abelian three-gluon vertices in the propagator – the gluon radiation off a propagator gluon, for example. Ultimately, all these results in the removal of ‘soft approximation’ in energy loss models, the next possible venture in relaxing the approximations at the level of single scattering, at least.

After a consistent way of incorporating multiple scattering with unapproximated matrix elements, we can set out for finding out the nuclear suppression factor for the energetic particles. The medium evolution has also to be incorporated in which arena the study of adiabatic approximation in evolution equations of both the probe and the medium will be worth perusing. While it is interesting to see how the collisional effects modify the radiation distribution off heavy quarks and the dead-cone vanishes, the effect of collision (or recoil due to collision, more precisely) on observables is yet to find out.

When comes the context of collision, who can forget the divergences in collisional cross-section due to massless particle exchange ? While the infra-red divergence in the longitudinal spectral functions are shielded by the HTL resummation, the magnetic scale divergence is shielded by adding magnetic screening mass much in the same way as the divergence in electric scale (t channel divergence) was shielded by Debye screening mass. The shielding of magnetic scale divergence calls for the consideration of density. So, Hard Dense Loop (HDL) calculations are natural extensions. But HDL is for zero-temperature plasma only. So, density plus temperature, still we don’t know how to tackle.

So, these are all we wanted to say. We tried to present a consistent and continuous story about radiations, or rather, our tryst with radiation. It was an interesting journey — adding an extra bit of information to a text-book based on the information we have. It is exciting — telling a story. It is exciting — to cook up the story. It gives pleasure — if someone enjoys the story.

Bibliography

- [1] S. K. Das and J. Alam, Phys. Rev. D **82**, 051502(R), (2010).
- [2] R. Abir, C. Greiner, M. Martinez, and M. G. Mustafa, Phys. Rev. D **83**, 011501 (R) (2011)
- [3] R. Abir, C. Greiner, M. Martinez, M. G. Mustafa and J. Uphoff, Phys. Rev. D **85**, 054012(2012).
- [4] R. Abir, Phys. Rev. D **87**, 034036(2013).

Appendix A:

In this appendix we derive Eq. 4.5 for the square of the invariant amplitude for the radiative process, $gg \rightarrow ggg$ upto orders $\mathcal{O}(k_\perp^0)$ and $\mathcal{O}(\frac{t^3}{s^3})$. Consider the reaction

$$g(k_1) + g(k_2) \rightarrow g(k_3) + g(k_4) + g(k_5), \quad (\text{A.1})$$

where k_5 is the four-momentum of the radiated gluon. The Mandelstam variables for the above process are defined as

$$\begin{aligned} s &= (k_1 + k_2)^2, & t &= (k_1 - k_3)^2 \\ u &= (k_1 - k_4)^2, & s' &= (k_3 + k_4)^2 \\ t' &= (k_2 - k_4)^2, & u' &= (k_2 - k_3)^2. \end{aligned} \quad (\text{A.2})$$

Because gluons massless we can write

$$\begin{aligned} k_1.k_2 &= \frac{s}{2}, & k_1.k_3 &= -\frac{t}{2} \\ k_1.k_4 &= -\frac{u}{2}, & k_3.k_4 &= \frac{s'}{2} \\ k_2.k_4 &= -\frac{t'}{2}, & k_2.k_3 &= -\frac{u'}{2}. \end{aligned} \quad (\text{A.3})$$

We also have the relations

$$\begin{aligned} k_1.k_5 &= \frac{s+t+u}{2}, & k_2.k_5 &= \frac{s+t'+u'}{2} \\ k_3.k_5 &= \frac{s+t'+u}{2}, & k_4.k_5 &= \frac{s+t+u'}{2}. \end{aligned} \quad (\text{A.4})$$

For soft gluon emission,

$$s+t+u+s'+t'+u'=0. \quad (\text{A.5})$$

The matrix element square of the radiative process $gg \rightarrow ggg$ is given by [1]

$$\begin{aligned} |M_{gg \rightarrow ggg}|^2 &= \frac{1}{2}g^6 \frac{N_c^3}{N_c^2 - 1} \frac{\mathcal{N}}{\mathcal{D}} [(12345) + (12354) + (12435) \\ &+ (12453) + (12534) + (12543) + (13245) + (13254) + (13425) \\ &+ (13524) + (14235) + (14325)], \end{aligned} \quad (\text{A.6})$$

where N_c is the number of colors, $g = \sqrt{4\pi\alpha_s}$ is the strong coupling,

$$\begin{aligned} \mathcal{N} &= (k_1.k_2)^4 + (k_1.k_3)^4 + (k_1.k_4)^4 + (k_1.k_5)^4 + (k_2.k_3)^4 + (k_2.k_4)^4 + (k_2.k_5)^4 \\ &+ (k_3.k_4)^4 + (k_3.k_5)^4 + (k_4.k_5)^4, \end{aligned} \quad (\text{A.7})$$

$$\mathcal{D} = (k_1.k_2)(k_1.k_3)(k_1.k_4)(k_1.k_5)(k_2.k_3)(k_2.k_4)(k_2.k_5)(k_3.k_4)(k_3.k_5)(k_4.k_5), \quad (\text{A.8})$$

and

$$(ijklm) = (k_i.k_j)(k_j.k_k)(k_k.k_l)(k_l.k_m)(k_m.k_i). \quad (\text{A.9})$$

Simplifying Eq. A.6 we get,

$$\begin{aligned}
|M_{\text{gg} \rightarrow \text{ggg}}|^2 &= 16g^6 \frac{N_c^3}{N_c^2 - 1} \mathcal{N} \left[\frac{1}{s'(s+u+t)(s+u'+t')} \left[\frac{1}{tt'} + \frac{1}{uu'} \right] \right. \\
&+ \frac{1}{s(s+u+t)(s+u'+t)} \left[\frac{1}{tt'} + \frac{1}{uu'} \right] - \frac{1}{t'(s+u+t)(s+u'+t')} \left[\frac{1}{uu'} + \frac{1}{ss'} \right] \\
&- \frac{1}{u'(s+u+t)(s+u'+t)} \left[\frac{1}{tt'} + \frac{1}{ss'} \right] - \frac{1}{u(s+u'+t')(s+u+t)} \left[\frac{1}{tt'} + \frac{1}{ss'} \right] \\
&\left. - \frac{1}{t(s+u'+t')(s+u'+t)} \left[\frac{1}{uu'} + \frac{1}{ss'} \right] \right]; \tag{A.10}
\end{aligned}$$

and \mathcal{N} can now be written as

$$\begin{aligned}
\mathcal{N} &= \frac{1}{16} [s^4 + t^4 + u^4 + s'^4 + t'^4 + u'^4 + (s+t+u)^4 + (s+t'+u')^4 \\
&\quad + (s+t'+u)^4 + (s+t+u')^4]. \tag{A.11}
\end{aligned}$$

For a soft gluon emission ($k_5 \rightarrow 0$) $s \rightarrow s'$, $t \rightarrow t'$, $u \rightarrow u'$. We can express the transverse momentum of the emitted gluon as

$$\begin{aligned}
k_\perp^2 &= 4(k_1 \cdot k_5)(k_2 \cdot k_5)/s \\
&= (s+t+u)(s+t'+u') \\
&= (s+t+u)^2/s \\
&\cdot \tag{A.12}
\end{aligned}$$

Using Eqs. A.10, A.11 and A.12, the square of the matrix element can be written as

$$\begin{aligned}
|M|_{\text{gg} \rightarrow \text{ggg}}^2 &= \frac{27}{2} g^6 (s^4 + t^4 + u^4 + 2s^2 k_{\perp}^4) \frac{1}{s k_{\perp}^2} \left[\frac{1}{s} \left(\frac{1}{t^2} + \frac{1}{u^2} \right) - \frac{1}{t} \left(\frac{1}{s^2} + \frac{1}{u^2} \right) - \frac{1}{u} \left(\frac{1}{t^2} + \frac{1}{s^2} \right) \right] \\
&= g^2 \left(\frac{27}{2} g^4 s^4 \right) \left(1 + \frac{t^4}{s^4} + \frac{u^4}{s^4} + 2 \frac{k_{\perp}^4}{s^2} \right) \frac{1}{s^2 k_{\perp}^2 t^2} \left[1 + \frac{t^2}{u^2} - \frac{t}{s} - \frac{st}{u^2} - \frac{s}{u} - \frac{t^2}{us} \right] \\
&= g^2 \left(\frac{9}{2} g^4 \frac{s^2}{t^2} \right) \left(3 + 3 \frac{t^4}{s^4} + 3 \frac{u^4}{s^4} + 6 \frac{k_{\perp}^4}{s^2} \right) \frac{1}{k_{\perp}^2} \\
&\quad \times \left[1 + \frac{t^2}{u^2} - \frac{t}{s} - \frac{st}{u^2} - \frac{s}{u} - \frac{t^2}{us} \right] \\
&= g^2 \left(\frac{9}{2} g^4 \frac{s^2}{t^2} \right) \left(3 \left(1 + \frac{u^4}{s^4} \right) + 3 \frac{t^4}{s^4} + 6 \frac{k_{\perp}^4}{s^2} \right) \frac{1}{k_{\perp}^2} \\
&\quad \times \left[1 - \frac{s}{u} - \left(1 + \frac{s^2}{u^2} \right) \frac{t}{s} + \left(\frac{s^2}{u^2} - \frac{s}{u} \right) \frac{t^2}{s^2} \right] \\
&= g^2 |M_{\text{gg} \rightarrow \text{gg}}|^2 \left(3 \left(1 + \frac{u^4}{s^4} \right) + 3 \frac{t^4}{s^4} + 6 \frac{k_{\perp}^4}{s^2} \right) \frac{1}{k_{\perp}^2} \\
&\quad \times \left[\left(1 - \frac{s}{u} \right) - \left(1 + \frac{s^2}{u^2} \right) \frac{t}{s} + \left(\frac{s^2}{u^2} - \frac{s}{u} \right) \frac{t^2}{s^2} \right], \tag{A.13}
\end{aligned}$$

where the subscript GB stands for the approximation used by Gunion and Bertsch [2]. For the elastic process,

$$|M_{\text{gg} \rightarrow \text{gg}}|^2 = \frac{9}{2} g^4 \frac{s^2}{t^2}. \tag{A.14}$$

On simplifying Eq. A.13 we obtain,

$$\begin{aligned}
|M|_{\text{gg} \rightarrow \text{ggg}}^2 &= g^2 |M_{\text{gg} \rightarrow \text{gg}}|^2 \frac{1}{k_{\perp}^2} \left[\left(3 - 3 \frac{s}{u} + 3 \frac{u^4}{s^4} - 3 \frac{u^3}{s^3} \right) - \left(3 \frac{t}{s} + 3 \frac{st}{u^2} + 3 \frac{u^4 t}{s^5} + 3 \frac{u^2 t}{s^3} \right) \right. \\
&\quad + \left(3 \frac{t^2}{u^2} - 3 \frac{t^2}{us} + 3 \frac{u^2 t^2}{s^4} - 3 \frac{u^3 t^2}{s^5} \right) + \left(3 \frac{t^4}{s^4} - 3 \frac{t^4}{us^3} \right) \\
&\quad - \left(3 \frac{t^5}{s^5} + 3 \frac{t^5}{u^2 s^3} \right) + \left(3 \frac{t^6}{u^2 s^4} - 3 \frac{t^6}{us^5} \right) + \left(6 \frac{k_{\perp}^4}{s^2} - 6 \frac{k_{\perp}^4}{us} \right) - \left(6 \frac{k_{\perp}^4 t}{s^3} + 6 \frac{k_{\perp}^4 t}{u^2 s} \right) \\
&\quad \left. + \left(6 \frac{k_{\perp}^4 t^2}{u^2 s^2} - 6 \frac{k_{\perp}^4 t^2}{us^3} \right) \right]. \tag{A.15}
\end{aligned}$$

In the proposed kinematic limit we set terms which are linear in k_\perp to zero and keep terms $\mathcal{O}(k_\perp^0)$, $\mathcal{O}(k_\perp^{-1})$, and $\mathcal{O}(k_\perp^{-2})$ in $|M|_{gg \rightarrow ggg}^2$. We also neglect terms $\mathcal{O}(\frac{t^4}{s^4})$ and higher order in the matrix element. To proceed further one needs to express the Mandelstam variable u in terms of s , t , and k_\perp by using the following relation:

$$\begin{aligned}
k_\perp^2 &= \frac{(s+t+u)^2}{s} \\
\Rightarrow u &= \sqrt{s}k_\perp - s - t \\
\Rightarrow \frac{1}{u} &= \frac{1}{(\sqrt{s}k_\perp - s - t)} \\
\Rightarrow \frac{1}{u} &= -\frac{1}{s} \left[1 - \left(\frac{k_\perp}{\sqrt{s}} - \frac{t}{s} \right) \right]^{-1} \\
\Rightarrow \frac{1}{u} &\approx -\frac{1}{s} \left[1 + \left(\frac{k_\perp}{\sqrt{s}} - \frac{t}{s} \right) + \left(\frac{k_\perp}{\sqrt{s}} - \frac{t}{s} \right)^2 + \left(\frac{k_\perp}{\sqrt{s}} - \frac{t}{s} \right)^3 + \left(\frac{k_\perp}{\sqrt{s}} - \frac{t}{s} \right)^4 + \left(\frac{k_\perp}{\sqrt{s}} - \frac{t}{s} \right)^5 + \dots \right]
\end{aligned} \tag{A.16}$$

The binomial expansion of $[1 - (\frac{k_\perp}{\sqrt{s}} - \frac{t}{s})]^{-1}$ converges if $(\frac{k_\perp}{\sqrt{s}} - \frac{t}{s}) < 1$. For the kinematic limit mentioned above *i.e.* for $k_\perp \rightarrow 0$ and keeping terms upto $\mathcal{O}(\frac{t^3}{s^3})$, the inequality $(\frac{k_\perp}{\sqrt{s}} - \frac{t}{s}) < 1$ is satisfied. We have checked that terms beyond $(\frac{k_\perp}{\sqrt{s}} - \frac{t}{s})^5$ in the expression of $\frac{1}{u}$ are not required for the kinematic limit under consideration. With all these we get,

$$\frac{1}{u} = -\frac{1}{s} \left[\left(1 - \frac{t}{s} + \frac{t^2}{s^2} - \frac{t^3}{s^3} \right) + \left(\frac{1}{\sqrt{s}} - \frac{2t}{s\sqrt{s}} + \frac{3t^2}{s^2\sqrt{s}} \right) k_\perp + \left(\frac{1}{s} - \frac{3t}{s^2} + \frac{6t^2}{s^3} \right) k_\perp^2 \right] \tag{A.17}$$

Similarly $1/u^2$ can be written as

$$\frac{1}{u^2} = \frac{1}{s^2} \left[\left(1 - \frac{2t}{s} + \frac{3t^2}{s^2} - \frac{4t^3}{s^3} \right) + \left(\frac{2}{\sqrt{s}} - \frac{6t}{s\sqrt{s}} + \frac{12t^2}{s^2\sqrt{s}} \right) k_\perp + \left(\frac{3}{s} - \frac{12t}{s^2} + \frac{30t^2}{s^3} \right) k_\perp^2 \right] \tag{A.18}$$

For the assumed kinematic conditions u^4/s^4 can be expressed as follows:

$$\frac{u^4}{s^4} = \left[\left(1 + \frac{4t}{s} + \frac{6t^2}{s^2} + \frac{4t^3}{s^3} \right) - \left(\frac{4}{\sqrt{s}} + \frac{12t}{s\sqrt{s}} + \frac{12t^2}{s^2\sqrt{s}} \right) k_{\perp} + \left(\frac{6}{s} + \frac{12t}{s^2} + \frac{6t^2}{s^3} \right) k_{\perp}^2 \right] \quad (\text{A.19})$$

Similarly,

$$\frac{u^3}{s^3} = - \left[\left(1 + \frac{3t}{s} + \frac{3t^2}{s^2} + \frac{t^3}{s^3} \right) - \left(\frac{3}{\sqrt{s}} + \frac{6t}{s\sqrt{s}} + \frac{3t^2}{s^2\sqrt{s}} \right) k_{\perp} + \left(\frac{3}{s} + \frac{3t^2}{s^2} \right) k_{\perp}^2 \right] \quad (\text{A.20})$$

and

$$\frac{u^2}{s^2} = \left[\left(1 + \frac{2t}{s} + \frac{t^2}{s^2} \right) - \left(\frac{2}{\sqrt{s}} + \frac{2t}{s\sqrt{s}} \right) k_{\perp} + \frac{1}{s} k_{\perp}^2 \right] \quad (\text{A.21})$$

Putting Eqs. A.17 to A.21 in A.15 we get,

$$\begin{aligned} |M|_{\text{gg} \rightarrow \text{ggg}}^2 &= 12g^2 |M_{\text{gg} \rightarrow \text{gg}}|^2 \frac{1}{k_{\perp}^2} \\ &\times \left[\left(1 + \frac{t}{2s} + \frac{5t^2}{2s^2} - \frac{t^3}{s^3} \right) - \left(\frac{3}{2\sqrt{s}} + \frac{4t}{s\sqrt{s}} - \frac{3t^2}{2s^2\sqrt{s}} \right) k_{\perp} + \left(\frac{5}{2s} + \frac{t}{2s^2} + \frac{5t^2}{s^3} \right) k_{\perp}^2 \right] \end{aligned} \quad (\text{A.22})$$

The terms $\mathcal{O}(k_{\perp}^{-1})$ and $\mathcal{O}(k_{\perp}^0)$ contribute to the energy loss of the gluons in a gluonic plasma and hence are important for heavy-ion phenomenology at RHIC and LHC energies. These terms were absent in the previous work [3] (also in [4])

Bibliography

- [1] F. A. Berendes *et al.*, Phys. Lett. B **103**, 124(1981).
- [2] J. F. Gunion and G. Bertsch, Phys. Rev. D **25**, 746(1982).
- [3] R. Abir, C. Greiner, M. Martinez, and M. G. Mustafa, Phys. Rev. D **83**, 011501 (R) (2011)
- [4] S. K. Das and J. Alam, Phys. Rev. D **82**, 051502(R), (2010).

Appendix B:

In this Appendix we show the calculation of the binary combination of amplitudes of the $Qq \rightarrow Qqg$ process.

1. Finding out the dot products with gluon momentum

Let us find out the dot products of the quark momenta with that of the emitted gluon which appear in the denominator of the matrix elements considering the following choice of four-momenta in centre of momentum (COM) frame in soft limit:

$$\begin{aligned} k_1 &\equiv (E_1, \vec{0}_\perp, k_{1z}), & k_2 &\equiv (E_2, \vec{0}_\perp, -k_{1z}), \\ k_3 &\equiv (E_3, \vec{q}_\perp, k_{3z}), & k_4 &\equiv (E_4, -\vec{q}_\perp, -k_{3z}) \\ k_5 &\equiv (\omega = k_\perp \operatorname{cosec} \theta, \vec{k}_\perp, k_z = k_\perp \cot \theta) \end{aligned} \tag{B.1}$$

Hence

$$\begin{aligned}
k_1.k_5 &= E_1 k_\perp \operatorname{cosec} \theta - k_{1z} k_\perp \cot \theta \\
&= \sqrt{k_{1z}^2 + M^2} k_\perp \operatorname{cosec} \theta - k_{1z} k_\perp \cot \theta \\
&= k_{1z} k_\perp \left(\sqrt{1 + M^2/k_{1z}^2} \operatorname{cosec} \theta - k_{1z} k_\perp \cot \theta \right) \\
&= \frac{s - M^2}{2\sqrt{s}} k_\perp \left(\sqrt{1 + \frac{4M^2/s}{(1 - M^2/s)^2}} \operatorname{cosec} \theta - \cot \theta \right) \\
&\quad \left(\text{putting } k_{1z} = \frac{(s - M^2)}{2\sqrt{s}} \right)
\end{aligned} \tag{B.2}$$

$$\begin{aligned}
k_2.k_5 &= E_2 k_\perp \operatorname{cosec} \theta + k_{1z} k_\perp \cot \theta \\
&= k_{1z} k_\perp \operatorname{cosec} \theta + k_{1z} k_\perp \cot \theta \\
&= k_{1z} k_\perp (\operatorname{cosec} \theta + \cot \theta)
\end{aligned} \tag{B.3}$$

Unlike the previous (eikonal) case where $k_1.k_5 = k_3.k_5$ and $k_2.k_5 = k_4.k_5$ (because q_\perp is zero), we can express $k_3.k_5$ and $k_4.k_5$ as factors of $k_1.k_5$ and $k_2.k_5$ respectively in the following way,

$$\begin{aligned}
k_3.k_5 &= E_3 k_\perp \operatorname{cosec} \theta - q_\perp k_\perp - k_{3z} k_\perp \cot \theta \\
&= k_{1z} k_\perp \left(\sqrt{1 + \frac{4M^2/s}{(1 - M^2/s)^2}} \operatorname{cosec} \theta - \sqrt{1 - \frac{q_\perp^2}{k_{1z}^2}} \cot \theta - \frac{q_\perp}{k_{1z}} \right) \\
&= k_{1z} k_\perp \left(\sqrt{1 + \frac{4M^2/s}{(1 - M^2/s)^2}} \operatorname{cosec} \theta - \cot \theta \right) \times \\
&\quad \underbrace{\left(1 + \frac{\cot \theta \left(1 - \sqrt{1 - \frac{q_\perp^2}{k_{1z}^2}} \right) - \frac{q_\perp}{k_{1z}}}{\left(\sqrt{1 + \frac{4M^2/s}{(1 - M^2/s)^2}} \operatorname{cosec} \theta - \cot \theta \right)} \right)}_{\mathcal{F}_{35}} \\
&= k_1.k_5 \mathcal{F}_{35}
\end{aligned} \tag{B.4}$$

So we see that the effect of non-eikonality is contained inside the factor \mathcal{F}_{35} . Much in the same way, the factor \mathcal{F}_{45} below appears once we consider the bending of the heavy quark jet.

$$\begin{aligned}
k_4.k_5 &= E_4 k_\perp \operatorname{cosec} \theta + q_\perp k_\perp + k_{3z} k_\perp \cot \theta \\
&= k_{1z} k_\perp \left(\operatorname{cosec} \theta + \sqrt{1 - \frac{q_\perp^2}{k_{1z}^2}} \cot \theta + \frac{q_\perp}{k_{1z}} \right) \\
&= k_{1z} k_\perp (\operatorname{cosec} \theta + \cot \theta) \underbrace{\left(1 - \frac{\cot \theta \left(1 - \sqrt{1 - \frac{q_\perp^2}{k_{1z}^2}} \right) - \frac{q_\perp}{k_{1z}}}{(\operatorname{cosec} \theta + \cot \theta)} \right)}_{\mathcal{F}_{45}} \\
&= k_2.k_5 \mathcal{F}_{45}
\end{aligned} \tag{B.5}$$

So, once we know the dot products in terms of the gluon emission angle θ , we can replace them in the denominator as will be done in the section to come.

2. The matrix elements

In the present section, we deliniate the calculation of amplitudes (genuine and interference) for the process $Q(k_1, k)q(k_2, n) \rightarrow Q(k_3, i)q(k_2, l)g(k_5, b)$, where k_i denote the four momenta of heavy quark (Q) or light quark (q) or gluon (g) with i, k, n, b denoting the colors.

Interference of Amplitudes with themselves (Genuine Amplitudes)

In the non-eikonal limit and within $\mathcal{O}(1/k_\perp^2)$ we have the following ‘genuine’ amplitudes.

$$\begin{aligned}
\mathcal{M}_1 \otimes \mathcal{M}_1^\dagger &\approx -g^6 \frac{8}{3 \times 36} \frac{(64M^6 - 128M^4s + 64M^2s^2 + 64M^2st + 32M^2t^2)}{t^2(2k_1 \cdot k_5)^2} \\
&= -g^6 \frac{8}{3 \times 36} 64M^2s^2 \left[\frac{\left(1 - \frac{M^2}{s}\right)^2 + \frac{t}{s} + \frac{t^2}{2s^2}}{t^2(2k_1 \cdot k_5)^2} \right] \\
&\approx -g^6 \frac{8}{3 \times 36} 64M^2s^2 \frac{\left(1 - \frac{M^2}{s}\right)^2 + \frac{t}{s} + \frac{1}{2} \frac{t^2}{s^2}}{\frac{(s-M^2)^2}{s} k_\perp^2 \left(\sqrt{1 + \frac{4M^2}{(1-\frac{M^2}{s})^2}} \operatorname{cosec} \theta - \cot \theta \right)^2} \\
&= \frac{128}{27} g^6 \frac{s^2}{t^2} \frac{1}{k_\perp^2} \left(\frac{-M^2}{s \tan^2 \frac{\theta}{2}} \right) \left(\frac{1 - \frac{M^2}{s}}{1 + \frac{M^2}{s \tan^2 \frac{\theta}{2}}} \right)^2 \left[1 + \frac{\frac{t}{s} \left(1 + \frac{t}{2s}\right)}{\left(1 - \frac{M^2}{s}\right)^2} \right] \\
&= \frac{128}{27} g^6 \frac{s^2}{t^2} \frac{1}{k_\perp^2} \left(-1 - \frac{M^2}{s \tan^2 \frac{\theta}{2}} + 1 \right) \left(\frac{1 - \frac{M^2}{s}}{1 + \frac{M^2}{s \tan^2 \frac{\theta}{2}}} \right)^2 \left[1 + \frac{\frac{t}{s} \left(1 + \frac{t}{2s}\right)}{\left(1 - \frac{M^2}{s}\right)^2} \right] \\
&= \frac{128}{27} g^6 \frac{s^2}{t^2} \frac{1}{k_\perp^2} \left(\frac{M^2}{s} - 1 + \frac{1 - \frac{M^2}{s}}{1 + \frac{M^2}{s \tan^2 \frac{\theta}{2}}} \right) \left(\frac{1 - \frac{M^2}{s}}{1 + \frac{M^2}{s \tan^2 \frac{\theta}{2}}} \right) \left[1 + \frac{\frac{t}{s} \left(1 + \frac{t}{2s}\right)}{\left(1 - \frac{M^2}{s}\right)^2} \right] \\
&= \frac{128}{27} g^6 \frac{s^2}{t^2} \frac{1}{k_\perp^2} (\Delta_M^2 - 1 + \mathcal{J}) \mathcal{J} \left(1 + \frac{f_1}{(1 - \Delta_M^2)^2} \right) \tag{B.6}
\end{aligned}$$

As well as,

$$\begin{aligned}
\mathcal{M}_3 \otimes \mathcal{M}_3^\dagger &\approx -g^6 \frac{8}{3 \times 36} \frac{\left(1 - \frac{M^2}{s}\right)^2 + \frac{t}{s} + \frac{t^2}{2s^2}}{4 \frac{(s-M^2)^2}{4s} k_\perp^2 \left(\sqrt{1 + \frac{4M^2}{(1-\frac{M^2}{s})^2}} \operatorname{cosec} \theta - \cot \theta\right)^2} \mathcal{F}_{35}^2 \\
&= \frac{128}{27} g^6 \frac{s^2}{t^2} \frac{1}{k_\perp^2} \left(\frac{-M^2}{s \tan^2 \frac{\theta}{2}}\right) \left(\frac{1 - \frac{M^2}{s}}{1 + \frac{M^2}{s \tan^2 \frac{\theta}{2}}}\right)^2 \left[1 + \frac{\frac{t}{s} (1 + \frac{t}{2s})}{(1 - \frac{M^2}{s})^2}\right] \frac{1}{\mathcal{F}_{35}^2} \\
&= \frac{128}{27} g^6 \frac{s^2}{t^2} \frac{1}{k_\perp^2} \left(-1 - \frac{M^2}{s \tan^2 \frac{\theta}{2}} + 1\right) \left(\frac{1 - \frac{M^2}{s}}{1 + \frac{M^2}{s \tan^2 \frac{\theta}{2}}}\right)^2 \left[1 + \frac{\frac{t}{s} (1 + \frac{t}{2s})}{(1 - \frac{M^2}{s})^2}\right] \frac{1}{\mathcal{F}_{35}^2} \\
&= \frac{128}{27} g^6 \frac{s^2}{t^2} \frac{1}{k_\perp^2} \left(\frac{M^2}{s} - 1 + \frac{1 - \frac{M^2}{s}}{1 + \frac{M^2}{s \tan^2 \frac{\theta}{2}}}\right) \left(\frac{1 - \frac{M^2}{s}}{1 + \frac{M^2}{s \tan^2 \frac{\theta}{2}}}\right) \left[1 + \frac{\frac{t}{s} (1 + \frac{t}{2s})}{(1 - \frac{M^2}{s})^2}\right] \frac{1}{\mathcal{F}_{35}^2} \\
&= \frac{128}{27} g^6 \frac{s^2}{t^2} \frac{1}{k_\perp^2} (\Delta_M^2 - 1 + \mathcal{J}) \mathcal{J} \left(1 + \frac{f_1}{(1 - \Delta_M^2)^2}\right) \frac{1}{\mathcal{F}_{35}^2} \tag{B.7}
\end{aligned}$$

Once we are done with the genuine (*i.e.* interference of any amplitude with itself) amplitudes, we turn towards the interference amplitudes which, again, can be divided into several types:

Interference between initial and final state radiations

$$\begin{aligned}
\mathcal{M}_1 \otimes \mathcal{M}_3^\dagger &\approx -g^6 \frac{1}{3 \times 36} \\
&\frac{(64M^6 - 128M^4s + 64M^2s^2 - 32M^4t + 128M^2st - 32s^2t + 32M^2t^2 - 32st^2 - 16t^3)}{t^2(4k_1 \cdot k_5 k_3 \cdot k_5)} \\
&= -g^6 \frac{1}{3 \times 36} 64M^2s^2 \left[\frac{\left(1 - \frac{M^2}{s}\right)^2 - \frac{M^2t}{2s^2} + \frac{2t}{s} - \frac{t}{2M^2} + \frac{t^2}{2s^2} - \frac{t^2}{2M^2s} - \frac{t^3}{4M^2s^2}}{t^2(4k_1 \cdot k_5 k_3 \cdot k_5)} \right] \\
&= -g^6 \frac{1}{3 \times 36} 64M^2s^2 \left[\frac{\left(1 - \frac{M^2}{s}\right)^2 - \frac{M^2t}{2s^2} + \frac{2t}{s} - \frac{t}{2M^2} + \frac{t^2}{2s^2} - \frac{t^2}{2M^2s} - \frac{t^3}{4M^2s^2}}{4 \frac{(s-M^2)^2}{4s} k_\perp^2 \left(\sqrt{1 + \frac{4M^2}{(1-\frac{M^2}{s})^2} \operatorname{cosec} \theta} - \cot \theta \right)^2} \right] \frac{1}{\mathcal{F}_{35}} \\
&= \frac{128}{27} g^6 \frac{s^2}{t^2} \frac{1}{k_\perp^2} \frac{1}{8} \left(\frac{-M^2}{s \tan^2 \frac{\theta}{2}} \right) \left(\frac{1 - \frac{M^2}{s}}{1 + \frac{M^2}{s \tan^2 \frac{\theta}{2}}} \right)^2 \\
&\quad \times \left[1 - \frac{\frac{M^2t}{2s^2} - \frac{2t}{s} + \frac{t}{2M^2} - \frac{t^2}{2s^2} + \frac{t^2}{2M^2s} + \frac{t^3}{4M^2s^2}}{\left(1 - \frac{M^2}{s}\right)^2} \right] \frac{1}{\mathcal{F}_{35}} \\
&= \frac{128}{27} g^6 \frac{s^2}{t^2} \frac{1}{k_\perp^2} \frac{1}{8} \left(-1 - \frac{M^2}{s \tan^2 \frac{\theta}{2}} + 1 \right) \left(\frac{1 - \frac{M^2}{s}}{1 + \frac{M^2}{s \tan^2 \frac{\theta}{2}}} \right)^2 \left[1 - \frac{f_2}{\left(1 - \frac{M^2}{s}\right)^2} \right] \frac{1}{\mathcal{F}_{35}} \\
&= \frac{128}{27} g^6 \frac{s^2}{t^2} \frac{1}{k_\perp^2} \frac{1}{8} \left(\frac{M^2}{s} - 1 + \frac{1 - \frac{M^2}{s}}{1 + \frac{M^2}{s \tan^2 \frac{\theta}{2}}} \right) \left(\frac{1 - \frac{M^2}{s}}{1 + \frac{M^2}{s \tan^2 \frac{\theta}{2}}} \right) \left[1 - \frac{f_2}{\left(1 - \frac{M^2}{s}\right)^2} \right] \frac{1}{\mathcal{F}_{35}} \\
&= \frac{128}{27} g^6 \frac{s^2}{t^2} \frac{1}{k_\perp^2} \frac{1}{8} (\Delta_M^2 - 1 + \mathcal{J}) \mathcal{J} \left(1 - \frac{f_2}{\left(1 - \Delta_M^2\right)^2} \right) \frac{1}{\mathcal{F}_{35}}
\end{aligned} \tag{B.8}$$

$$\begin{aligned}
\mathcal{M}_2 \otimes \mathcal{M}_4^\dagger &\approx g^6 \frac{1}{3 \times 36} \frac{32M^4t - 64M^2st + 32s^2t + 32st^2 + 16t^3}{4t^2k_2.k_5k_4.k_5} \\
&= g^6 \frac{1}{3 \times 36} 32s^2t \left[\frac{\left(1 - \frac{M^2}{s}\right)^2 + \frac{t^2}{2s^2} + \frac{t}{s}}{4t^2k_2.k_5k_4.k_5} \right] \\
&= \frac{128}{27} g^6 \frac{s^2}{t^2} \frac{1}{k_\perp^2} \frac{1}{16} \tan^2 \frac{\theta}{2} \left[\frac{t}{s} \left(1 + \frac{\frac{t}{s} \left(1 + \frac{t}{2s}\right)}{\left(1 - \frac{M^2}{s}\right)^2}\right) \right] \frac{1}{\mathcal{F}_{45}}
\end{aligned} \tag{B.9}$$

$$\begin{aligned}
\mathcal{M}_2 \otimes \mathcal{M}_3^\dagger &\approx g^6 \frac{7}{3 \times 36} \\
&\frac{-32M^6 + 96M^4s + 32M^4t - 96M^2s^2 - 96M^2st - 16M^2t^2 + 16s^6t^3 + 32s^3 + 64s^2t + 48st^2}{t^2(4k_2.k_5k_3.k_5)} \\
&= g^6 \frac{7}{3 \times 36} 32s^3 \frac{\left(1 - \frac{M^2}{s}\right)^3 + \frac{M^4t}{s^3} - \frac{3M^2t}{s^2} + \frac{2t}{s} - \frac{M^2t^2}{2s^3} + \frac{3t^2}{2s^2} + \frac{t^3}{2s^3}}{t^2(4k_2.k_5k_3.k_5)} \\
&= \frac{128}{27} g^6 \frac{s^2}{t^2} \frac{1}{k_\perp^2} \frac{7}{16} \left(1 - \frac{M^2}{s}\right)^2 \frac{1}{\left(1 + \frac{M^2}{s \tan^2 \frac{\theta}{2}}\right)} \\
&\times \left[1 + \frac{\frac{M^4t}{s^3} - \frac{3M^2t}{s^2} + \frac{2t}{s} - \frac{M^2t^2}{2s^3} + \frac{3t^2}{2s^2} + \frac{t^3}{2s^3}}{\left(1 - \frac{M^2}{s}\right)^3} \right] \frac{1}{\mathcal{F}_{35}} \\
&= \frac{128}{27} g^6 \frac{s^2}{t^2} \frac{1}{k_\perp^2} \frac{7}{16} \left(1 - \frac{M^2}{s}\right) \mathcal{J} \left[1 + \frac{f_4}{\left(1 - \frac{M^2}{s}\right)^3} \right] \frac{1}{\mathcal{F}_{35}}
\end{aligned} \tag{B.10}$$

$$\begin{aligned}
\mathcal{M}_1 \otimes \mathcal{M}_4^\dagger &\approx g^6 \frac{7}{3 \times 36} \\
&\frac{-32M^6 + 96M^4s + 32M^4t - 96M^2s^2 - 96M^2st - 16M^2t^2 + 16s^6t^3 + 32s^3 + 64s^2t + 48st^2}{t^2(4k_1 \cdot k_5 k_4 \cdot k_5)} \\
&= g^6 \frac{7}{3 \times 36} 32s^3 \frac{\left[\left(1 - \frac{M^2}{s}\right)^3 + \frac{M^4t}{s^3} - \frac{3M^2t}{s^2} + \frac{2t}{s} - \frac{M^2t^2}{2s^3} + \frac{3t^2}{2s^2} + \frac{t^3}{2s^3} \right]}{t^2(4k_1 \cdot k_5 k_4 \cdot k_5)} \\
&= \frac{128}{27} g^6 \frac{s^2}{t^2} \frac{1}{k_\perp^2} \frac{7}{16} \left(1 - \frac{M^2}{s}\right)^2 \frac{1}{\left(1 + \frac{M^2}{s \tan^2 \frac{\theta}{2}}\right)} \\
&\times \left[1 + \frac{\frac{M^4t}{s^3} - \frac{3M^2t}{s^2} + \frac{2t}{s} - \frac{M^2t^2}{2s^3} + \frac{3t^2}{2s^2} + \frac{t^3}{2s^3}}{\left(1 - \frac{M^2}{s}\right)^3} \right] \frac{1}{\mathcal{F}_{45}} \\
&= \frac{128}{27} g^6 \frac{s^2}{t^2} \frac{1}{k_\perp^2} \frac{7}{16} \left(1 - \frac{M^2}{s}\right) \mathcal{J} \left[1 + \frac{f_4}{\left(1 - \frac{M^2}{s}\right)^3} \right] \frac{1}{\mathcal{F}_{45}} \tag{B.11}
\end{aligned}$$

Interference of final state radiations

$$\begin{aligned}
\mathcal{M}_3 \otimes \mathcal{M}_4^\dagger &= g^6 \frac{2}{3 \times 36} \frac{32s^3}{\mathcal{F}_{35}\mathcal{F}_{45}} \left[\frac{\left(1 - \frac{M^2}{s}\right)^3 - \frac{M^2t}{s^2} + \frac{t}{s} - \frac{M^2t^2}{2s^3} + \frac{t^2}{2s^2}}{4 \frac{(s-M^2)^2}{4s} k_\perp^2 \left(\sqrt{1 + \frac{4\frac{M^2}{s}}{\left(1 - \frac{M^2}{s}\right)^2} \text{cosec } \theta - \cot \theta} \right) (\text{cosec } \theta + \cot \theta)} \right] \\
&= \frac{128}{27} g^6 \frac{s^2}{t^2} \frac{1}{k_\perp^2} \frac{1}{8} \left(1 - \frac{M^2}{s}\right)^2 \left[\frac{1 - \frac{\frac{M^2t}{s^2} - \frac{t}{s} - \frac{t^2}{2s^2} + \frac{M^2t^2}{2s^3}}{\left(1 - \frac{M^2}{s}\right)^3}}{\left(1 + \frac{M^2}{s \tan^2 \frac{\theta}{2}}\right)} \right] \frac{1}{\mathcal{F}_{35}\mathcal{F}_{45}} \\
&= \frac{128}{27} g^6 \frac{s^2}{t^2} \frac{1}{k_\perp^2} \frac{1}{8} \left(1 - \frac{M^2}{s}\right) \mathcal{J} \left[1 - \frac{f_3}{\left(1 - \frac{M^2}{s}\right)^3} \right] \frac{1}{\mathcal{F}_{35}\mathcal{F}_{45}} \tag{B.12}
\end{aligned}$$

Interference of initial state radiations

$$\begin{aligned}
\mathcal{M}_1 \otimes \mathcal{M}_2^\dagger &= g^6 \frac{2}{3 \times 36} 32s^3 \left[\frac{\left(1 - \frac{M^2}{s}\right)^3 - \frac{M^2 t}{s^2} + \frac{t}{s} - \frac{M^2 t^2}{2s^3} + \frac{t^2}{2s^2}}{4 \frac{(s-M^2)^2}{4s} k_\perp^2 \left(\sqrt{1 + \frac{4M^2}{(1-M^2/s)^2} \operatorname{cosec} \theta - \cot \theta} \right) (\operatorname{cosec} \theta + \cot \theta)} \right] \\
&= \frac{128}{27} g^6 \frac{s^2}{t^2} \frac{1}{k_\perp^2} \frac{1}{8} \left(1 - \frac{M^2}{s}\right)^2 \left[\frac{1 - \frac{M^2 t}{s^2} - \frac{t}{s} - \frac{t^2}{2s^2} + \frac{M^2 t^2}{2s^3}}{\left(1 - \frac{M^2}{s}\right)^3} \right] \\
&= \frac{128}{27} g^6 \frac{s^2}{t^2} \frac{1}{k_\perp^2} \frac{1}{8} \left(1 - \frac{M^2}{s}\right) \mathcal{J} \left[1 - \frac{f_3}{\left(1 - \frac{M^2}{s}\right)^3} \right] \tag{B.13}
\end{aligned}$$

3. Color factors of the diagrams

The calculation of colour factor is pretty straightforward. However, for sake of completeness we show here the calculation of \mathcal{C}_{11} , the colour factor corresponding to \mathcal{M}_{11} . We may easily find out that the factor $t_{ij}^a t_{jk}^b t_{ln}^a$, ($t^a = \frac{\lambda^a}{2}$, where λ^a are Gell-Mann matrices; and b (a) is the color of the emitted (propagator) gluon.) when squared yields \mathcal{C}_{11} . Hence,

$$\begin{aligned}
\mathcal{C}_{11} &= t_{ij}^a t_{jk}^b t_{ln}^a \{t_{ij}^a t_{jk}^b t_{ln}^a\}^\dagger \\
&= (t^a t^b)_{ik} t_{ln}^a \{(t^a t^b)_{ik} t_{ln}^a\}^\dagger \\
&= \chi_k^\dagger t^a t^b \chi_i \chi_n^\dagger t^a \chi_l \chi_l^\dagger t^{a'} \chi_n \chi_i^\dagger t^b t^{a'} \chi_k \\
&= \underbrace{\chi_n^\dagger t^a \chi_l \chi_l^\dagger t^{a'} \chi_n \chi_k^\dagger t^a t^b \chi_i \chi_i^\dagger t^b t^{a'} \chi_k}_{\text{Tr}(t^a t^{a'}) \text{Tr}(t^a t^b t^b t^{a'})} \\
&= \frac{4}{3} \mathcal{I} \text{Tr}(t^a t^{a'}) \text{Tr}(t^a t^{a'}) \quad \left[t^b t^b = \frac{4}{3} \mathcal{I} \text{ (}\mathcal{I} \text{: Identity matrix)} \right] \\
&= \frac{4}{3} \mathcal{I} \cdot \frac{1}{2} \delta^{aa'} \cdot \frac{1}{2} \delta^{aa'} \\
&= \frac{8}{3} \tag{B.14}
\end{aligned}$$

where χ_i, χ_j, χ_k are the quark colour states denoted by three mutually orthogonal vectors: $(1,0,0)$, $(0,1,0)$ and $(0,0,1)$. Below we list down all the \mathcal{C}_{ij} s we have obtained corresponding to \mathcal{M}_{ij} s in Eq. 5.17.

	1	2	3	4
1	$\frac{8}{3}$	$-\frac{2}{3}$	$-\frac{1}{3}$	$\frac{7}{3}$
2			$\frac{7}{3}$	$-\frac{1}{3}$
3			$\frac{8}{3}$	$-\frac{2}{3}$
4				